EXPLORATION GEOCHEMICAL MAPPING IN THE NORTHERN SECTOR OF THE MOROKWENG IMPACT STRUCTURE, SOUTH AFRICA.

By

JINGJING XU

Submitted in partial fulfillment
of the requirements for the degree of

MAGISTER SCIENTIAE

Department of Earth Science,
Faculty of Science,
University of the Western Cape.

Supervisor: Prof. C.Okujeni **May 2006**

DECLARATION

I declare that this work "*Exploration Geochemical Mapping in the Northern Sector of the Morokweng Impact Structure, South Africa*" is my own work, that it has not been submitted for degree or examination at any other university, and that all the sources I have used or quoted have been indicated and acknowledged by means of complete references.

.....

Jingjing Xu
May, 2006.

ACKNOWLEDGEMENTS

The one who deserves my sincere thanks is Prof. C.Okujeni, my supervisor of this thesis who gave me great encouragement and assistance during the course of the project. He inspired me always and was patient throughout the whole process of study.

Sincere thanks goes to Prof. J. Van Bever Donker, who has given me suggestions on the geology and also helped resolve problems related to student matters.

My special thanks goes to Mr. William Baugaard, Mr. Patrick Ackon and Mr. Segun Akinyemi who gave me suggestions on the structural geology and also helped me with proof reading of this thesis.

I would like to thank Dr. Marco Andreoli for his various ways to support. My gratitude goes to Prof. Nebo Jovanovic for giving me his support during this project.

Finally, I would like to thank my parents and Jade Yang who supported me financially as well as emotionally through my years of studies.

ABSTRACT

Geochemical mapping was undertaken to delineate concealed bedrocks and Ni-PGE mineralization beneath aeolian regolith overlying the Morokweng Impact Structure (MIS), which is situated in the Northwest province of South Africa. The regolith overlying MIS is covered entirely by wind-blown Kalahari sand and few isolated exposures of calcretes.

About 40 samples were collected from an area of about 50 square kilometers. Samples were sieved into <75μm, 75μm-125μm, and >125μm, then each fraction was extracted with both cold and hot hydroxylamine leach at a concentration range of 0.1M, 0.15M, 0.2M and 0.25M.

Patterns of element extractability can be grouped into: 1.) The rapid reaction group comprising of Mn, Ba, Cu, Sr, Pb, Ni, Co, Pd and U. 2.) The group of elements having higher extractability with an increased hydroxylamine concentration: As, V, Au and Cr. 3.) A group of elements with variable extractability patterns: Zn, Se, Ag, Pt, Ru, Cd, Ir, Re and Rh. Elements such as Ba, Rb and Sr do not reflect anomalies around melt sheet despite their high level of extractability. Most elements show the best reflection of bedrock and possible mineralization in 0.1M and 0.25M hydroxylamine partial extraction. Elevated As, V, Ir, Pt, Ni and Au values are located around the magnetic highs in the western part and at the boundary between the impact melt sheet and the surrounding basement rocks. These two areas fall within the NE-SW trending geochemical anomalous zones. These zones of geochemical anomalies coincide with the orientation of radial dykes / faults emanating from the impact melt structure.

KEY WORDS

Morokweng Impact Structure, Aeolian sand, Geochemical anomalies, Hydroxylamine hydrochloride, Regolith, Partial extraction, Ni-mineralization.

ABBREVIATIONS

AAS	-	Atomic Absorption Spectrometer
CH	-	Cold Hydroxylamine Hydrochloride
Concen.	-	Concentration
Fig.	-	Figure
ICP-MS	-	Inductively Coupled Plasma Mass Spectrometry
g	-	gram
HH	-	Hot Hydroxylamine Hydrochloride
km	-	kilometers
M	-	Molar
Ma	-	Million years
MIS	-	Morokweng Impact Structure
MMI	-	Mobile Metal Ion
ml	-	Milliliter
Min.	-	Minutes
μm	-	Micrometer
NECSA	-	South African Nuclear Energy Corporation
PCA	-	Principal Component Analysis
PGM	-	Platinum Group Metal
PGE	-	Platinum Group Element
ppm	-	parts per million
ppb	-	parts per billion

TABLE OF CONTENTS

LIST OF FIGURES

LIST OF TABLES

LIST OF PLATES

LIST OF APPENDICES

CHAPTER 1

1.1 Introduction

The Morokweng impact structure is located the Northwestern province of South Africa as a circular feature of about 70km diameter. Recent studies have revealed that this structure hosts impact melt rocks beneath the Kalahari sediments and are widely accepted as a source of anomalous signatures in the regional aeromagnetic map (Hart et al., 1997). The presence of a deeply buried meteorite is confirmed by the discovery of impact characteristic shock metamorphic effects in basement rocks and impact melt rocks have also been intercepted at depth in drilled cores. Chemical analysis of samples impact melt rocks from drillholes have shown a significant abundance of siderophile elements indicated by the presence of about 5% by weight of meteoritic component (Hart et al., 1997)

Previous work (McDonald et al., 2001, Hart et al., 2002) has shown that the impact melt sheet contains Ni rich sulphides and oxides significantly enriched in platinum group element (PGE) and chromium. The area has attracted some exploration interest because of its similarities to the Sudbury Impact Structure in Canada. The latter hosts world class magmatic deposit of Ni, Cu and Platinum Group Elements (PGEs) (Reimold et al., 2000).

The Morokweng impact structure and the surrounding areas are generally characterized by poor outcrop exposure due to the thick pervasive sand and calcrete cover of the Cenozoic Kalahari Group. This thick regolith cover makes the underlain melt rocks inaccessible and a great challenge to understanding the geology. The available structural and geological information on the study area were obtained through the interpretation of geophysical and drilled boreholes data (Hart et al., 1997).

The occurrence of aeolian sand / calcretes dominated regolith covering the entire area does pose serious problem in exploration for mineralization in MIS. Geochemical anomalies have often been associated with ferruginized aeolian sand overlying mineralization in several parts of South Africa.

The nature of occurrence of anomalies in ferruginized sediments can be very diverse due to the complex nature of element adsorption to Fe-Mn oxides (Okujeni et al., 2005). Recent studies by Okujeni et al., (2005) indicated that Fe-Mn oxides are the major components in aeolian sand and controls the distribution patterns of mobile metal ions. Those are either bound or unbound to colloid surfaces in soil. Iron and Manganese oxide composition could greatly vary depending on its source, environment of formation. This could ultimately affect their ability to adsorb trace elements. Davy et al., (1999), Okujeni et al., (2005) and others have recommended the use of hydroxylamine hydrochloride for selectively targeting Fe-Mn oxides in aeolian regolith.

The northwestern sector of the Morokweng impact structure was selected for investigation because of the possible existence of impact melt rocks beneath the surface cover as inferred from geophysical and geological data (Reimold et al., 2000). The aim of study with a view clearly defines the geochemical signature of the concealed impact melt rock in overlying aeolian sand. Selective leach techniques like hydroxylamine hydrochloride can be useful in unraveling the relationship between element extractability in regolith and signatures from bedrock and mineralization.

This project is therefore designed as a step in first developing technique that has the potential to fingerprint geochemical signatures that can characterize underlying bedrock and the impact melt zone from the surrounding shock metamorphosed basement.

1.1.1 Climate

The study area is located in a semi-arid region of South Africa. Annual rainfall ranges from around 180~300mm per annum and is characterized by cold winters and hot summers with an average minimum and maximum temperatures occurring in the summer season (18.2℃ and 33.7℃ respectively). July is the coldest month or the winter period and has a minimum and maximum average temperature of 2℃ and 20.1℃ respectively.

1.1.2 Vegetation and Drainage

The primary vegetation in the area is the Kalahari Plains Thorny Bushveld which is characterized by a well-developed tree stratum, a shrub layer and a basal grass cover. Dominant trees are the *Acacia erioloba, Boscia albitrunca. Acacia mellifera, Acacia hebeclada, Lycium hirstum, Grewia flava* and *Acacia heamatoxylon* are the domininant shrubs. The most conspicuous grasses are *lehmannia Eragrostis*, *Schmidtia kalahariensis* and *Stiptagrostis uniplumis*. The regional drainage direction of the proto-Molopo had been towards the northwest, but was later connected to a major southwest trending drainage system of the Permo-Carboniferous (-300 Ma) Kalahari Basin. The Proto-Molopo was strongly affected by the formation of the large MIS, which influenced the general drainage direction and pattern (Bootsman et al., 1999). Reconstruction of the post-impact drainage pattern, as it existed in the Late Cretaceous (-75 Ma) just before the formation of the rejuvenated Cenozoic Kalahari Basin, shows a generally southward flowing Moshaweng River with annular drainage pattern components. With the filling of the Kalahari Basin since Tertiary times, the affinity between the Molopo drainage and the Morokweng impact structure became less obvious (Bootsman et al., 1999).

CHAPTER 2

Geology

2.1 Regional Geology

The regional geology of the Morokweng area has been well documented by Corner et al., (1997), Hart et al., (2002), Andreoli et al., (1999) and Reimold et al., (2000). The basement consists of Archaean (ca.3.0 to 2.9 Ga) granitoids and some occurrences of Kraaipan Group meta-volcanics (greenstones) overlain by Proterozoic metasediments which consist of extensive carbonates deposits and banded iron formations of Griqualand West Supergroup (Poujol et al., 2000; Anhaeusser and Walraven, 1999). These, in turn, are overlain by what are now remnants of an originally extensive cover of (ca. 300 Ma old) Dwyka sediments of the Karoo Supergroup and Cenozoic deposits (sands, silcretes and calcretes) of the Kalahari Group ca. 70 Ma. Other mafic intrusives and extrusives rocks besides the Kraaipan Group include ca. 2.7 Ga Ventersdorp Lava, Ongeluk Lava which is an equivalent of the Hekpoort Andesite (2.2 to 2.3 Ga) in the Morokweng area (Corner et al., 1997).

2.1.1 Ganyesa Dome

The geology of the Morokweng region is not well defined. With the exception of limited exposures in the environs of the Ganyesa Dome, sands and silcretes / calcretes of the Cenozoic Kalahari Group cover the whole area. Only sporadic outcrop, mainly to the southeast of the Dome which consists of Archaean granitoid basement is accessible. The central part of the region contains Archaean granitoids. To the east of the Ganyesa Dome, Dwyka diamictites occur in patches. It is possible that small inliers of amphibolite schists occur in the central part, and they may be related to the Archaean Kraaipan Group (Anhaeusser and Walraven, 1999), that also occurs further to the east.

To the west of the Dome, metasediments of the Proterozoic Transvaal Supergroup and Griqualand West Group occur (Reimold, et al., 2000). Conglomerates quartzites, dolomites and shales of the Vryburg Formation are exposed to the northwest of Morokweng where they overly the granitoids and are in turn overlain by quartzite and stromatolitic dolomite which have been correlated with the Smidtsdrif subgroup (Hart et al., 2002). The Ongeluk Formation of the Postmasburg Group consists of dark-green andesitic lava which mainly exposed along the *Moshaweng* and *Kgokgole* Rivers in the vicinity of *Severn* to the most southwest of the project area.

2.2 Local Geology -The Morokweng Impact Structure

A circular aeromagnetic anomaly to the south of the town of Morokweng has been recognized by Hart et al., (2002); Corner et al., (1997) to be the result of a meteorite impact. The age of the impact event has been constrained to 145±2 Ma. The impact origin of this structure and its associated melt rocks have been confirmed by the existence of shock metamorphic clasts within the melt rocks (Koeberl and Reimold, 2003). The melt rocks are mostly unaltered and contains a large number of gabbroic and felsic clasts. The impact melt rock body shows no statistically pronounced variation or trend in chemical composition with depth or geographic location (Koeberl et al., 1997).

In this study, the geochemical mapping was carried out in an area bounded by Latitudes S26°15' to S26°26"2' and Longitudes E23°21'2" to E23°45'. It is bordered on the west by flowing Molopo River that also forms a common boundary between South Africa and Botswana. The topography is mostly flat (Fig. 2.1) with an N-S trending ranges of low sinous hills. The major rivers, namely the *Molopo, Kuruman, Moshaweng, Kgokgole* and *Phepane* Rivers, are all ephemeral.

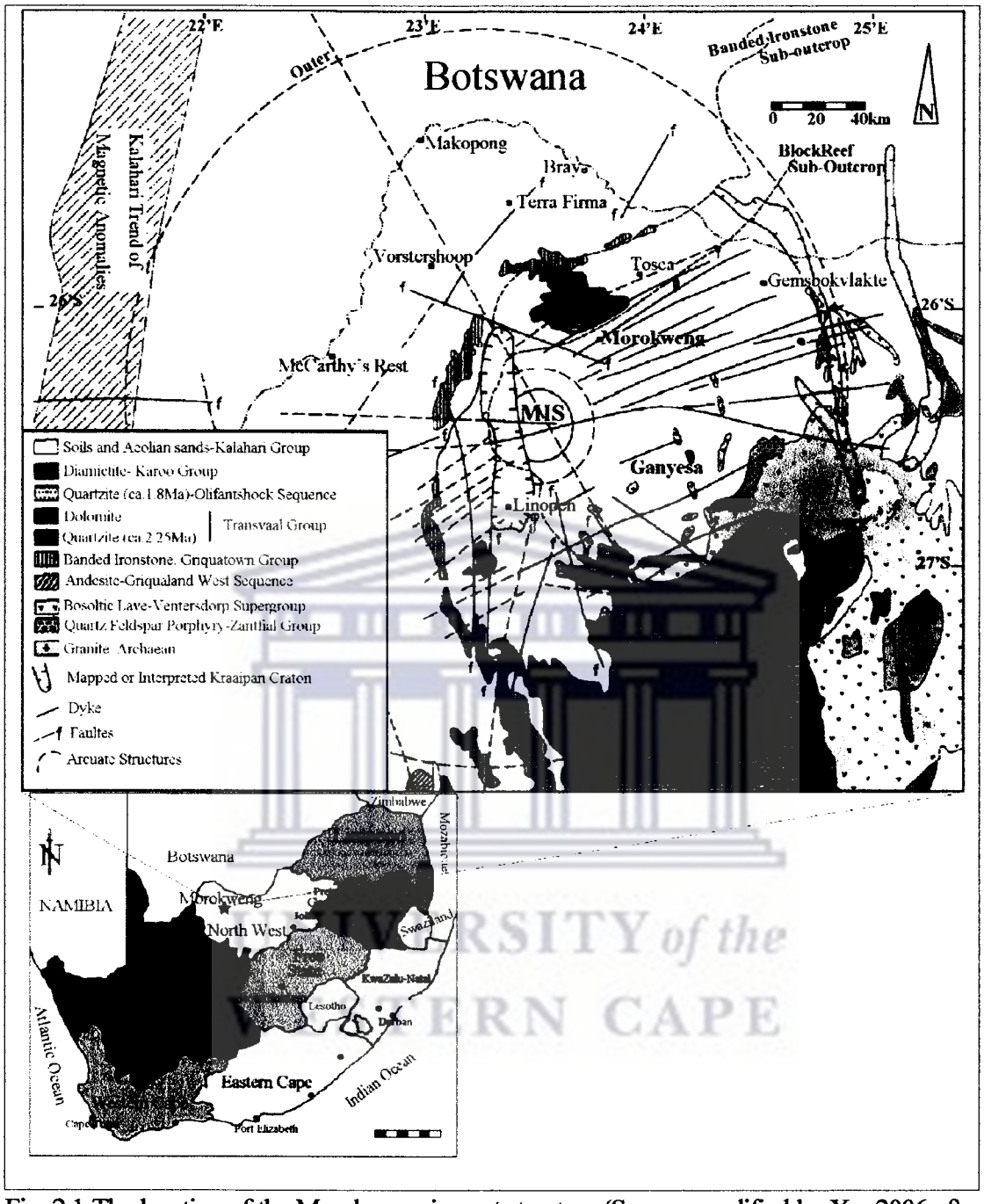

Fig. 2.1 The location of the Morokweng impact structure (Source: modified by Xu, 2006 after Koeberl et al., 2003).

2.2.1 Structural Trends

Reimold et al., (2000) summarized the major features of the impact structure as follows:

1. A number of radial faults (Fig. 2.1) occur within or cut the outer circular structure at the east and south of the central MIS. These radial features are termed the Morokweng Lineaments.

2. Within the MIS there are circular structures and also North-South to NW-SE trending magnetic anomalies. These lineaments and arcuate structures show typical magnetic dykes patterns that are discontinuous (Hart et al., 2002).

3. Certain dykes appear to extend further eastwards and westwards, but some are considered to be of different age and origin from the others. It is though that they belong to a much more widespread set of east-west trending dykes traversing the craton; a prominent east-west trending Machive dyke passes through the centre of the structure and is about 600km in length (Machaive dyke) (Koeberl and Reimold, 2003).

2.2.2 Subsurface Geology of the Morokweng Impact Structure

The MIS was first identified as a circular aeromagnetic anomaly of up to 1000 nT and about 30km diameter. Boreholes drilled into the centre of the anomaly intercept a sheet of differentiated granophyric to noritic rocks (Hart et al., 2002). The underlying rocks are brecciated and consist of shock-metamorphosed basement gneisses.

Direct petrological information on the impact melt sheet has been derived from a series of three boreholes WF3, WF4, and WF5 (Fig. 2.2). The drill holes intercepted. 1.) An upper sediment cover comprising of calcretes. 2.) An altered melt rock. 3.) A heterogeneous quartz-norite. The thickness of calcretes (Tertiary to Holocene) intersected in the three boreholes varies between 20 - 92m; about 20 meters in its

central parts of MIS.

The melt rocks directly underlie the calcretes and reach a thickness of about 125 m in borehole WF5 (Koeberl and Armstrong, 1997). The calcretes are underlain by norites which are mainly comprised of a 160m thick medium-grained quartz-norite and a heterogeneous quartz-norite (Koeberl and Armstrong, 1997). The homogenous quartz norite contains minor veins of granophyres in the upper zone. A zone of mafic nodules with minor sulphides occurs at a depth between 356-357m. Brecciated and hydrothermally altered quartz-norites occur at 400m to 440m depth (Hart et al., 2002; Koeberl et al., 1997). The lower contact of the melt rock was intersected in WF5, where the granitic rocks were encountered at a depth of 225 m whereas the other holes bottomed out in the melt rock unit (Reimold and Koeberl, 2003). In M3 borehole, there appear to contain granophyre heterogeneous norite and granophyric norite. (Hart et al, 2002). The Platinum Group Elements (PGE) in the granophyric norite occurs as disseminated inclusions in sulphides, oxides and ultramafic silicates throughout the melt sheet. Although these inclusions contain high PGE and Ni concentrations, their origins are unclear, as the PGE appear to be fractionated relative to chondrites and the bulk granophyric norite (Andreoli et al., 1999).

According to Hart et al., (2002), the bulk PGEs concentration in the inclusion-rich zone is indistinguishable from the inclusion poor melt rocks. This suggests that a similar PGE bearing material is present in the inclusion-rich and inclusion poor melt rocks. The bulk PGE signature of the altered melt rock is chondritic and it is clear that there has been a millimeter to sub-millimeter scale fractionation of PGE into different inclusion components. Pd and Rh tend to fractionate into sulphides at the expense of oxides while Pt is depleted in the oxide portion and fractionate into either a sulphide or Pt metal.

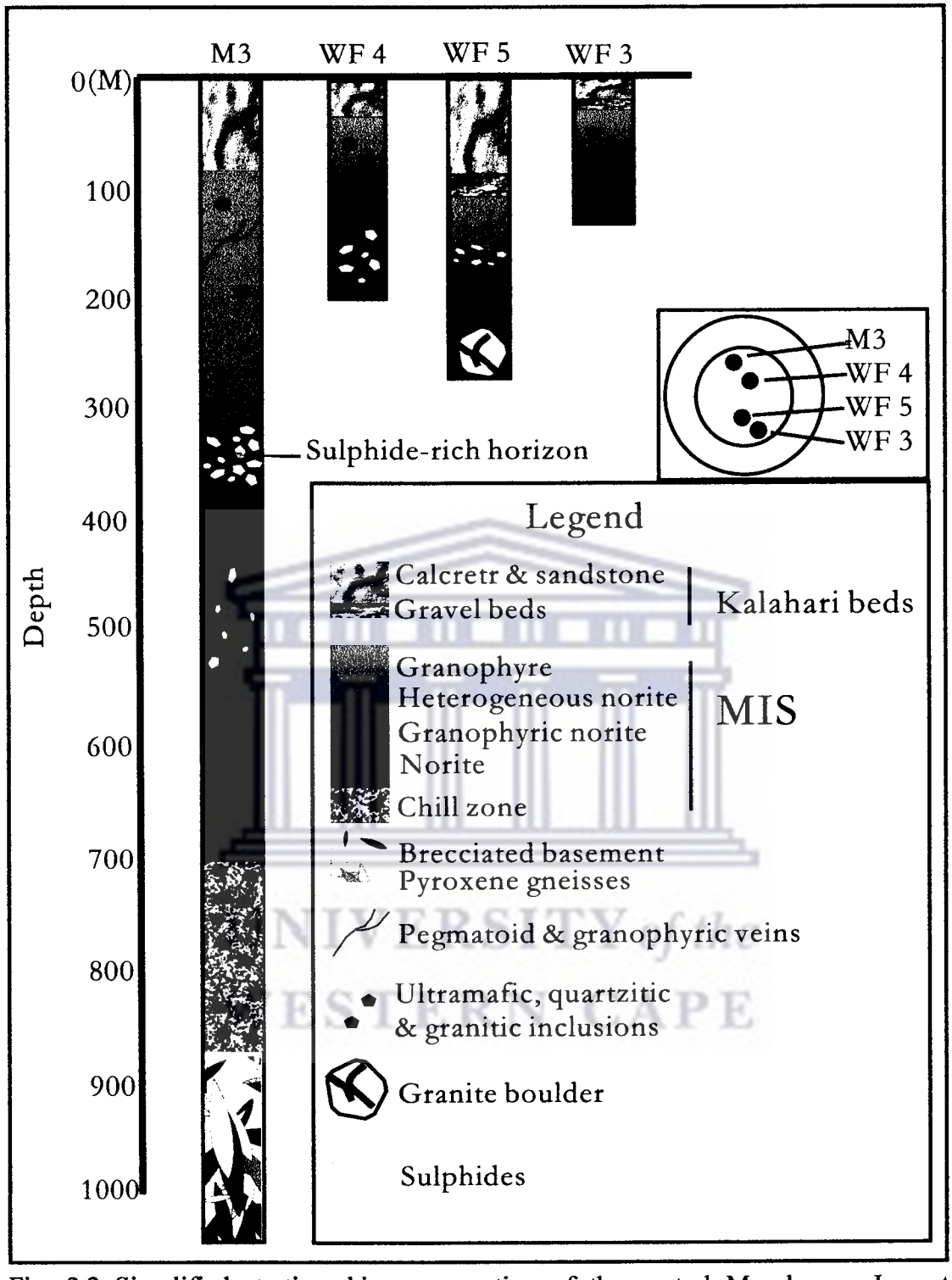

Fig. 2.2 Simplified stratigraphic cross-section of the central Morokweng Impact Structure which was deduced from three boreholes drilled by the Geological Survey of South Africa. After Hart et al., (2002).

The Morokweng melt rocks contain between 2.6 and 6.5wt% impactor. At this crustal melt ratio, over 99% of the Re and Os in the melt rock is derived from impactor. In the fresh melt rock, the oxide / sulphide mixture shows a slight enrichment in Rh and Pd and a very strong enrichment in Pt relative to Ru and Ir (Hart et al., 2002). The sulphide mixture has a high concentration of PGEs and a slight Pd and strong Pt enrichment relative to Ir, Rh and Ru (Hart et al., 2002).

2.3 Mineralization Potential of Impact Melt Rocks

As mentioned elsewhere, the study area is completely covered by Kalahari Group sands and calcretes. The main rock underlying the Kalahari beds comprise of a medium-grained, homogeneous quartz-norite. The quartz-norites consist of *plagioclase* (60%), *quartz* (10%), *K-feldspar* (5%), *orthopyroxene* (15%), *clinopyroxenes* (5%) and *opaques* (5%). The opaque minerals generally consist of *magnetite* and *ilmenite* (Koeberl et al., 1997). Three magnetic domains can be identified within the melt sheet. The contact between three of these domains, R1, R2 and R3, (Fig. 2.2) as well as the contact with the footwall rocks may represent potential sites for mineralization. Magnetic anomalies R1 and R2 in the melt sheet are areas of moderate magnetization while R3 encircled by the orange line has a high magnetic signature.

CHAPTER 3

Methodology

3.1 Field Work

Field mapping was preceded by a desk study involving the collection of existing information on the Morokweng impact structure. Geophysical and geochemical data (http://www.unb.ca/passc/impactdatabase) from previous investigations were also integrated in the planning of the grid regolith mapping. Field mapping and soil sampling was done over a period of two weeks in December 2004.

3.1.1 Regolith mapping

A rectilinear grid sampling plan was adopted and the traverses were laid at intervals of 1.5km with spacing. The traverses were orientated in such a way that it cuts across areas and high magnetic intensities in the melt sheet. Samples were collected at intervals of 1km so that samples could fall within each area of geophysical anomaly in the field (Fig. 3.1). The sampling sites were located with the aid of Global Position System (GPS) and recorded on a control map. Sample were numbered and labelled in accordance to their relative grid position on the control map (Fig. 3.1).

3.1.2 Soil sampling

The top soil comprising of loose sand with organic matter was scrapped off with a hand shovel until a colour change is observed and then sampled (Plate 3.1). Samples were collected in plastic bags, labelled and left to air dry at the field camp. The plastic bags were closed tightly and subsequently put into a field bay ready to be dispatched to the laboratory.

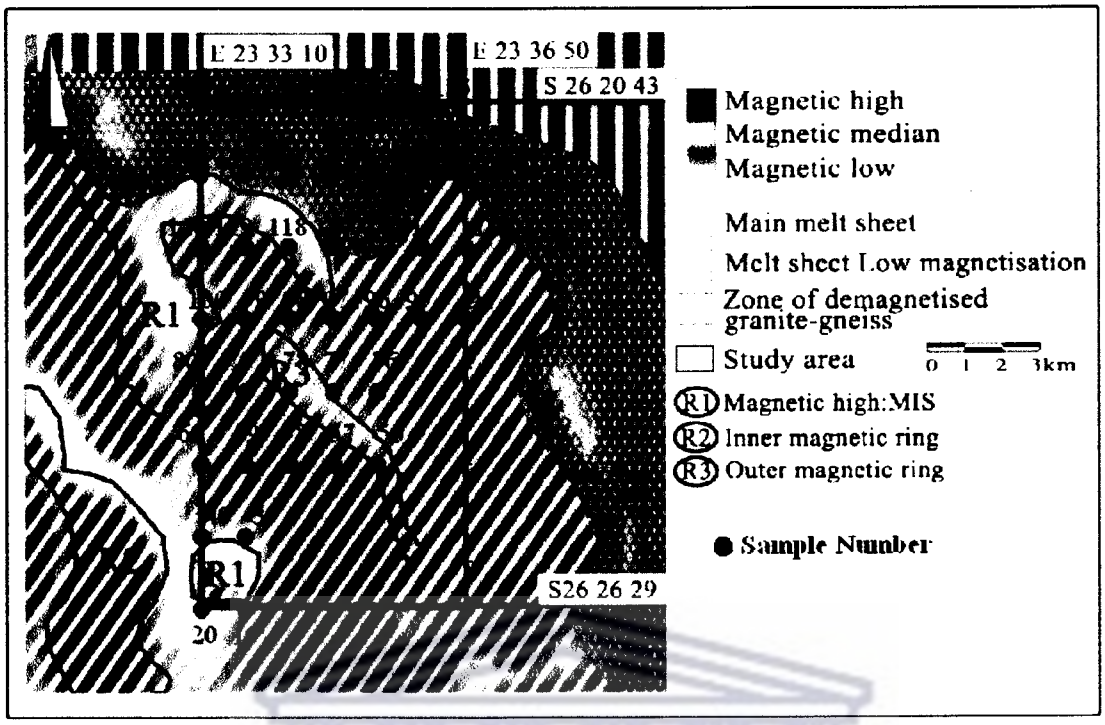

Fig. 3.1 Location of the study area and sampling grid.

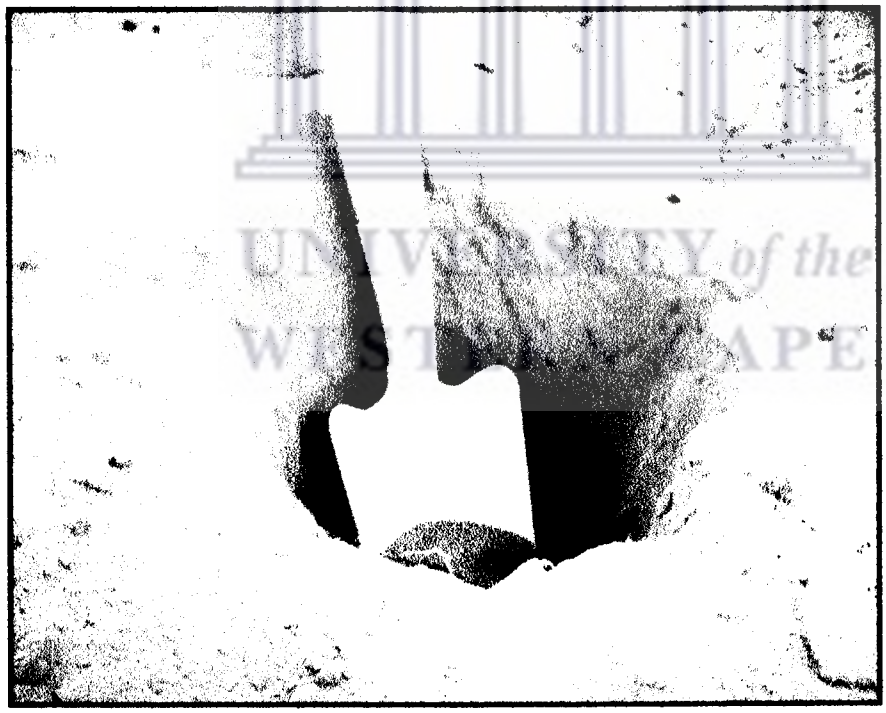

Plate 3.1 Soil sampling procedure.

	Regolith components observed				Physical properties					
Sample ID	quartz	calcretes	FeO%	Impurity	Grain Size	Mottled%	Colour	Glassy %	Milkiness	Angularity
19	25-50%	<25%	<25%	-	fine	dark	dark-yellow	>75%	<25%	sub
20	>75%	<25%	<25%	-	fine	dark	brown	>75%	<25%	sub
39	>75%	<25%	<25%	-	fine	dark	brown	>75%	<25%	sub
40	>75%	<25%	<25%	-	fine	dark	brown	>75%	<25%	sub
56	>75%	<25%	<25%	-	medium coarse	light	light yellow	50-75%	25-50%	well
57	>75%	<25%	<25%	-	medium coarse	light	light yellow	>75%	<25%	well
58	>75%	<25%	<25%	-	fine	light	light yellow	>75%	<25%	sub
59	>75%	<25%	<25%	cow dung	fine	light	light yellow	>75%	<25%	sub
60	>75%	<25%	<25%	cow dung	fine	medium	yellow	>75%	<25%	sub
76	>75%	<25%	<25%	-	fine	dark	brown	>75%	<25%	sub
77	25-50%	25-50%	<25%	-	fine	dark	brown	50-75%	25-50%	sub
78	>75%	<25%	<25%	-	fine	dark	brown	>75%	<25%	sub
79	>75%	<25%	<25%	-	fine	dark	dark-yellow	>75%	<25%	sub
80	>75%	<25%	<25%	-	medium coarse	light	milky	>75%	<25%	well
94	>75%	<25%	<25%	-	fine	medium	yellow	>75%	<25%	sub
95	>75%	<25%	<25%	-	fine	medium	yellow	>75%	<25%	sub
96	25-50%	25-50%	<25%	-	fine	medium	yellow	50-75%	25-50%	sub
97	25-50%	25-50%	<25%	-	fine	medium	yellow	50-75%	25-50%	sub
98	>75%	<25%	<25%	-	fine	medium	yellow	>75%	<25%	sub
99	>75%	<25%	<25%	insect	fine	light	light yellow	>75%	<25%	sub
100	>75%	<25%	<25%	-	fine	light	milky	>75%	<25%	sub
114	>75%	<25%	<25%	-	fine	light	light yellow	>75%	<25%	sub
115	25-50%	<25%	<25%	grass	medium coarse	light	milky	>75%	<25%	well
117	25-50%	<25%	<25%	insect	fine	light	light yellow	>75%	<25%	sub
118	25-50%	25-50%	<25%	-	fine	light	milky	50-75%	25-50%	sub
119	>75%	25-50%	<25%	-	fine	light	milky	50-75%	25-50%	sub
120	>75%	25-50%	<25%	-	fine	light	milky	50-75%	25-50%	sub
135	25-50%	25-50%	<25%	-	fine	medium	yellow	50-75%	25-50%	sub
136	25-50%	25-50%	<25%	-	fine	light	milky	50-75%	25-50%	sub
137	>75%	<25%	<25%	-	fine	dark	brown	>75%	<25%	sub
138	>75%	25-50%	<25%	grass	fine	dark	dark-yellow	50-75%	25-50%	sub
139	>75%	25-50%	<25%	-	fine	dark	dark-yellow	50-75%	25-50%	sub
140	25-50%	25-50%	<25%	cow dung	fine	medium	yellow	50-75%	25-50%	sub
155	>75%	<25%	<25%	-	fine	dark	dark-yellow	>75%	<25%	sub
156	25-50%	25-50%	<25%	-	fine	medium	yellow	50-75%	25-50%	sub
157	>75%	25-50%	<25%	-	fine	dark	dark-yellow	50-75%	25-50%	sub
158	>75%	25-50%	<25%	-	fine	dark	brown	50-75%	25-50%	sub
159	25-50%	25-50%	<25%	-	fine	dark	brown	50-75%	25-50%	sub
160	25-50%	25-50%	<25%	-	medium coarse	light	light yellow	50-75%	25-50%	well

Table 3.1 Sample description

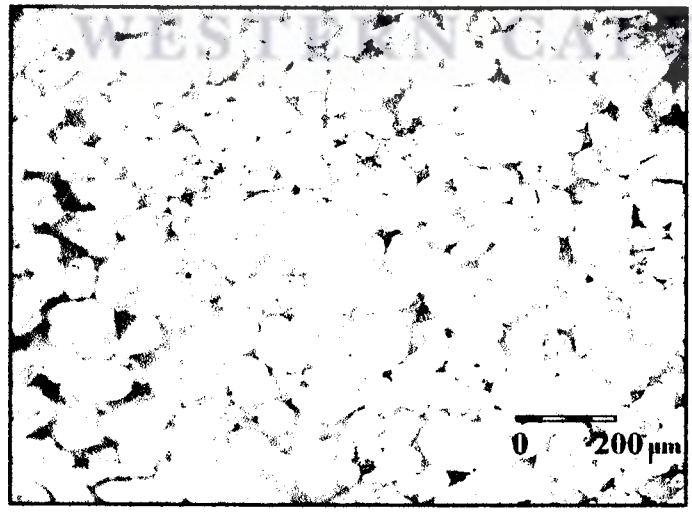

Plate 3.2 Aeolian sand under binocular microscope.

3.2 Laboratory work

3.2.1 Petrography

In this section the characteristics of the soils were described as comprehensively as possible in relation to their various physical properties. This comprises the general physical observation and description of the samples with respect to colour, grain sizes and organic matter content. Descriptions of colour, grain sizes, organic matter content, angularity, mineral composition were also undertaken in Table 3.1. Relative proportions of these components were estimated and the degree of mottleness for each sample was determine and plotted in Fig. 3.2.

Aeolian sand samples are mainly composed of varieties of quartz that range from glassy, milky and mottled quartz. Plate 3.2 shows the soil sample at 40x magnification under binocular microscope.

3.2.2 Sample preparation

Soil samples were sieved in the laboratory (University of Western Cape) in order to determine the optimum fraction for subsequent chemical analysis. The samples were loaded into the screen then sieved into less than 75μm; between 75μm and 125μm and greater than 125μm and mechanically agitated for 30 minutes. Sieved samples along with unsieved samples were preserved in separate sample bags for further laboratory work.

3.3 Partial extraction techniques

Selective extraction techniques can be very useful in investigating the nature of the distribution of elements in various mineral phases in soils (Hlavay et al., 2004). These extractions techniques are used in geochemical exploration, because they enhance a clear separation of anomalous component from background concentration to noise.

There are many of these techniques in use today by industry e.g. Mobile Metal Ions (MMI). Reasons for selecting hydroxylamine hydrochloride for this study have been given earlier. Hydroxylamine hydrochloride was used to partially extract elements that are mostly adsorped by secondary Fe-Mn oxides and hydroxides (Gray, 1999).

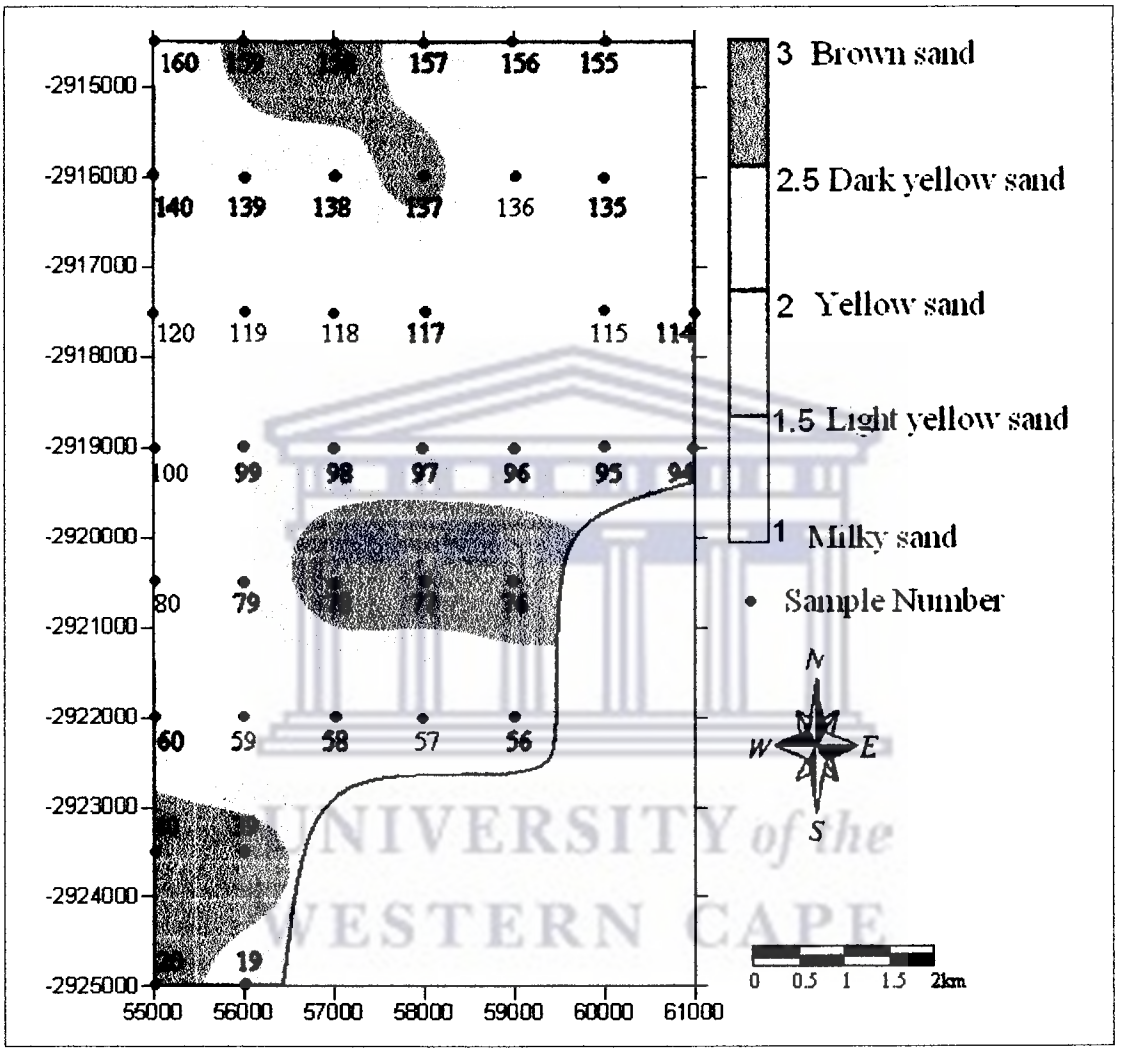

Fig. 3.2 Degree of mottleness in samples

Two leaching conditions of hydroxylamine hydrochloride were used during the extraction of the soil samples. These were cold hydroxylamine hydrochloride which selectively dissolves manganese oxides and amorphous hydrous iron oxide but does not dissolve crystalline iron oxides. Hot hydroxylamine hydrochloride on the other hand dissolves manganese oxides; amorphous hydrous iron oxides and less than 1% of the crystalline iron oxide (Gray, 1999).

3.3.1 Hydroxylamine partial extraction method

Hydroxylamine partial geochemical extractions allow variation of single parameters at a time, while maintaining other conditions constant. Manganese forms several oxidations states and exists in a variety of amorphous and crystalline forms. As a result Mn oxide has an extraordinarily high cation exchange capacity, accommodating many different trace elements on its surfaces. Therefore, this leach does not dissolve crystalline iron oxides but does dissolve very small amounts of amorphous hydrous iron oxide (Kelley et al., 2003). The hot hydroxylamine leach, which combines a higher concentration of hydroxylamine with elevated temperature (50℃) under reducing acid environment, is capable of effectively dissolving amorphous hydrous Fe oxide while leaving crystalline iron oxide substantially intact. As amorphous hydrous Fe oxide is a more effective scavenger than crystalline forms of Fe oxide, this leachant can be quite informative about metal ion mobility (Kelley et al., 2003).

The hydroxylamine hydrochloride leachant prepared procedure using a reagent with 98% purity as follows:

(1) 0.1M hydroxylamine hydrochloride = 6.95g $NH_2OH.HCL$ add 10ml 10% nitric acid and add distilled water till 1000ml then churn to dissolve.

(2) 0.15M hydroxylamine hydrochloride = 10.43g $NH_2OH.HCL$ add 15ml 10% nitric acid and add distilled water 1000ml then churn to dissolve.

(3)0.2M hydroxylamine hydrochloride = 13.9g $NH_2OH.HCL$ add 20ml 10% nitric acid and add distilled water 1000ml then churn to dissolve.

(4) 0.25M hydroxylamine hydrochloride = 17.37g $NH_2OH.HCL$ add 25ml 10% nitric acid and add distilled water 1000ml then churn to dissolve.

3.3.2 Cold hydroxylamine hydrochloride

0.1M hydroxylamine hydrochloride in concentrated nitric acid was added to 1g of soil sample in a plastic container. It was then sealed and placed in a shaker for 30 minutes. The solution was removed from the shaker and allowed to settle before filtration into a vial and subsequent analyzed by Atomic Absorption Spectrometer (AAS). By using the "add on" technique, 0.15M solution of hydroxylamine and concentrated nitric acid was then added to the soil residue in the containers and again shaken for 30 minutes. This procedure was repeated for 4 different concentrations of hydroxylamine, increasing by 0.05M up to 0.25M.

3.3.3 Hot hydroxylamine hydrochloride

The same concentrations of hydroxylamine hydrochloride with nitric acid were added to 1g of soil sample. However, the containers (not sealed) were placed in a bath at 50℃ for 1 hour. The solution was again allowed to settle and then filtered. The residue was put back into the leach vessels and the procedure replaced three times for 0.15, 0.2 and 0.25M hydroxylamine hydrochloride.

3.4 Analytical methods

Sample solutions were analyzed using flame atomic absorption spectroscopy (AAS) in the Department of Earth Science, University of the Western Cape. Further analysis was undertaken by ICP-MS in the geochemical laboratories at the University of Cape Town. ICP-MS provides a much lower detection limit for a wide range of elements (also refractory elements) than is possible with AAS.

3.5 Quality Control

Data quality measures were used in the orientation study to ensure reliable analysis. These measures were introduced by inclusion of duplicate samples at a rate of one per 20 samples analyzed. In addition, the laboratory maintained its own internal data

quality procedures that included analysis of reference standards and blanks.

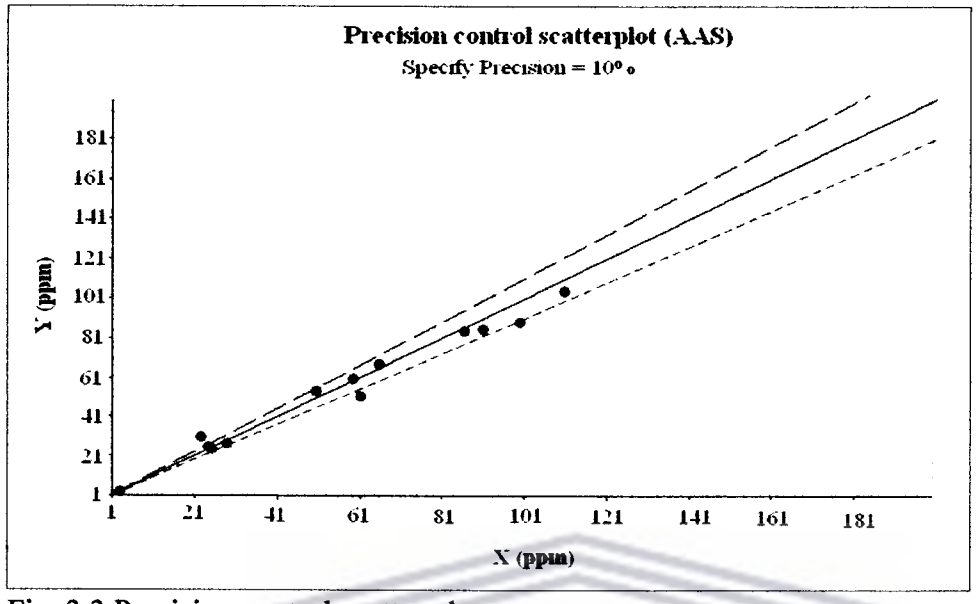

Fig. 3.3 Precision control scatter plot

Fig. 3.3 shows an estimated analytical (precision) diagram. Twenty duplicate samples were selected and leached twice by the same method and show an error of less than 10%. The data from the first leach and the duplicate were plotted using scatter plot, an Excel® based programme provided by the University of British Columbia, Canada.

3.6 Data evaluation

The software used for data evaluation included Xlstatistic 2006®, SigmaPlot 9.0® Surfer 8® and Excel 2003®. Principal Components Analysis (PCA) was used to reveal simpler patterns within a complex set of variables. It is very useful statistical tool to characterize and map interrelationships in geochemical data sets. This method seeks to establish if the observed variables can be explained largely or entirely by a much smaller number of variables called components. Principal component analysis is a mathematical method designed to reveal the relationships between two or more variables (Fang et al., 2003).

The geological significance of the components can help in the exploration and

location of the ore bodies that are deeply buried, especially around the MIS where exploration is difficult because the area is extensively covered by aeolian sand / calcretes.

CHAPTER 4

Results

The results of the investigation into the regolith geochemistry of the Northern section of the Morokweng impact structure is presented in two parts. Results for the orientation studies undertaken to optimize the hydroxylamine hydrochloride selective extraction techniques are first presented. Orientation studies focused on selective extraction of twenty aeolian soil samples under various conditions, e.g. by varying the sample mass, concentration of leach liquor, temperature and agitation time as well as variable sieve fraction size. The results are presented in section 4.1.

The second part of the study presents analytical data for all the samples collected from entire area. Samples were selectively extracted under optimized conditions using hydroxylamine hydrochloride. These results are presented in section 4.2.

4.1 Orientation Study

The result of the orientation study has been summarized in tables and plotted in various graphs of element extractability in leach liquor relative to variation in grain size of samples, duration of agitation and concentration or strength of leachant. The main objective of this work was to determine the optimum leach duration, sample weight, grain size and hydroxylamine concentration to be used in selective extraction of soils around the MIS.

The hydroxylamine hydrochloride leach is used to selectively extract elements from the iron / manganese mineral phases in the soil. In this orientation study concentration of cold hydroxylamine hydrochloride ($NH_2OH{\cdot}HCl$) was varied between 0.1M and 0.25M in nitric acid (HNO_3). The weight of sample was varied from 1g to 3g in an

attempt to set an optimum weight sample extraction. The samples were then extracted into 90ml of hydroxylamine and the solutions, agitated for 1 hour and allowed to settle down. The extractants was filtered into an Erlenmeyer conical flask and subsequently put inside sample bottles for measurement. Hot hydroxylamine hydrochloride was performed using the same concentration of hydroxylamine hydrochloride ($NH_2OH{\cdot}HCl$) but in addition heated in a water bath at 50℃ after heating for 1 hour the sample was allowed to cool down.

The extracts for both cold and hot hydroxylamine hydrochloride were analyzed with Atomic Absorption Spectrometry (AAS) for Fe, Mn, Ni, Cu and Co.

4.1.1 Temperature

Analytical data for hydroxylamine leach at room temperature (cold) and 50℃ (hot) (see Table 4.1.1 and Fig. 4.1.1) shows variable trends. Higher Mn, Cu and Ni contents occur in cold hydroxylamine hydrochloride extracts while the relative values for Fe and Co are higher in the hot extraction. Maximum extractability of manganese occurs at 0.1M hydroxylamine hydrochloride.

Cold hydroxylamine leach has been used extensively because it is known to be more selective for manganese oxides. Manganese oxide has an extraordinarily high cation exchange capacity, which can accommodate many different trace elements on its surfaces. This leach does not dissolve crystalline iron oxides but does dissolve very small amounts of amorphous hydrous iron oxide. Hot hydroxylamine leach, which combines a higher concentration of hydroxylamine with elevated temperature (50℃) and a reducing acid environment, is capable of effectively dissolving amorphous hydrous iron oxide while leaving crystalline iron oxide substantially intact (typically <1% dissolution). As amorphous hydrous iron oxide is a much more effective scavenger than crystalline forms of iron oxide, this leach can be quite informative about metal ion mobility (Kelley et al, 2003).

4.1.2 Grain size

Table 4.1.1 shows the summary for the 10 samples that were analyzed for Mn, Co, Cu, Ni and Fe; different fraction in aeolian sand and unsieved samples also under variable concentration of hydroxylamine hydrochloride. The results are presented in the Table 4.1.1 and plotted in Fig. 4.1.1. Element extractability of the leach versus variable grain size (unsieved samples >125μm, 75μm -125μm and <75μm size fraction) generally shows increased Mn, Cu, Fe contents towards finer grain fraction at 0.1M concentration. Increased extractability is observed in Fe and partly Co at higher hydroxylamine hydrochloride concentration. An overall trend suggesting an increase in element extractability with decreasing grain size corroborates work done by Hlavay et al., (2004). Variations in the behavior of different elements with particle size is attributed largely to differences in their relative potential for sorption on clay minerals, hydrous oxides, and organic matter surfaces, all of which tend to be concentrated in smaller grain sizes (Hlavay et al., 2004).

4.1.3 Sample weight

The sample weight used for partial extraction was varied between 1g and 3g. The concentration of the hydroxylamine hydrochloride was also varied between 0.1M and 0.25M (in 0.05M increment) Mn, Co, Fe, Ni and Cu all shows elevated element extractability at 1g compare to 2g and 3g.

The results from various concentrations of hot hydroxylamine hydrochloride plots (Fig. 4.1.2) appear to point to the fact that 1g sample weight shows higher element extractability. Therefore, the ensuing investigations will use the 1g sample as the analytical weight.

Cold Hydroxylamine hydrochloride							Hot Hydroxylamine hydrochloride						
Samples Average							Samples Average						
Range	Concen.	Mn	Co	Ni	Fe	Cu	Range	Concen.	Mn	Co	Ni	Fe	Cu
<75μm	0.1M	11.20	0.11	3.67	3.44	4.25	<75μm	0.1M	10.82	2.05	1.51	14.56	2.18
	0.15M	1.94	0.15	4.32	4.12	3.67		0.15M	1.42	4.70	1.76	9.29	1.44
	0.2M	1.91	0.21	5.78	5.96	3.71		0.2M	1.04	6.20	2.45	16.22	1.49
	0.25M	2.07	0.25	6.46	7.56	3.71		0.25M	1.21	6.49	2.27	12.26	2.20
75-125μm	0.1M	5.08	0.12	3.87	2.63	3.56	75-125μm	0.1M	4.27	3.49	1.48	6.73	1.37
	0.15M	2.11	0.16	4.77	4.09	4.59		0.15M	1.04	5.28	2.05	4.48	1.33
	0.2M	1.80	0.20	5.70	5.51	3.60		0.2M	0.99	6.37	2.30	7.87	1.35
	0.25M	2.02	0.24	6.23	6.66	3.69		0.25M	2.57	7.51	1.91	6.53	1.35
>125μm	0.1M	4.91	0.14	4.14	2.97	3.55	>125μm	0.1M	4.39	4.78	1.55	5.45	1.35
	0.15M	1.84	0.18	5.13	3.62	3.58		0.15M	1.04	4.36	2.25	2.99	1.30
	0.2M	2.03	0.19	5.42	6.16	3.6		0.2M	1.08	6.21	2.29	9.95	1.33
	0.25M	1.96	0.23	6.05	5.94	3.63		0.25M	2.12	7.52	1.87	5.54	1.30
Un-Sieved	0.1M	10.10	0.39	2.34	6.08	0.22	Un-Sieved	0.1M	3.20	1.77	1.64	3.24	1.35
	0.15M	6.35	1.08	2.48	5.96	0.18		0.15M	1.13	4.18	1.76	4.05	1.35
	0.2M	6.08	1.08	2.48	5.87	0.22		0.2M	1.04	4.83	2.39	5.99	1.31
	0.25M	6.16	1.09	2.50	5.45	0.25		0.25M	0.99	7.20	2.34	6.41	1.28

Table 4.1.1 Summary statistics of element extractability in hot and cold hydroxylamine hydrochloride leach vs. grain size (All values in ppm).

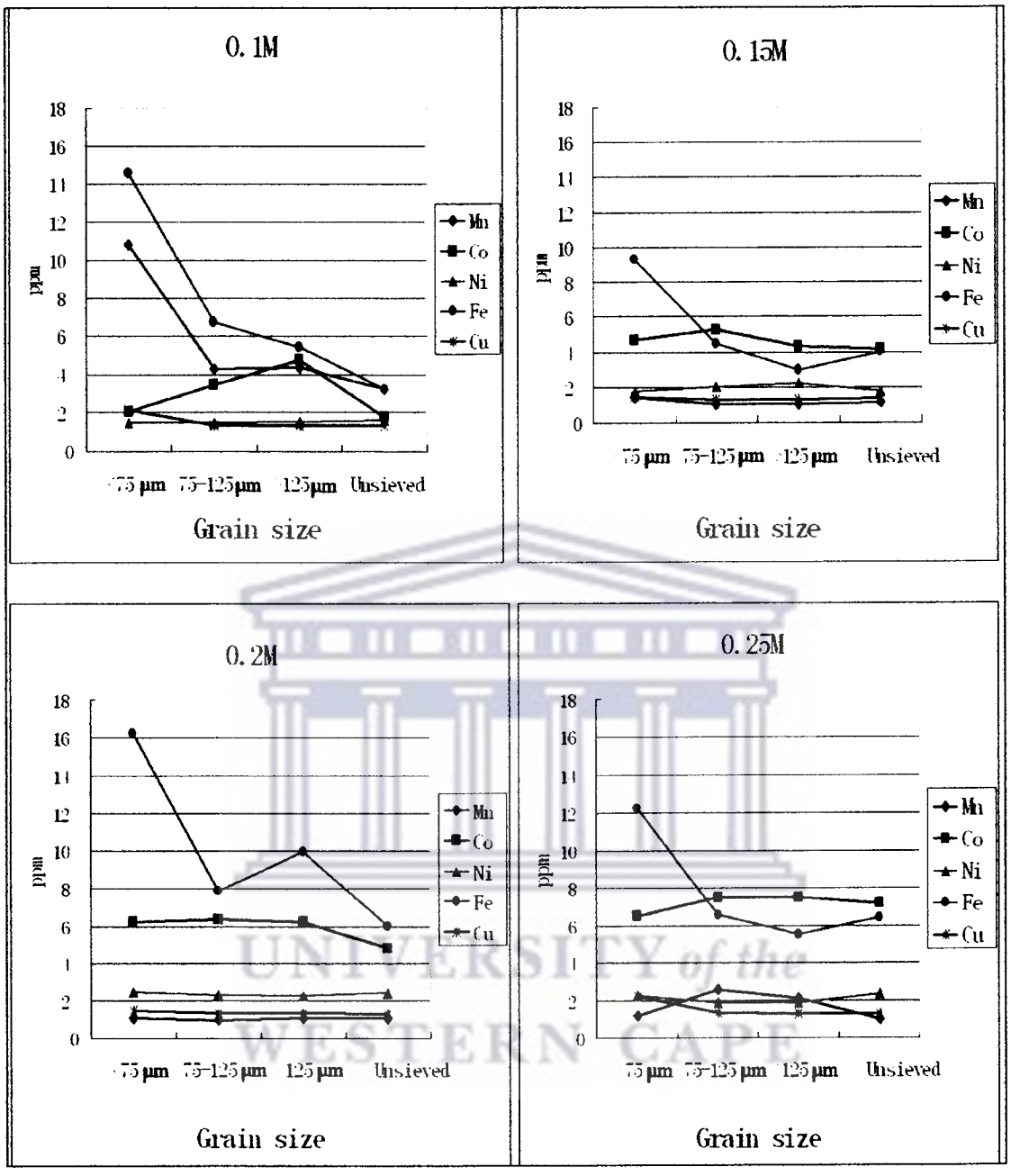

Fig. 4.1.1 Element extractability in hydroxylamine hydrochloride vs. grain size.

Samples No. 1-5 weight hot hydroxylamine leaching (ppm)						
Average		Mn	Co	Ni	Fe	Cu
1g	0. 1M	3. 83	3. 31	0. 41	4. 70	1. 91
	0. 15M	2. 29	2. 95	0. 90	5. 76	2. 68
	0. 2M	0. 50	5. 89	1. 04	8. 12	2. 84
	0. 25M	0. 76	7. 16	1. 75	4. 28	2. 92
2g	0. 1M	2. 03	1. 28	0. 31	2. 57	1. 09
	0. 15M	0. 41	2. 04	0. 48	4. 23	1. 37
	0. 2M	0. 27	3. 60	0. 45	5. 13	1. 44
	0. 25M	0. 43	4. 19	0. 92	3. 52	1. 49
3g	0. 1M	2. 38	1. 42	0. 27	2. 77	0. 83
	0. 15M	0. 37	1. 90	0. 23	3. 01	0. 93
	0. 2M	0. 25	2. 17	0. 38	3. 52	0. 97
	0. 25M	0. 25	2. 52	0. 55	2. 85	1. 00

Table 4.1.2 Summary statistics of element extractability vs. sample weight (All values in ppm).

This illustrates that the effect of increasing sample weight to optimize representatively and enhance detection limit capability is accompanied by a marked reduction in extraction efficiency which might be due to the processes of precipitation, colloid aggregation or sorption at exchange sites (Hall et. al., 1995).

4.1.4 Time

Table 4.3 and Fig. 4.1.4 shows the plot of extraction duration (10, 30, 60, 90 minutes) versus element extractability. Nickel and cobalt show a maximum extractability after a 90 minute leach period. Variable trends are observed in Fe, Mn and Cu, especially at higher concentration hydroxylamine hydrochloride. It is because of this trend in element extractability that further work will concentrate on leaching for 90 minutes.

4.1.5 Hydroxylamine Hydrochloride concentration

Solutions of various concentrations of hydroxylamine hydrochloride are used to selectively reduce and dissolve relatively insoluble Fe and Mn oxides of various compositions and crystallinities and thereby release adsorbed elements.

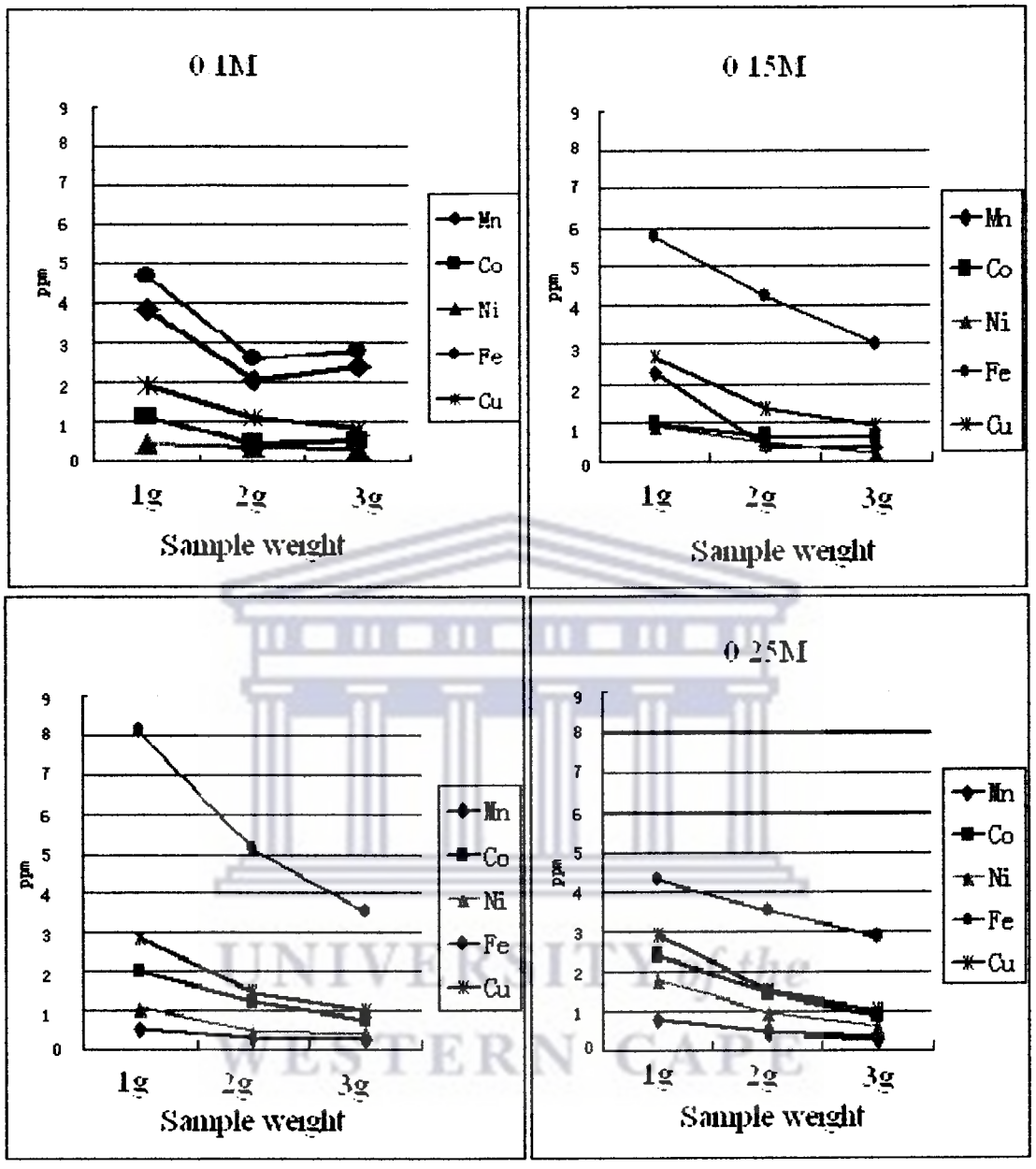

Fig. 4.1.2 Effect of sample weight on element extractability into hot hydroxylamine hydrochloride.

Samples duration hot hydroxylamine leaching (ppm)						
Average		Mn	Co	Ni	Fe	Cu
10 minutes	0.1M	3.53	3.00	1.57	4.84	2.99
	0.15M	1.19	2.71	1.76	5.40	2.95
	0.2M	1.12	2.73	1.71	6.23	3.01
	0.25M	1.03	2.89	2.02	7.29	2.97
30 minutes	0.1M	5.11	2.97	2.27	8.93	3.02
	0.15M	1.46	3.42	2.29	9.43	2.99
	0.2M	1.37	3.19	2.20	9.71	2.97
	0.25M	1.24	3.36	2.30	5.73	3.02
60 minutes	0.1M	3.94	2.98	2.66	4.52	2.97
	0.15M	1.60	3.51	3.06	4.10	2.93
	0.2M	1.73	3.44	3.10	4.70	2.99
	0.25M	1.48	3.56	3.00	5.54	2.97
90 minutes	0.1M	5.40	3.64	3.22	7.25	3.01
	0.15M	1.89	3.79	3.08	6.64	2.99
	0.2M	2.07	3.83	3.28	7.40	2.99
	0.25M	1.89	3.64	3.71	8.23	2.99

Table 41.3 Summary statistics of element extractability into hydroxylamine hydrochloride vs. each duration (All values in ppm).

The orientation studies so far suggests the use of 1g samples, sieved to a grain size fraction of <75µm and subsequently leached for at least 90 minutes. Randomly selected samples were leached using various hydroxylamine concentrations from 0.1 to 0.25M.

The resulting leach solution hydroxylamine concentration of 0.1M, 0.15M, 0.2M and 0.25M were analyzed by ICP-MS. A total of 24 elements analyzed by the ICP-MS which include V, Cr, Mn, Ni, Cu, Zn, Co, Ru, Rh, Pd, Ag, Cd, Re, Os, Ir, Pt, Au, Rb, Sr, Ba, As, Se, Pb and U.

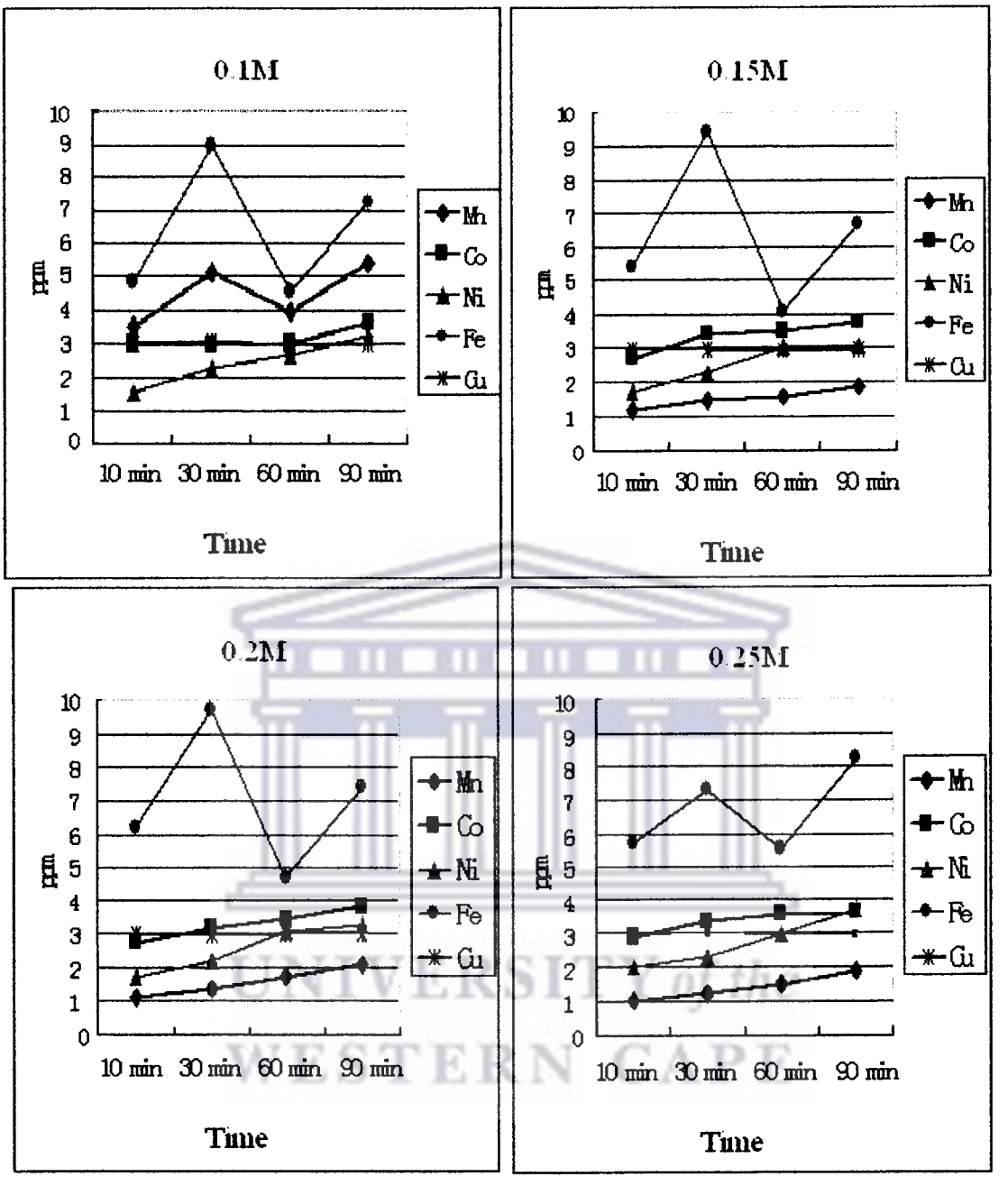

Fig. 4.1.3 Relationship between leach duration and element extractability.

The main objective of this study is to determine the optimum hydroxylamine concentration for the selective leach of various groups of elements that could occur adsorbed to various phases of Fe-Mn oxides.

Table 4.1.4 shows a summary of the distribution pattern of elements in 0.1 to 0.25M hydroxylamine hydrochloride leach. Variable trends in the distribution pattern of elements occur with an increasing strength of hydroxylamine hydrochloride and are

summarized as follows:

- Elements with concentration levels generally above 10 ppb, whose contents decrease with increasing strength of hydroxylamine are Mn, Ni, Co, Pb, Rb, Ba, Sr, and Cu.

- The second group of elements has a concentration level above 10ppb but contents increases with an increasing strength of hydroxylamine hydrochloride are V, As and Au.

- The third group with variable but low contents, generally below 10ppb levels; an increase in hydroxylamine hydrochloride is generally weak to flat or variable e.g., U, Pt, Ag, Cd, Re, Ru, Ir, Rh and Pd.

Group one also referred to as the rapid reaction group (Dalrymple et al., 2005) typically approaches a maximum level of extractability at low pH and low hydroxylamine concentration. These groups contain Ba and Sr with alkali earth elements as well as Co, Mn and Cu which agree with recently published works of Nolan et al., (2005).

Group two resemble a hydroxylamine stabilized metal group whose level of extractability is weak at low pH and hydroxylamine concentration (Dalrymple et al., 2005). Increased pH and hydroxylamine concentration prevent absorption of the element to Fe oxide.

These results (Fig. 4.1.4) underpins a variable pattern of element extractability, which in turn is related to the relative pattern association of the minor and trace elements to hydrous Fe and Mn oxide or even their crystalline varieties. Understanding the pattern of variability of trace elements with increasing strength of hydroxylamine will immensely contribute to interpretation of ensuing geochemical signature especially as this relates to their source. The data were therefore further studied using principal

component analysis.

The PCA were outlined in the previous chapter. The reader is referred to Pwa et al., (1999) and Davis, (1986) for further details. Principal components were calculated from a correlation matrix in order to reduce the effect to interference on concentration range between the elements. R-Mode principal components analysis was employed and bivariate plots of the four principal components accounting for 70% the data was used for the plots, which are presented as star plots in quadrants I to IV (Fig. 4.1.5 to Fig. 4.1.7)

Principal component star plots for element in 0.1M hydroxylamine hydrochlorides shows 3 major clusters of elements starting from the IV quadrant in a clockwise fashion (Rb, Mn, Co, Ni, Sr and Zn), (U, Pb, Rh, Pd, Os, Se and Ir) and (Au, Ru, Cr, Ag, Cu, Cd, Rh, As and V). A weak breakdown in this pattern into more subgroups can be observed in 0.15M hydroxylamine hydrochloride strength.

Two major element clusters are depicted by the principal component plot (V, Pt, Ru, U, Cr, Cd, Cu, Ir, Au, Rh and As) and (Mn, Zn, Sr, Ba, Rb and Pb).

Principal component plots for data derived from 0.2 and 0.25M hydroxylamine hydrochloride show increased bundling of the most elements into one cluster or association. The above trends suggest a release of elements from Fe and Mn phases of hydrous Fe-Mn oxides at low-hot hydroxylamine hydrochloride concentration. (0.1-0.15M) and increased release of elements from a single mineral phase; predominantly Fe-oxyhydroxides at higher hot hydroxylamine hydrochloride concentrations.

HH	0.1M			0.15M			0.2M			0.25M		
ppb	Minimum	Maximum	Mean	Minimum	Maximum	Mean	Minimum	Maximum	Mean	Minimum	Maximum	Mean
Mn	447.83	1726.17	1142.20	51.58	238.39	89.51	19.79	102.91	48.87	11.22	62.18	39.41
Ni	11.85	23.32	18.09	5.88	11.02	8.36	7.30	10.96	9.24	8.58	13.86	11.25
V	11.94	40.71	29.12	28.24	50.45	38.61	41.46	62.08	51.67	58.52	82.56	68.05
Cu	3.86	211.10	45.20	2.33	57.27	25.62	3.33	61.56	27.00	3.64	36.54	18.87
Zn	0.66	135.88	39.83	13.71	74.37	35.02	4.13	153.78	38.45	15.83	74.24	38.88
As	18.81	28.71	23.20	28.79	37.44	33.65	42.27	53.48	45.94	50.74	61.22	56.25
Sr	21.99	67.16	42.85	2.82	6.08	3.77	2.36	5.25	3.14	3.00	6.47	3.72
Ba	122.07	495.30	214.00	8.52	57.29	20.70	4.47	23.45	9.34	3.01	18.16	9.43
Os	0.00	234.94	58.28	1.21	151.98	45.55	0.02	424.06	71.23	0.00	252.96	46.34
Rb	4.93	16.37	12.30	1.33	3.51	2.73	0.83	2.26	1.29	0.60	1.32	0.85
Pb	9.38	22.80	17.13	7.52	13.44	10.25	4.09	19.62	8.88	3.69	11.18	7.14
Au	0.00	6.11	2.82	0.42	7.89	4.18	1.25	21.25	7.73	0.00	13.49	5.43
Co	7.24	27.70	18.01	0.24	1.98	1.01	0.39	1.20	0.85	0.00	0.98	0.43
Pd	0.27	1.40	0.83	0.32	1.27	0.74	0.01	3.83	1.00	0.00	1.56	0.46
Se	0.00	14.71	5.73	0.70	25.74	11.45	0.98	38.59	12.49	0.00	27.00	6.88
U	0.07	0.26	0.16	0.09	0.21	0.13	0.11	0.29	0.16	0.07	0.20	0.16
Pt	0.00	0.21	0.04	0.02	0.35	0.21	0.16	0.46	0.28	0.00	0.58	0.10
Ag	0.00	0.94	0.15	0.10	0.27	0.19	0.25	1.47	0.17	0.00	0.19	0.02
Cd	0.04	0.66	0.29	0.01	0.64	0.26	0.06	0.31	0.22	0.00	0.50	0.17
Re	0.00	0.21	0.04	0.02	0.19	0.09	0.01	0.21	0.08	0.00	0.17	0.06
Ru	0.00	0.35	0.12	0.15	0.40	0.26	0.16	0.43	0.32	0.00	0.36	0.13
Ir	0.00	0.43	0.16	0.07	0.31	0.16	0.01	0.91	0.22	0.00	0.38	0.13
Rh	0.00	0.23	0.05	0.06	0.37	0.17	0.03	0.35	0.17	0.00	0.19	0.05
Cr	0.00	35.23	9.68	15.41	43.61	29.26	11.03	39.19	25.74	0.00	39.17	12.05

Table 4.1.4 Summary statistics of element extractability in different concentrations of hot hydroxylamine hydrochloride (All values in ppb).

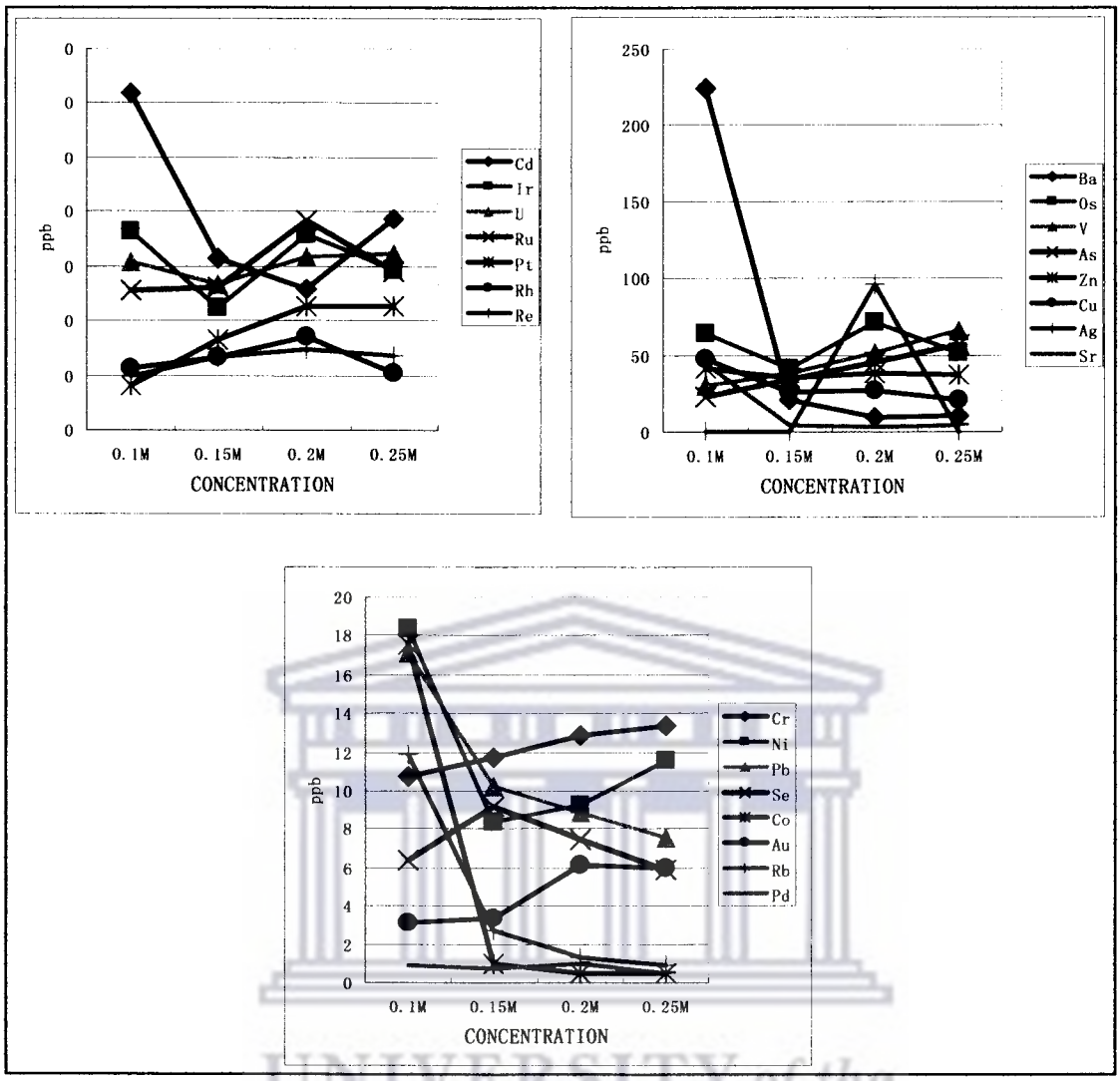

Fig. 4.1.4 Average element extractability vs. the concentration of hydroxylamine hydrochloride.

The above is corroborated by the plot of element extractability versus the hydroxylamine hydrochloride concentration is Fig. 4.1.5-4.1.8. Three major patterns of elements distribution can be observed:

1. Elements whose extractability decreases with an increasing hydroxylamine concentration e.g. Mn extractability gives the elevated values at 0.1M than 0.2M.
2. Elements whose extractability increase with increasing hydroxylamine concentration and suggest the release of elements from Fe-Mn oxyhydroxides at low hydroxylamine concentration and increasingly from Fe-bearing phases with increasing hot hydroxylamine hydrochloride concentration.

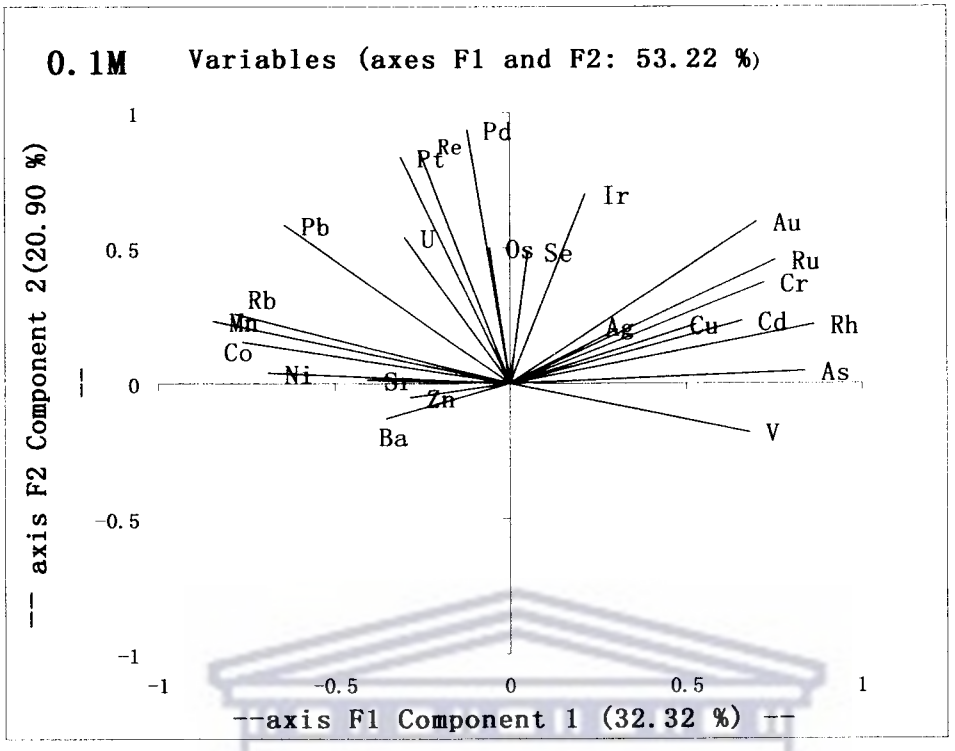

Fig. 4.1.5 Principal component plot for element data in 0.1M hydroxylamine hydrochloride.

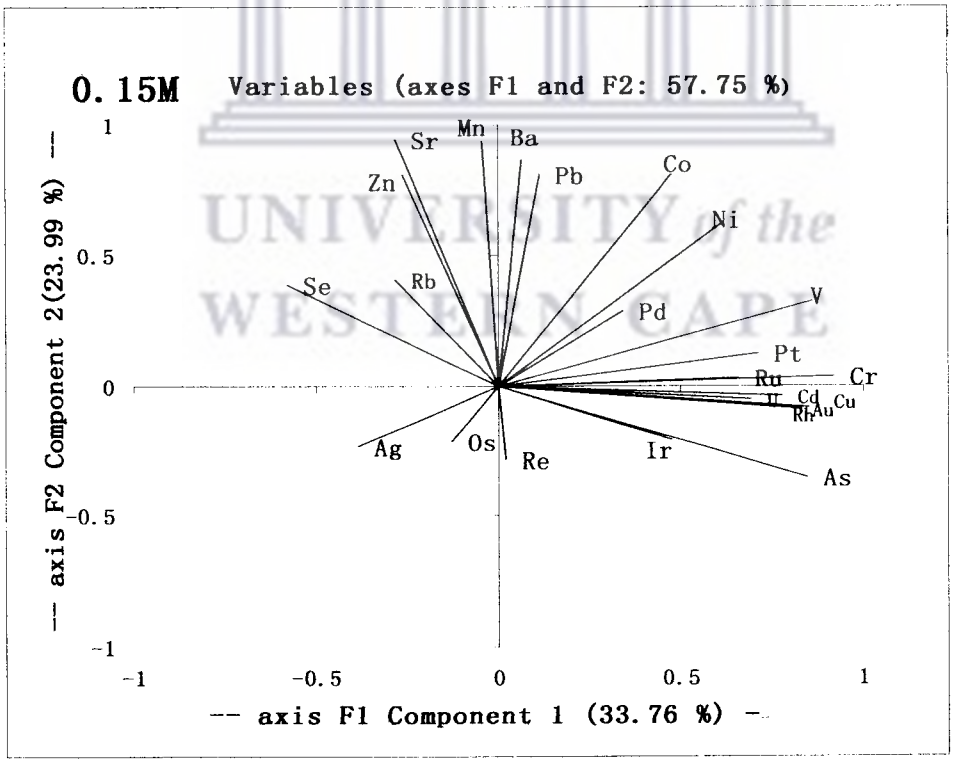

Fig.4.1.6 Principal component plot for element data in 0.15M hydroxylamine hydrochloride.

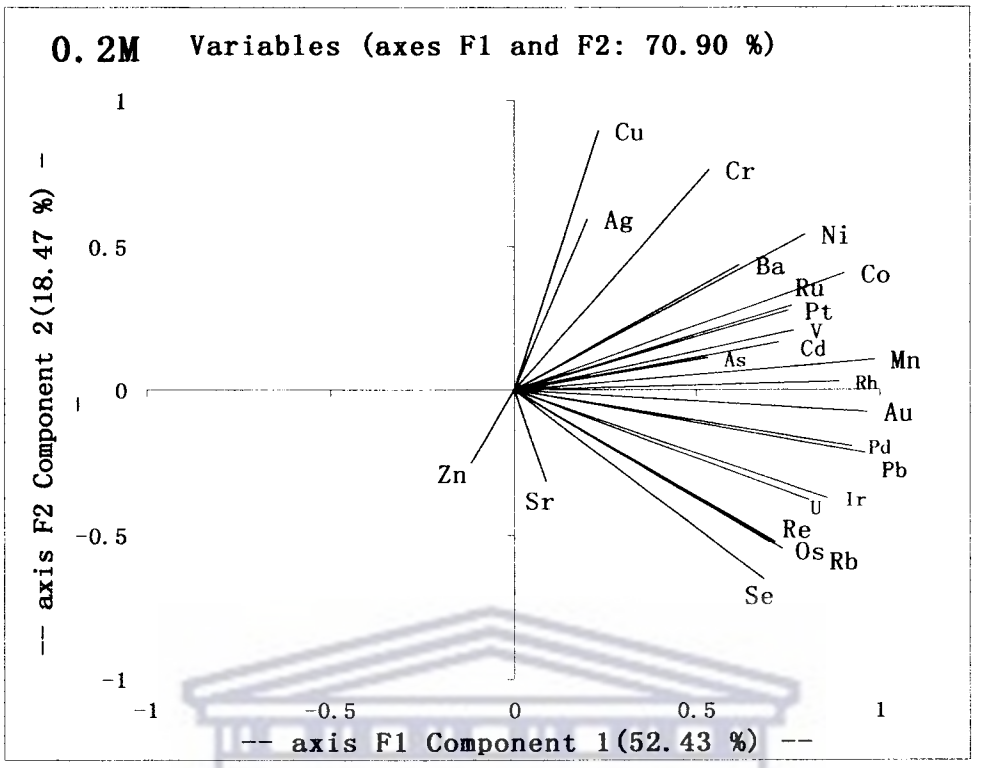

Fig. 4.1.7 Principal component plot for element data in 0.2M hydroxylamine hydrochloride.

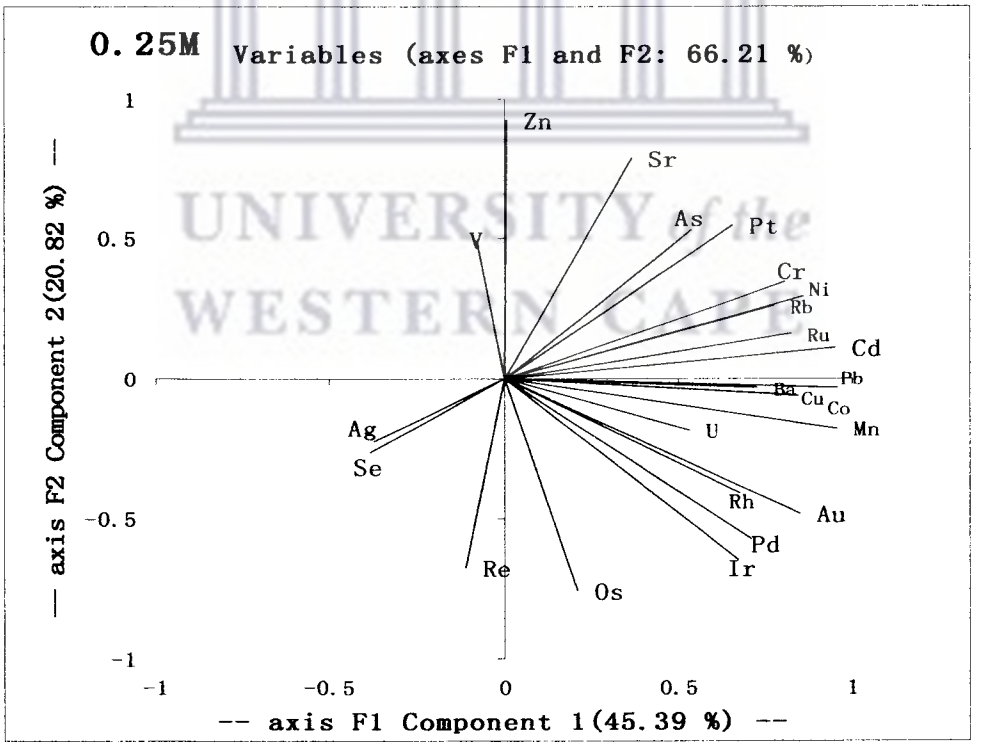

Fig. 4.1.8 Principal component plot for element data in 0.25M hydroxylamine hydrochloride.

0.1M	F1	F2	F3	F4	F5	F6
Eigen value	7.757	5.016	3.477	3.126	2.323	0.959
Variance %	32.321	20.901	14.488	13.024	9.679	3.995
Cumulative %	32.321	53.222	67.710	80.734	90.414	94.409
0.15M	F1	F2	F3	F4	F5	F6
Eigen value	8.102	5.758	3.275	2.442	1.956	1.064
Variance %	33.760	23.991	13.646	10.174	8.150	4.433
Cumulative %	33.760	57.752	71.398	81.572	89.721	94.154
0.2M	F1	F2	F3	F4	F5	F6
Eigen value	12.584	4.432	2.731	1.927	0.833	0.558
Variance	52.433	18.468	11.378	8.028	3.470	2.324
Cumulative %	52.433	70.901	82.279	90.307	93.777	96.100
0.25M	F1	F2	F3	F4	F5	F6
Eigen value	10.893	4.997	2.290	1.594	1.352	1.215
Variance %	45.389	20.820	9.540	6.641	5.634	5.061
Cumulative %	45.389	66.209	75.749	82.390	88.025	93.085

Table 4.1.5 Principal component analysis of Eigen value obtained from 0.1, 0.15, 0.2 and 0.25M hydroxylamine partial extraction results (data)

Noteworthy is the variable behavior of the PGE, which supports their variable migrating patterns in the secondary environment and adsorption pattern in Fe-Mn oxyhydroxides.

4.2 Regolith geochemical survey results

The results in the previous section 4.1 show that the element contrast can be enhanced by using the fine grain size fraction of aeolian sand for analysis. Based on these results 1g of fine grained size fraction of less than 75µm was used for a 0.1M and 0.25M hydroxylamine hydrochloride extraction of all the aeolian samples collected for this investigation. These were analyzed for 24 elements (see Appendix II). The resulting data are statistically summarized into tables and as box and whiskers plots in Fig. 4.2.1 and Table 4.2.

The data were further treated with principal component analysis (PCA) to identify groups of elements that behave similarly and also to determine possible changing

patterns of element association in regolith components. This could significantly contribute to understanding the distribution of elements related to the bedrock.

4.2.1 Element distribution and association patterns in regolith

Table 4.2.1 shows a statistical summary of analytical data of 40 samples which have been partially extracted by 0.1M and 0.25M hydroxylamine hydrochloride. All elements except the PGEs, Ag, U and Cd occur at levels greater than 1ppb. Higher value of V, Zn, Sr, Co, Pd, Cd occur in 0.25M hydroxylamine extraction while Mn, Cu, Pb, Ni, Au, Pt are significantly higher in 0.1M. A comparison of data from within the impact melt area to these of aeolian sand overlying granites to the east shows higher values for Mn, Cu, Pb, Au, Pt for the latter while V, Zn, Sr, Pd and Cd are more enriched in soils overlying the impact melt sheet. The PGE contents are slightly higher in the impact melt zone especially in the 0.1M hydroxylamine extract.

Data for aeolian sand overlying granites rocks outside the impact melt zone (Yang 2006) have been included in Table 4.2.1 for comparison. The patter of element correlation has been presented in Table 4.2.2 and 4.2.3. Significant positive correlative above 0.6 exist between Co-Mn, As-V, Os-Au, Ba-Sr and Ir-Os. Degrees of correlation between Fe-Mn, Cu-Zn are the strongest in 0.25M while correlative between Ni-As are strongest in 0.1M extraction. These corroborate the changing patterns of element correlative between 0.1 and 0.25M partial extraction.

Principal components were calculated from the correlation matrix (Table 4.2.2) in order to reduce the effect of interference on concentration range between the elements. R-mode principal components analysis was employed and the first 4 principal components account for 75% of the total variability of the data. Table 4.2.4 shows plots of the first 2 principal components that account for over 40% of data and these are presented for 0.1M and 0.25M partial extraction data (Fig. 4.2.1- 4.2.2).

Fig. 4.2.1 shows principal component plots for elements at 0.1M hydroxylamine hydrochlorides. There major clusters of elements starting from the quadrant IV in a clockwise fashion (Ru, Se, V, Ni, Cd, As, Zn, Pb, Cu, U, Pd and Ag), (Pt, Rh, Os, Ir, Re and Au) and (Cr, Fe, Sr, Ba, Co, Mn and Rb) are apparent. A changing pattern of element association is in the star plot of the principal components (Fig. 4.2.2) for data derived at 0.25M hydroxylamine hydrochloride can also be seen. Increased bundling of most elements into two clusters or associations occurs from the quadrant IV in a clockwise fashion (Se, V, Rb, As, Ru, Mn, Co, Sr, Ba, Fe and Ni) and (Pt, Au, Pd, Rh, Ir, Os, Ag, Pb, Zn, U and Cu).

4.2.2 Separation of background and anomaly

Box and whiskers plots of element content in regolith are presented in Fig. 4.2.3 and Fig. 4.2.4. These are particularly useful in visualizing the distribution pattern and populations variables. An estimate of background threshold and anomalous values were made using parameters inherent in various box and whiskers plots. For example, all outliners are classified as anomalous and threshold/anomaly boundary is fixed at the 75th percentile. Threshold lies between 50th and 75th percentile while values below 50th percentile are classified as background. The separation between background and anomaly using classical statistical treatment was not used, since this would have not allowed consideration of various populations inherent in the data. The background / anomaly estimates made from the box and whiskers plot was tabulated in Table 4.2.5.

4.2.3 Geochemical maps

Geochemical dot maps in Fig. 4.2.5 to 4.3.6 were prepared using SURFER8®and MapInfo7®. Dots of variable sizes are used to represent concentration ranges of elements which would be interpreted in this section in relation to possible bedrock types and mineralization.

Section									
	West								East
HH	0.1M				0.25M				0.1M
(ppb)	Minimum	Maximum	Mean	Median	Minimum	Maximum	Mean	Median	Median
Mn	209.44	2210.21	966.76	827.11	11.22	114.44	54.15	52.42	972.45
V	11.94	79.89	48.34	48.07	58.52	150.45	102.88	102.64	4.85
Cu	3.86	211.10	23.99	15.18	3.64	90.41	15.17	10.71	40.23
Zn	0.66	145.89	45.78	39.72	3.16	83.95	24.46	19.20	19.56
As	9.47	28.71	18.55	18.57	40.34	66.98	54.55	54.81	22.86
Sr	21.99	161.76	57.28	51.59	1.57	9.44	3.45	3.11	16.77
Ba	96.71	835.11	215.80	184.40	0.00	70.80	7.64	3.95	54.73
Pb	9.38	64.17	22.90	19.00	3.69	42.63	12.83	10.40	215.79
Os	0.00	234.94	21.84	3.76	0.00	252.96	20.57	2.72	29.40
Rb	4.93	25.77	12.95	12.38	0.60	10.27	3.98	4.43	13.01
Ni	0.00	23.32	10.04	10.70	0.00	16.76	7.51	8.42	20.85
Co	6.12	29.07	17.46	16.58	0.00	2.63	0.64	0.60	1.84
Se	0.00	20.39	9.21	9.23	0.00	31.86	10.86	6.82	18.33
Cr	0.00	53.98	3.97	0.00	0.00	241.84	13.84	4.46	0.90
Au	0.00	6.11	1.18	0.48	0.00	13.49	2.63	1.56	14.15
Pd	0.13	1.40	0.67	0.66	0.00	1.92	0.80	0.81	0.30
Cd	0.04	1.15	0.44	0.42	0.00	0.71	0.15	0.08	0.00
U	0.07	0.38	0.19	0.18	0.07	0.40	0.20	0.19	0.01
Pt	0.00	0.21	0.04	0.01	0.00	0.58	0.06	0.02	0.18
Ag	0.00	0.94	0.10	0.07	0.00	0.23	0.07	0.03	0.00
Ru	0.00	0.35	0.04	0.00	0.00	0.36	0.05	0.00	0.00
Ir	0.00	0.43	0.05	0.00	0.00	0.38	0.05	0.00	0.01
Rh	0.00	0.23	0.02	0.00	0.00	0.19	0.03	0.02	0.01
Re	0.00	0.21	0.02	0.00	0.00	0.17	0.03	0.02	0.00

Table 4.2.1 Statistical summary of analytical results (all values are in ppb).

	Mn	Ni	V	Cu	Zn	As	Sr	Ba	Os	Rb	Pb	Au	Co	Pd	Se	U	Pt	Ag	Cd	Re	Ru	Ir	Rh	Cr	Fe
Mn	1.00	0.14	-0.09	**-0.48**	-0.31	-0.26	0.30	**0.49**	-0.01	**0.56**	-0.22	0.05	**0.85**	-0.22	0.10	-0.18	-0.04	-0.22	0.23	0.04	-0.05	0.00	0.08	0.29	**0.48**
Ni	0.14	1.00	**0.59**	0.24	0.37	**0.67**	-0.04	0.03	-0.37	0.28	0.34	-0.18	0.09	-0.05	0.29	0.12	-0.12	0.19	0.36	-0.27	0.15	-0.35	-0.24	**0.42**	0.29
V	-0.09	**0.59**	1.00	0.17	0.28	**0.80**	-0.05	0.08	**-0.53**	0.01	0.28	**-0.40**	-0.27	-0.24	0.24	-0.17	-0.18	0.01	**0.42**	-0.27	0.30	**-0.50**	-0.28	-0.08	0.10
Cu	**-0.48**	0.24	0.17	1.00	0.31	**0.42**	-0.25	-0.28	0.02	-0.25	**0.49**	-0.08	**-0.49**	**0.48**	-0.05	**0.39**	0.01	**0.43**	0.13	-0.08	-0.18	-0.10	-0.06	-0.07	-0.37
Zn	-0.31	0.37	0.28	0.31	1.00	0.22	-0.08	-0.19	-0.17	-0.05	**0.42**	-0.15	-0.26	0.10	0.30	**0.56**	-0.01	**0.42**	0.33	-0.26	0.05	-0.19	0.14	-0.02	-0.02
As	-0.26	**0.67**	**0.80**	**0.42**	0.22	1.00	-0.26	-0.17	**-0.44**	-0.13	**0.41**	-0.30	**-0.42**	0.06	0.37	0.10	-0.22	-0.01	0.27	-0.33	**0.37**	**-0.43**	**-0.39**	0.10	0.01
Sr	0.30	-0.04	-0.05	-0.25	-0.08	-0.26	1.00	**0.69**	0.18	0.12	-0.32	0.23	**0.48**	-0.19	-0.11	-0.06	0.08	0.33	-0.17	0.22	-0.01	0.08	0.05	0.03	**0.41**
Ba	**0.49**	0.03	0.08	-0.28	-0.19	-0.17	**0.69**	1.00	0.07	0.03	-0.16	0.05	**0.53**	-0.04	-0.14	-0.19	-0.07	0.26	-0.01	-0.06	-0.12	0.06	-0.07	-0.02	**0.47**
Os	-0.01	-0.37	**-0.53**	0.02	-0.17	**-0.44**	0.18	0.07	1.00	-0.10	-0.14	**0.91**	0.23	**0.42**	-0.06	0.11	**0.48**	0.33	-0.31	**0.40**	-0.20	**0.95**	**0.57**	-0.05	-0.03
Rb	**0.56**	0.28	0.01	-0.25	-0.05	-0.13	0.12	0.03	-0.10	1.00	-0.30	0.02	**0.51**	**-0.39**	0.15	-0.21	-0.07	-0.31	**0.40**	-0.10	0.03	-0.05	-0.06	0.17	0.00
Pb	-0.22	0.34	0.28	**0.49**	**0.42**	**0.41**	-0.32	-0.16	-0.14	-0.30	1.00	-0.23	-0.25	**0.57**	-0.09	**0.53**	0.07	**0.45**	**0.51**	0.03	-0.08	-0.09	0.13	0.06	0.06
Au	0.05	-0.18	**-0.40**	-0.08	-0.15	-0.30	0.23	0.05	**0.91**	0.02	-0.23	1.00	0.30	0.31	0.07	0.06	**0.45**	0.26	-0.27	**0.39**	-0.01	**0.87**	**0.53**	0.17	0.09
Co	**0.85**	0.09	-0.27	**-0.49**	-0.26	**-0.42**	**0.48**	**0.53**	0.23	**0.51**	-0.25	0.30	1.00	-0.15	0.11	-0.18	0.04	-0.02	0.13	0.04	-0.16	0.24	0.19	0.23	**0.47**
Pd	-0.22	-0.05	-0.24	**0.48**	0.10	0.06	-0.19	-0.04	**0.42**	**-0.39**	**0.57**	0.31	-0.15	1.00	-0.18	**0.61**	0.24	**0.52**	0.11	0.25	-0.30	**0.37**	0.27	0.19	0.01
Se	0.10	0.29	0.24	-0.05	0.30	0.37	-0.11	-0.14	-0.06	0.15	-0.09	0.07	0.11	-0.18	1.00	-0.01	-0.18	-0.14	0.16	**-0.50**	**0.50**	-0.08	-0.10	-0.11	-0.17
U	-0.18	0.12	-0.17	**0.39**	**0.56**	0.10	-0.06	-0.19	0.11	-0.21	**0.53**	0.06	-0.18	**0.61**	-0.01	1.00	0.15	**0.39**	0.06	0.06	-0.15	0.08	0.23	0.21	0.16
Pt	-0.04	-0.12	-0.18	0.01	-0.01	-0.22	0.08	-0.07	**0.48**	-0.07	0.07	**0.45**	0.04	0.24	-0.18	0.15	1.00	0.35	-0.26	**0.46**	0.06	**0.50**	**0.64**	0.08	0.30
Ag	-0.22	0.19	0.01	**0.43**	**0.42**	-0.01	0.33	0.26	0.33	-0.31	**0.45**	0.26	-0.02	**0.52**	-0.14	**0.39**	0.35	1.00	0.17	0.22	-0.16	0.22	0.33	0.01	0.18
Cd	0.23	0.36	**0.42**	0.13	0.33	0.27	-0.17	-0.01	-0.31	**0.40**	**0.51**	-0.27	0.13	0.11	0.16	0.06	-0.26	0.17	1.00	-0.15	0.03	-0.24	0.04	-0.01	-0.02
Re	0.04	-0.27	-0.27	-0.08	-0.26	-0.33	0.22	-0.06	**0.40**	-0.10	0.03	**0.39**	0.04	0.25	**-0.50**	0.06	**0.46**	0.22	-0.15	1.00	0.11	**0.37**	**0.38**	0.24	0.20
Ru	-0.05	0.15	0.30	-0.18	0.05	**0.37**	-0.01	-0.12	-0.20	0.03	-0.08	-0.01	-0.16	-0.30	**0.50**	-0.15	0.06	-0.16	0.03	0.11	1.00	-0.15	-0.08	-0.02	0.02
Ir	0.00	-0.35	**-0.50**	-0.10	-0.19	**-0.43**	0.08	0.06	**0.95**	-0.05	-0.09	**0.87**	0.24	**0.37**	-0.08	0.08	**0.50**	0.22	-0.24	**0.37**	-0.15	1.00	**0.61**	-0.08	0.02
Rh	0.08	-0.24	-0.28	-0.06	0.14	**-0.39**	0.05	-0.07	**0.57**	-0.06	0.13	**0.53**	0.19	0.27	-0.10	0.23	**0.64**	0.33	0.04	**0.38**	-0.08	**0.61**	1.00	-0.09	0.19
Cr	0.29	**0.42**	-0.08	-0.07	-0.02	0.10	0.03	-0.02	-0.05	0.17	0.06	0.17	0.23	0.19	-0.11	0.21	0.08	0.01	-0.01	0.24	-0.02	-0.08	-0.09	1.00	**0.55**
Fe	**0.48**	0.29	0.10	-0.37	-0.02	0.01	**0.41**	**0.47**	-0.03	0.00	0.06	0.09	**0.47**	0.01	-0.17	0.16	0.30	0.18	-0.02	0.20	0.02	0.02	0.19	**0.55**	1.00

Table 4.2.2 Correlation matrix of 0.1M hydroxylamine hydrochloride *(In bold, significant values except diagonal) at the level of significance alpha=0.050 (two-tailed test).*

	Mn	Ni	V	Cu	Zn	As	Sr	Ba	Os	Rb	Pb	Au	Co	Pd	Se	U	Pt	Ag	Cd	Re	Ru	Ir	Rh	Cr	Fe
Mn	1.00	0.26	0.18	-0.14	0.03	-0.01	**0.57**	**0.63**	0.18	**0.59**	0.01	0.23	**0.81**	0.28	0.16	-0.11	0.07	0.02	-0.14	-0.12	0.07	0.17	0.15	-0.12	**0.66**
Ni	0.26	1.00	0.23	-0.03	0.04	**0.46**	0.00	0.24	0.17	-0.09	-0.24	0.25	**0.37**	0.32	-0.19	-0.08	0.33	**0.67**	0.00	0.18	**0.37**	0.17	0.11	-0.06	0.34
V	0.18	0.23	1.00	-0.06	-0.24	**0.69**	0.09	0.04	**-0.43**	0.29	-0.26	-0.10	0.23	**-0.38**	**0.40**	-0.23	0.12	-0.10	-0.28	**-0.51**	0.25	**-0.45**	-0.21	-0.07	0.05
Cu	-0.14	-0.03	-0.06	1.00	**0.79**	0.07	-0.17	0.00	0.03	-0.11	0.08	-0.02	0.02	0.05	-0.18	0.01	0.34	-0.03	0.03	**0.38**	-0.04	0.02	-0.20	-0.08	-0.09
Zn	0.03	0.04	-0.24	**0.79**	1.00	-0.14	0.12	0.32	0.11	-0.06	0.27	-0.08	0.26	0.12	**-0.42**	0.00	**0.44**	0.00	0.27	**0.50**	-0.12	0.06	0.00	-0.12	0.07
As	-0.01	**0.46**	**0.69**	0.07	-0.14	1.00	-0.08	0.03	-0.02	-0.20	-0.27	0.33	0.10	0.13	0.14	0.13	**0.46**	0.24	-0.11	-0.17	0.26	-0.06	-0.07	-0.02	0.19
Sr	**0.57**	0.00	0.09	-0.17	0.12	-0.08	1.00	**0.83**	0.17	**0.38**	**0.44**	0.15	**0.69**	0.28	-0.16	0.00	0.29	-0.05	0.16	-0.05	-0.15	0.12	0.13	0.01	**0.63**
Ba	**0.63**	0.24	0.04	0.00	0.32	0.03	**0.83**	1.00	0.21	0.19	0.24	0.22	**0.76**	**0.46**	-0.23	0.17	**0.44**	0.09	0.14	0.14	0.00	0.16	0.19	-0.02	**0.71**
Os	0.18	0.17	**-0.43**	0.03	0.11	-0.02	0.17	0.21	1.00	-0.05	0.33	**0.88**	0.17	**0.81**	-0.29	0.26	0.23	**0.47**	**0.38**	**0.37**	-0.08	**0.98**	**0.56**	-0.08	**0.55**
Rb	**0.59**	-0.09	0.29	-0.11	-0.06	-0.20	**0.38**	0.19	-0.05	1.00	0.15	-0.12	**0.55**	-0.25	0.24	-0.28	-0.24	-0.24	-0.11	-0.20	-0.23	-0.06	0.11	-0.09	0.29
Pb	0.01	-0.24	-0.26	0.08	0.27	-0.27	**0.44**	0.24	0.33	0.15	1.00	0.11	0.23	0.24	-0.32	0.13	0.10	0.20	**0.83**	**0.38**	-0.14	0.24	**0.37**	-0.10	0.10
Au	0.23	0.25	-0.10	-0.02	-0.08	0.33	0.15	0.22	**0.88**	-0.12	0.11	1.00	0.17	**0.83**	-0.04	0.31	0.30	**0.45**	0.16	0.09	0.08	**0.87**	**0.44**	-0.14	**0.57**
Co	**0.81**	**0.37**	0.23	0.02	0.26	0.10	**0.69**	**0.76**	0.17	**0.55**	0.23	0.17	1.00	0.27	-0.04	-0.05	0.36	0.16	0.12	0.12	0.01	0.11	0.25	0.00	**0.71**
Pd	0.28	0.32	**-0.38**	0.05	0.12	0.13	0.28	**0.46**	**0.81**	-0.25	0.24	**0.83**	0.27	1.00	-0.30	**0.46**	0.33	**0.49**	0.29	0.34	0.10	**0.79**	**0.43**	-0.19	**0.59**
Se	0.16	-0.19	**0.40**	-0.18	**-0.42**	0.14	-0.16	-0.23	-0.29	0.24	-0.32	-0.04	-0.04	-0.30	1.00	-0.07	-0.27	-0.31	**-0.49**	**-0.43**	0.28	-0.27	-0.21	-0.16	-0.16
U	-0.11	-0.08	-0.23	0.01	0.00	0.13	0.00	0.17	0.26	-0.28	0.13	0.31	-0.05	**0.46**	-0.07	1.00	0.14	0.09	0.22	0.24	0.00	0.21	0.24	0.04	0.08
Pt	0.07	0.33	0.12	0.34	**0.44**	**0.46**	0.29	**0.44**	0.23	-0.24	0.10	0.30	0.36	0.33	-0.27	0.14	1.00	0.24	0.14	0.34	0.22	0.11	0.22	0.18	0.36
Ag	0.02	**0.67**	-0.10	-0.03	0.00	0.24	-0.05	0.09	**0.47**	-0.24	0.20	**0.45**	0.16	**0.49**	-0.31	0.09	0.24	1.00	**0.50**	**0.48**	0.28	**0.41**	**0.46**	-0.16	0.19
Cd	-0.14	0.00	-0.28	0.03	0.27	-0.11	0.16	0.14	**0.38**	-0.11	**0.83**	0.16	0.12	0.29	**-0.49**	0.22	0.14	**0.50**	1.00	**0.57**	-0.04	0.27	**0.53**	-0.12	0.07
Re	-0.12	0.18	**-0.51**	**0.38**	**0.50**	-0.17	-0.05	0.14	**0.37**	-0.20	**0.38**	0.09	0.12	0.34	**-0.43**	0.24	0.34	**0.48**	**0.57**	1.00	-0.10	0.29	**0.43**	-0.08	0.11
Ru	0.07	**0.37**	0.25	-0.04	-0.12	0.26	-0.15	0.00	-0.08	-0.23	-0.14	0.08	0.01	0.10	0.28	0.00	0.22	0.28	-0.04	-0.10	1.00	-0.12	0.10	-0.06	-0.05
Ir	0.17	0.17	**-0.45**	0.02	0.06	-0.06	0.12	0.16	**0.98**	-0.06	0.24	**0.87**	0.11	**0.79**	-0.27	0.21	0.11	**0.41**	0.27	0.29	-0.12	1.00	**0.46**	-0.07	**0.53**
Rh	0.15	0.11	-0.21	-0.20	0.00	-0.07	0.13	0.19	**0.56**	0.11	**0.37**	**0.44**	0.25	**0.43**	-0.21	0.24	0.22	**0.46**	**0.53**	**0.43**	0.10	**0.46**	1.00	-0.21	**0.40**
Cr	-0.12	-0.06	-0.07	-0.08	-0.12	-0.02	0.01	-0.02	-0.08	-0.09	-0.10	-0.14	0.00	-0.19	-0.16	0.04	0.18	-0.16	-0.12	-0.08	-0.06	-0.07	-0.21	1.00	-0.05
Fe	**0.66**	0.34	0.05	-0.09	0.07	0.19	**0.63**	**0.71**	**0.55**	0.29	0.10	**0.57**	**0.71**	**0.59**	-0.16	0.08	0.36	0.19	0.07	0.11	-0.05	**0.53**	**0.40**	-0.05	1.00

Table 4.2.3 Correlation matrix of 0.25M hydroxylamine hydrochloride *(In bold, significant values except diagonal) at the level of significance alpha=0.050 (two-tailed test).*

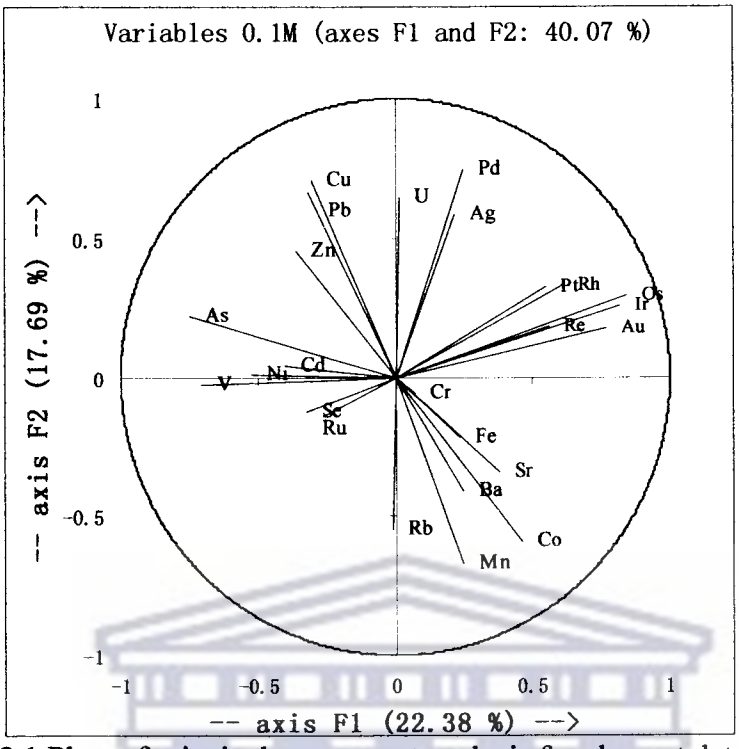

Fig. 4.2.1 Plots of principal component analysis for element data for 0.1M hydroxylamine hydrochloride extraction

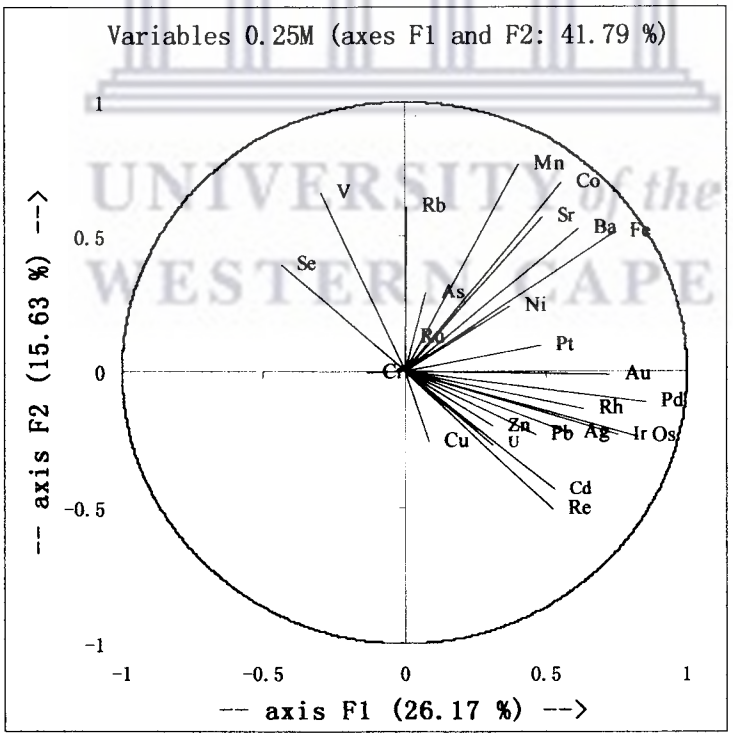

Fig. 4.2.2 Plots of principal component analysis for element data for 0.25M hydroxylamine hydrochloride extraction

		F1	F2	F3	F4	F5	F6
0.1M	Eigen value	5.595	4.423	3.217	1.995	1.730	1.617
	Variance %	22.381	17.693	12.867	7.982	6.919	6.466
	Cumulative %	22.381	40.075	52.942	60.923	67.842	74.308
0.25M	Eigen value	6.542	3.907	2.980	2.508	1.716	1.405
	Variance %	26.167	15.626	11.919	10.032	6.863	5.619
	Cumulative %	26.167	41.794	53.713	63.745	70.609	76.228

Table 4.2.4 Eigen values for first 6 principal components in element data (0.1M and 0.25M hot hydroxylamine hydrochloride)

The geochemical maps were overlain on the top of geophysical maps which have been provided. The investigated area has been classified into various zones based on the geophysical signatures as follows: 1.) R1 to R3 are magnetic highs in the western parts of the project area (also termed as zone A). This zone interspersed by streaks of magnetic fabrics and intensely faulted. 2.) Zone B still site within melt sheet around the (trend) magnetic rings to the east. 3.) Zone C is the boundary of the melt sheet and the surrounding basement rocks which shows low magnetization to the north.

Geochemical maps were constructed and overlain on to geophysical maps (Fig. 4.2.5 to 4.3.5). These maps will be discussed in the light of the descriptive and multivariate statistical results. The objective is to infer a possible relationship between element chemistry and underlying bedrock.

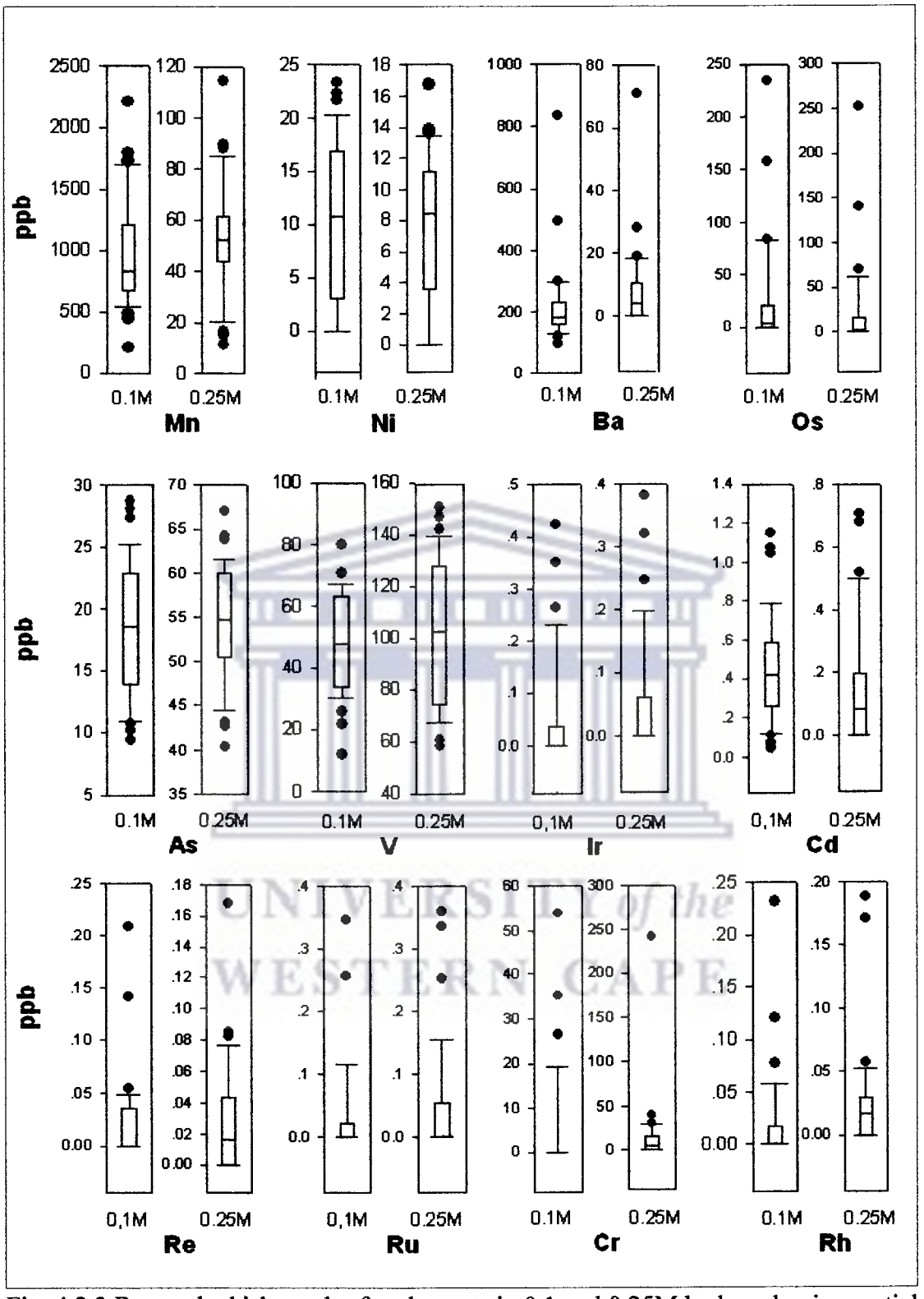

Fig. 4.2.3 Box and whiskers plot for elements in 0.1 and 0.25M hydroxylamine partial extraction.

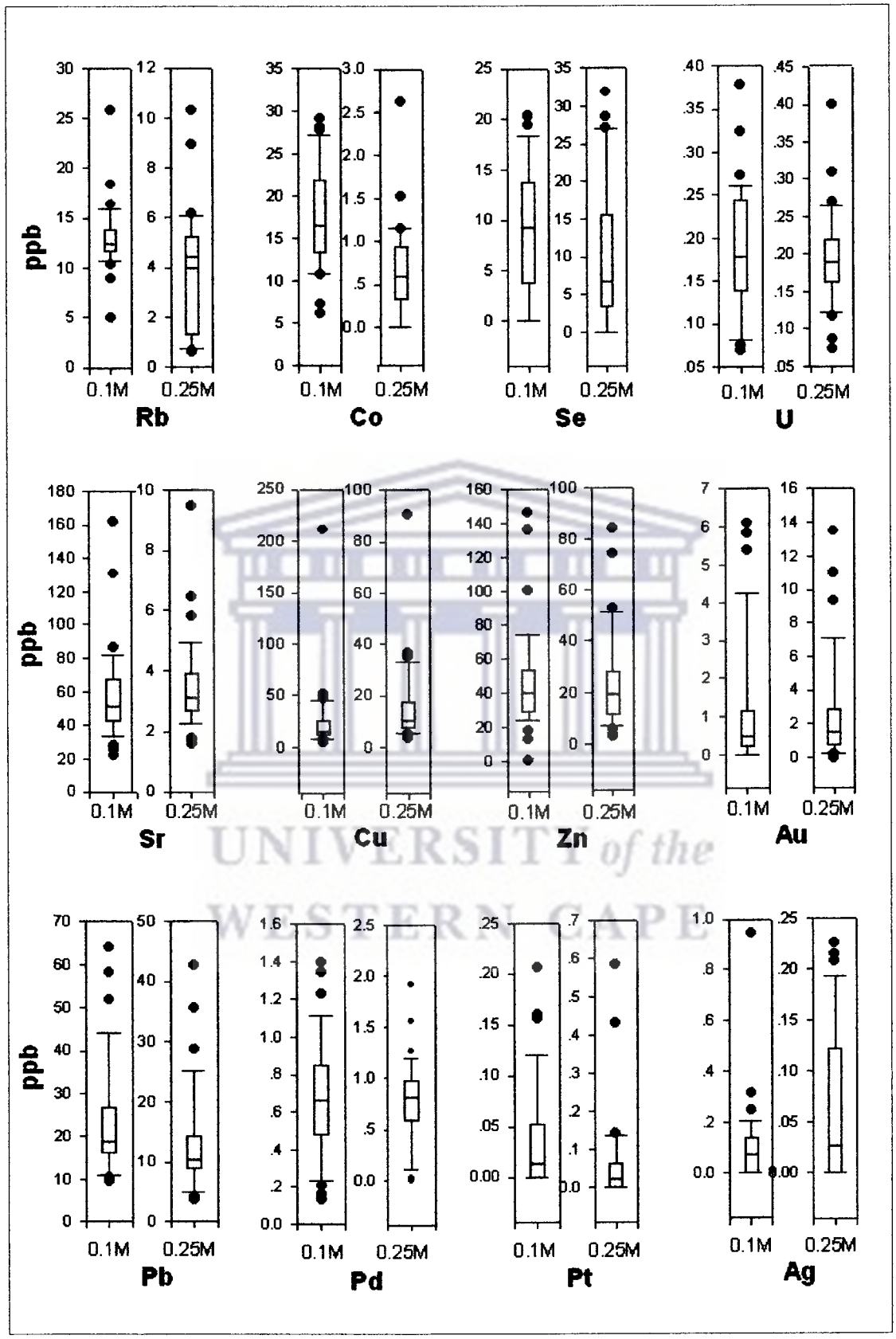

Fig. 4.2.4 Box and whiskers plot for elements in 0.1 and 0.25M hydroxylamine partial extraction.

	0.1M			0.25M		
Element	Background	Threshold	Anomaly	Background	Threshold	Anomaly
Mn	0-650	1300	>1300	0-55	60	>60
Ni	0-11	17	>25	0-8.5	11.4	>11.4
Ba	0-119.5	210	>210	0-5.5	10	>10
Os	0-10	25	>25	0-8.5	11	>11
As	0-19	22.5	>22.5	35-55	60	>60
V	0-48	62	>62	40-102	128	>128
Ir	0.0-0.04	0.23	>0.23	0.0-0.07	0.2	>0.2
Cd	0.0-0.41	0.6	>0.6	0.0-0.15	0.2	>0.2
Re	0.00-0.04	0.05	>0.05	0.00-0.02	0.04	>0.04
Ru	0.0-0.03	0.12	>0.12	0.0-0.06	0.17	>0.17
Cr	0.00	20	>20	0-11	20	>20
Rh	0-0.02	0.06	>0.06	0.00-0.03	0.04	>0.04
Rb	0-13	14	>14	0-4.3	5.8	>5.8
Co	0-16	21	>21	0-0.6	1.0	>1.0
Se	0-8	14	>14	0-7	15	>15
U	0.05-0.17	0.24	>0.24	0.05-0.18	0.22	>0.22
Sr	0-50	70	>70	0-3.1	4	>4
Cu	0-20	30	>30	0-15	19	>19
Zn	0-40	58	>58	0-20	28	>28
Au	0.0-0.5	1.2	>1.2	0.0-1.8	2.3	>2.3
Pb	0-19	28	>28	0-11	15	>15
Pd	0.0-0.7	0.82	>0.82	0.0-0.7	1.0	>1.0
Pt	0.00-0.02	0.05	>0.05	0.0-0.03	0.08	>0.08
Ag	0.00-0.14	0.18	>0.18	0.00-0.3	0.13	>0.13

Table 4.2.5 Estimated background-anomalous values of the various elements (all values are in ppb)

Manganese

Manganese contents vary from 20-2500ppb. Manganese values in 0.1M partial extraction are higher than those of 0.25M and these have a mean of 700 and 45ppb and an estimated background anomaly value of 1300ppb and 69ppb respectively (Table 4.2.1 and Fig. 4.2.3). Manganese oxyhydroxides may be host for several of the elements considered in this study and a higher extractability and release of associated trace elements are expected at 0.1M hydroxylamine concentration.

Distribution pattern of manganese in 0.1M and 0.25M geochemical maps are similar.

Elevated Mn contents above 1300ppb (0.1M) and 60ppb (0.25M) occur in the south eastern parts of the project are and towards the north in 0.1M Mn partial extraction. Manganese in 0.25M extraction appears to show an almost extensive band of NNE trending elevated values.

The box and whiskers plot shows three outliers of manganese values of 650ppb, 1300ppb, 2500ppb which are located in Zone A and Zone C in the SE and N of the project area. These areas are coincident with the occurrence of highly magnetic anomalies or trends. Manganese distributions are similar to those of Ba, Sr and Rh though some of the elevated values may not coincide with each other (Fig. 4.2.5).

Barium

Barium levels are high in soils formed from limestone, feldspars and granites. Barium in soils would not be expected to be very mobile because of the formation of water insoluble salts and its inability to form soluble complexes with humic and fulvic materials.

Barium contents the samples studied vary from 96-835ppb. Barium contents in 0.1M partial extraction are higher than those of 0.25M. A possible release of Ba from Mn oxides may be inferred from results of correlation analysis (r=+0.85 for Mn-Ba) and the clustering in principal component plots (Table 4.2.1 and Fig. 4.2.6).
Distribution pattern of barium in 0.1M and 0.25m geochemical maps (Fig. 4.2.6) are almost identical. To the north where elevated values above 210ppb (0.1M) and 10ppb (0.25M) occur distribution pattern of anomalous values differ slightly towards the south. The overall pattern of Ba distribution in 0.25M hydroxylamine bears a closer resemblance to those of 0.1M Mn partial extraction.

The box and whiskers plot shows three outliers of barium values at (120ppb, 210ppb and 1000ppb) at 0.1M concentration which occur in the north (Zone A). In the 0.25M hydroxylamine concentration, the anomalous values also occur in the north (Zone A) and it shows an almost extensive band of NE-SW trending elevated values (Zone B). These areas are coincident with the occurrence of highly magnetic anomalies or trends (Fig. 4.2.6).

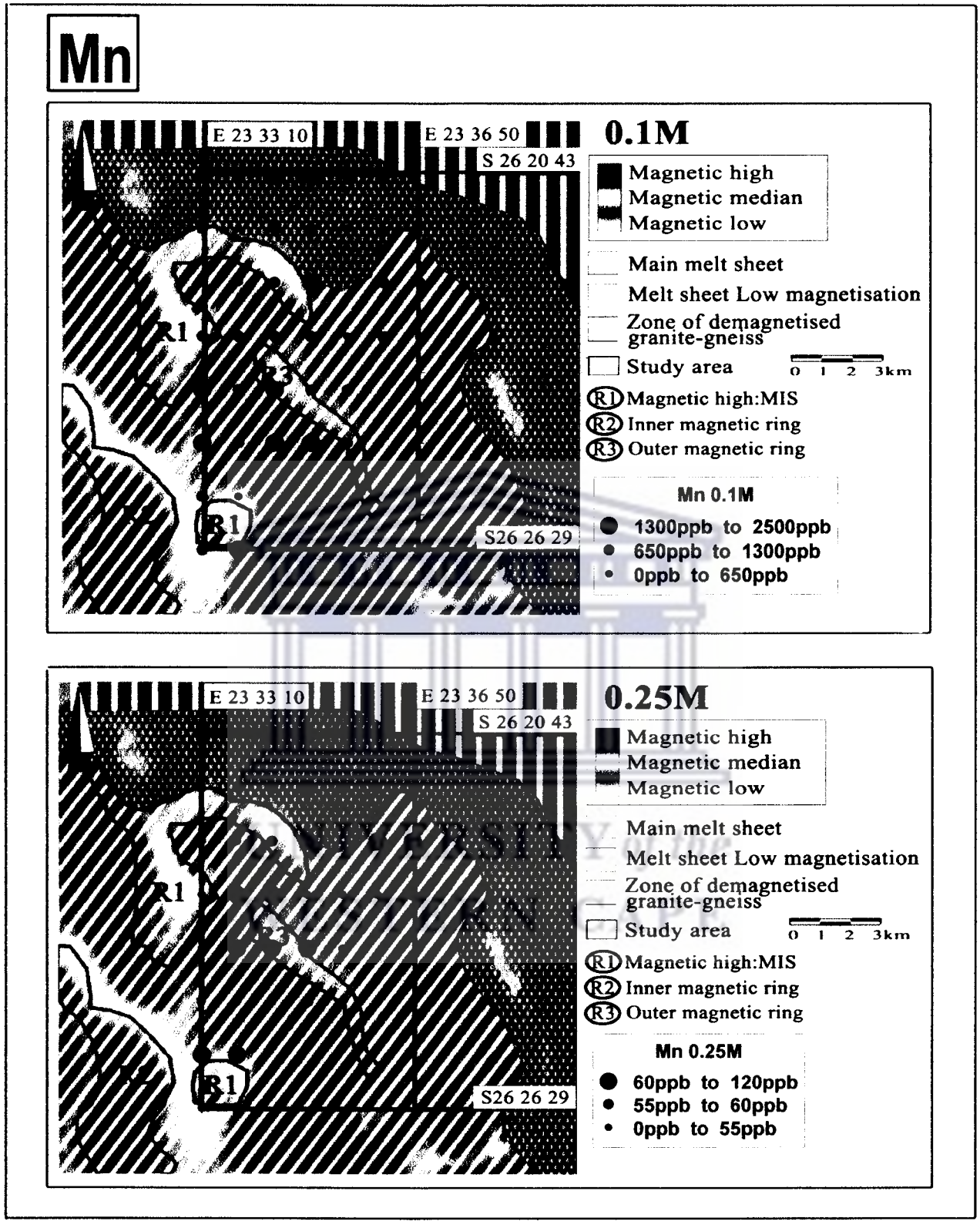

Fig. 4.2.5 Geochemical map of Mn (0.1M, 0.25M hydroxylamine concentration)

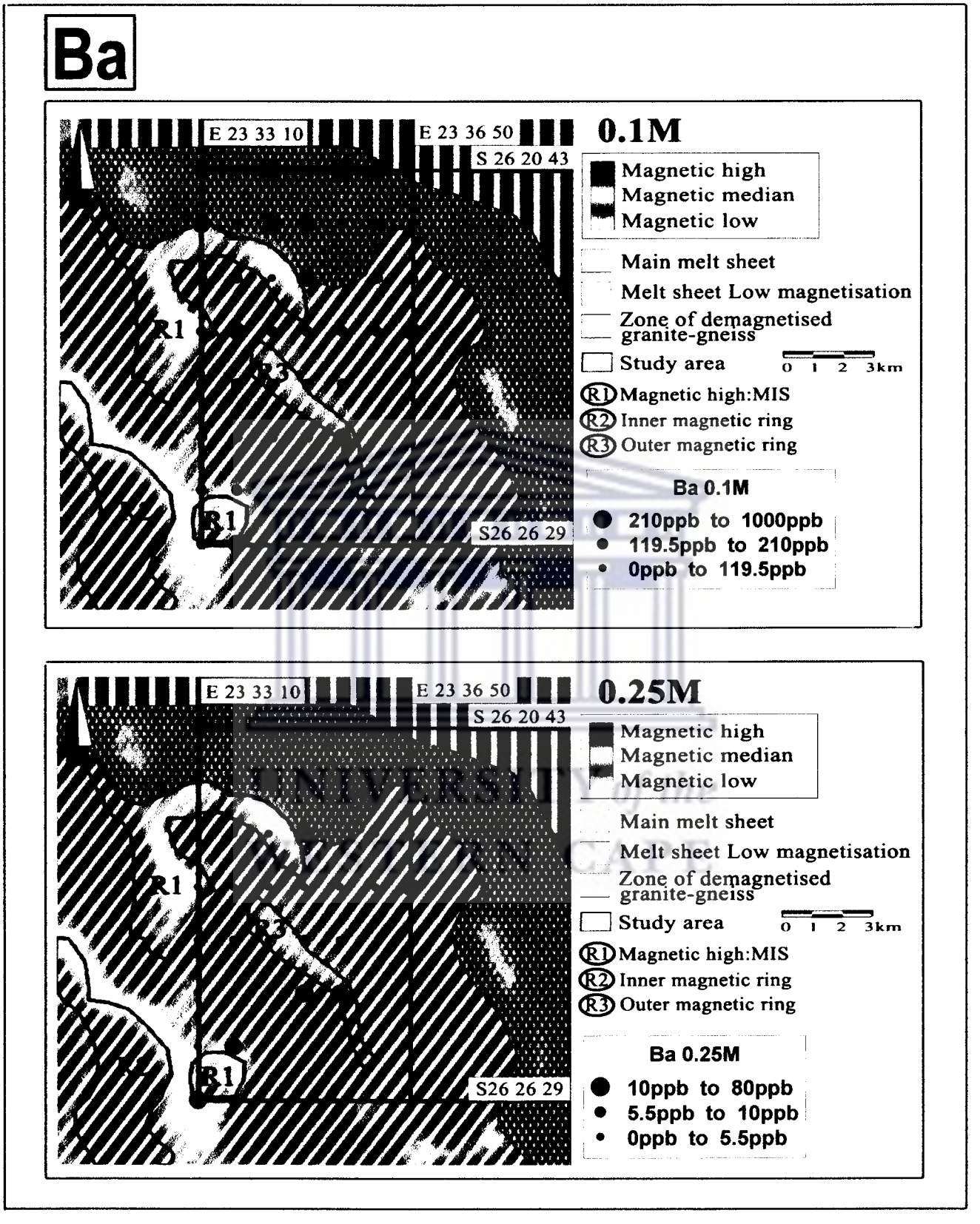

Fig. 4.2.6 Geochemical map of Ba (0.1M, 0.25M hydroxylamine concentration).

Copper

Copper often occurs in association with many sulphide ore deposits. Its contents vary from 3.6-211.1ppb. Copper contents in 0.1M partial extraction are higher than 0.25M and these have an average values of 24ppb and 15.17ppb and estimated background anomaly values at 20ppb and 30ppb respectively.

Distribution patterns of copper in the 0.1m and 0.25M partial leach are similar. Elevated Cu values above 30ppb (0.1M) and 19ppb (0.25M) occur from south to southeast. Patterns of distribution of anomalous Cu values differ slightly towards north.

The box and whiskers plot shows three outliers copper values of 20ppb, 30ppb, and 250ppb (0.1M) occur in the south and north (Zone A and Zone B). Patterns of Cu distribution in the south (Zone B) give the pronounced values in 0.1M and 0.25M extraction (Fig. 4.2.7).

Nickel

High Ni contents would typically reflect the occurrence of ultramafic rocks. Nickel is basically scavenged by Fe-Mn oxyhydroxides in the weathering environment. Amorphous Fe-Mn oxides are abundant in aeolian sand. Ni contents of up to 0.74% have been reported in the ores associated with the impact melt rock of the MIS. Unmineralized rocks show Ni contents of about 500ppm (McDonald et al., 2001).

Nickel content partial extractions vary from 7-23ppb. Nickel correlation in 0.1M partial extraction are higher than those of 0.25M and these have average contents of 10ppb and 8ppb and an estimated background anomaly values at 17ppb and 11.4ppb respectively (Table 4.2.1 and Fig. 4.2.3).

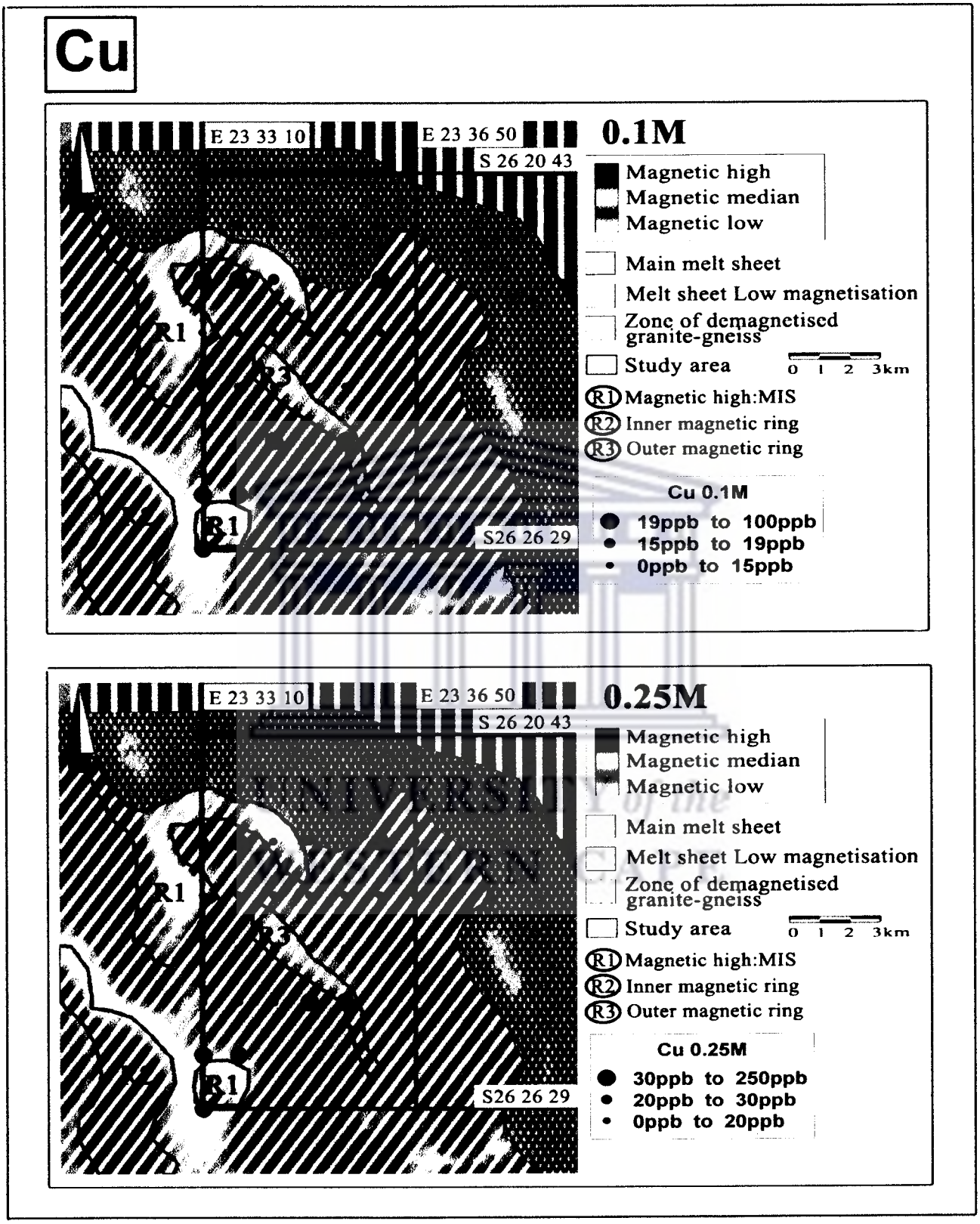

Fig. 4.2.7 Geochemical map of Cu (0.1M, 0.25M hydroxylamine concentration)

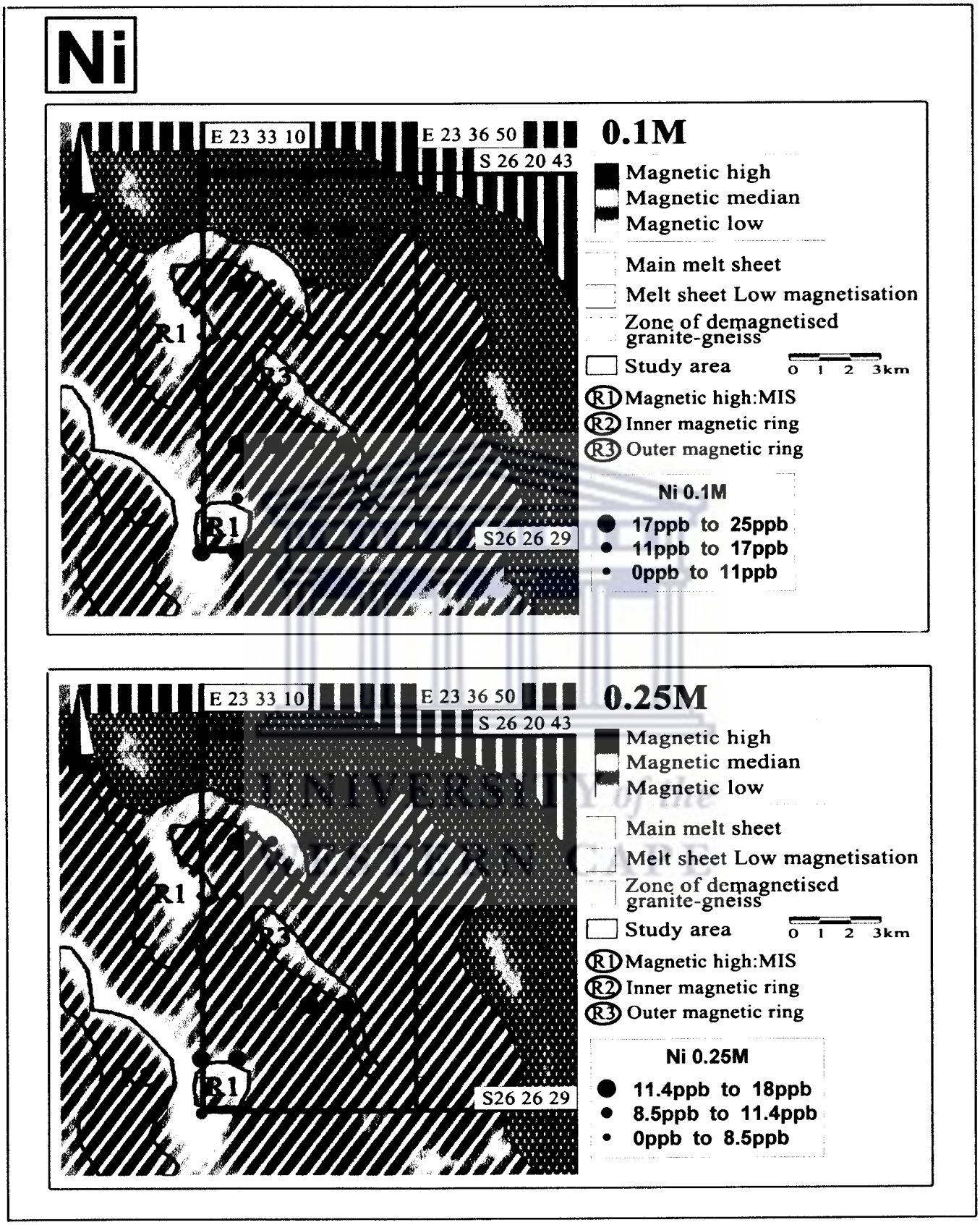

Fig. 4.2.8 Geochemical map of Ni (0.1M, 0.25M hydroxylamine concentration)

Distribution patterns of nickel in 0.1M and 0.25M geochemical maps are almost identical. Elevated Ni values above 17ppb (0.1M) and 11.4ppb (0.25M) occur in the northern parts of the project area and towards to the south in the 0.1M and 0.25M partial extraction. These areas are located in a zone of melt sheet with a low magnetization and main melt sheet intensives respectively.

The box and whiskers plots show three outliers in the nickel values (11ppb, 17ppb and 25ppb) of 0.1M which occurs in the north (Zone A) and in the south (Zone B). In 0.25M, it gives the similar element distribution as 0.1M (Fig.4.2.8).

Arsenic

Arsenic contents vary from 10-67ppb. Arsenic value in 0.1M partial extraction are lower than those of 0.25M and these have average values of 19 and 55ppb and an estimated background anomaly values at 23ppb and 60ppb respectively (Table 4.2.1 and Fig. 4.2.3).

Distribution pattern of arsenic in 0.1M and 0.25M geochemical maps are similar. Elevated values above 22.5ppb (0.1M) and 60ppb (0.25M) occur in the southern part of the project area which is located in zone of melt sheet of low magnetization area and main melt sheet intensives respectively.

The box and whiskers plots show three outliers arsenic values of 55ppb, 60ppb, 70ppb (0.25M) which occurs in the south (Zone B) and on the boundary of (Zone A and B) (Fig. 4.2.9).

Gold

Gold is generally associated with PGM ore deposits types. For instance there is up to 10x (over 100ppb) enrichment of Au in sulphides associated with Morokweng impact melt rocks. Au contents of up to 0.13% have been reported in the ores associated with the impact melt rock of the MIS. Unmineralized rocks show Au contents of about 12ppb (McDonald et al., 2001).

Gold contents in aeolian sand vary from 1.2-16ppb. Gold contents in 0.1M partial extraction are lower than 0.25M and these have average values of 1.2 and 2.7ppb and estimated background anomaly values of 1.8ppb and 2.3ppb respectively.

Distribution pattern of gold in 0.1M and 0.25M in the geochemical maps are almost identical. Elevated Au values above 1.2ppb (0.1M) and 2.3ppb (0.25M) occur towards the north and eastern parts of the study area. Pattern of distribution of anomalous Au values differ slightly towards the south.

The box and whiskers plot shows three outliers gold values of 1.8ppb, 2.3ppb, 16ppb (0.25M) which occur in the north and east (boundary of Zone A and Zone B). Patterns of Au distribution in 0.25M are similar to arsenic (0.25M) though elevated values may not coincide with each other. These areas are coincident with occurrence of highly magnetic anomalies or trends (Fig. 4.3.1).

Iridium

Impact melt rocks in the MIS have Ir contents of up to 31ppb in unmineralized rocks. Ir contents of up to 0.02% have been reported in the ores associated with the impact melt rock of the MIS (McDonald et al., 2001).

Iridium contents in soil vary from 0.1-0.5ppb. Iridium contents in 0.1M partial extraction are higher than 0.25M and these have average values of 0.5ppb for both 0.1M and 0.25M partial extraction and an estimated background anomaly values at 0.23ppb and 0.2ppb respectively.

Distribution pattern of iridium in both geochemical maps are similar. Elevated values above 0.23ppb (0.1M) and 0.2ppb (0.25M) occur in the southern parts of the project area.

The box and whiskers plot shows three outliers iridium values of 0.07ppb, 0.23ppb, 0.5ppb (0.1M) occur in the south (Zone B). Distributions of elevated values in 0.25M are similar to 0.1M of iridium (Fig. 4.3.2).

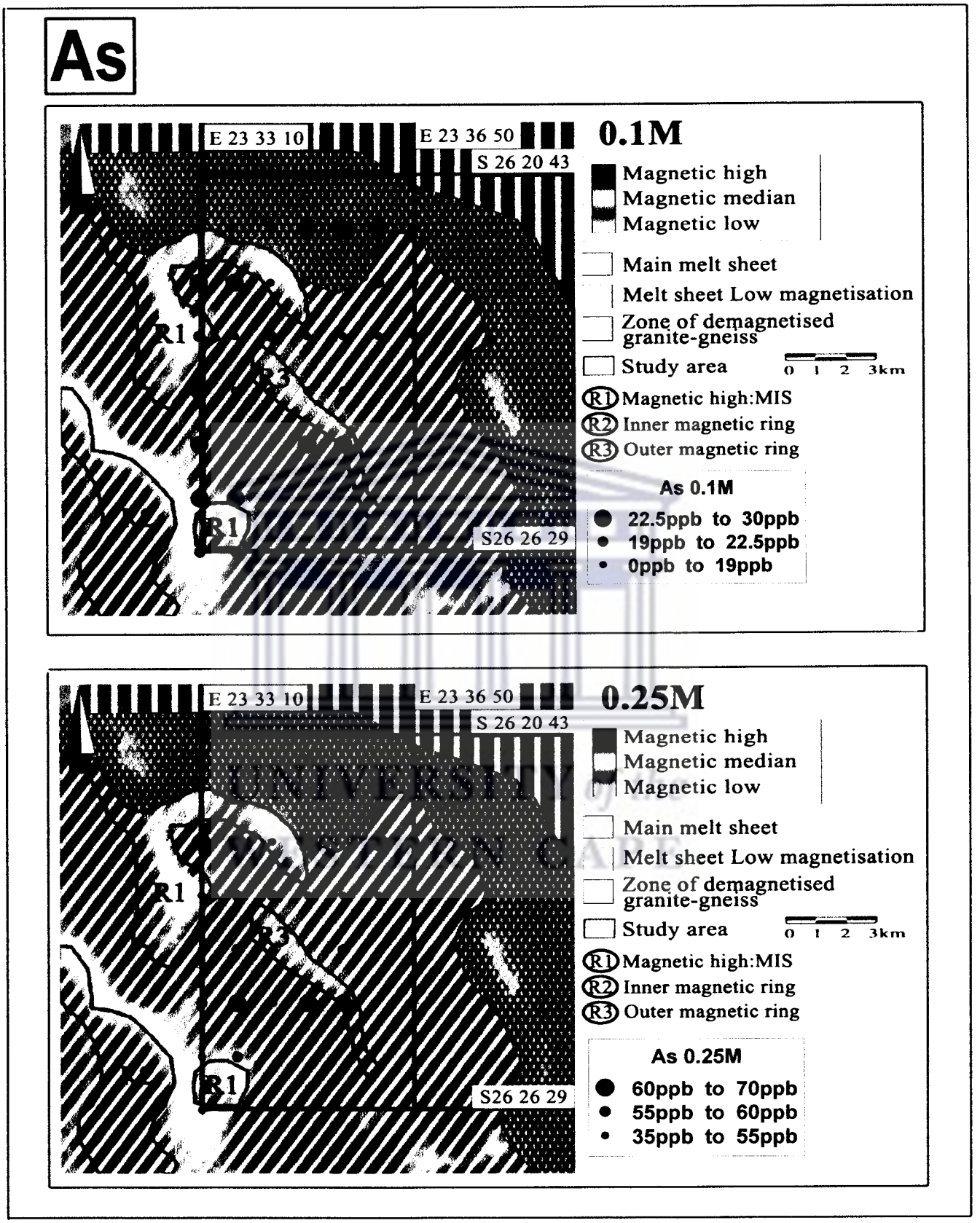

Fig. 4.2.9 Geochemical map of As (0.1M, 0.25M hydroxylamine concentration)

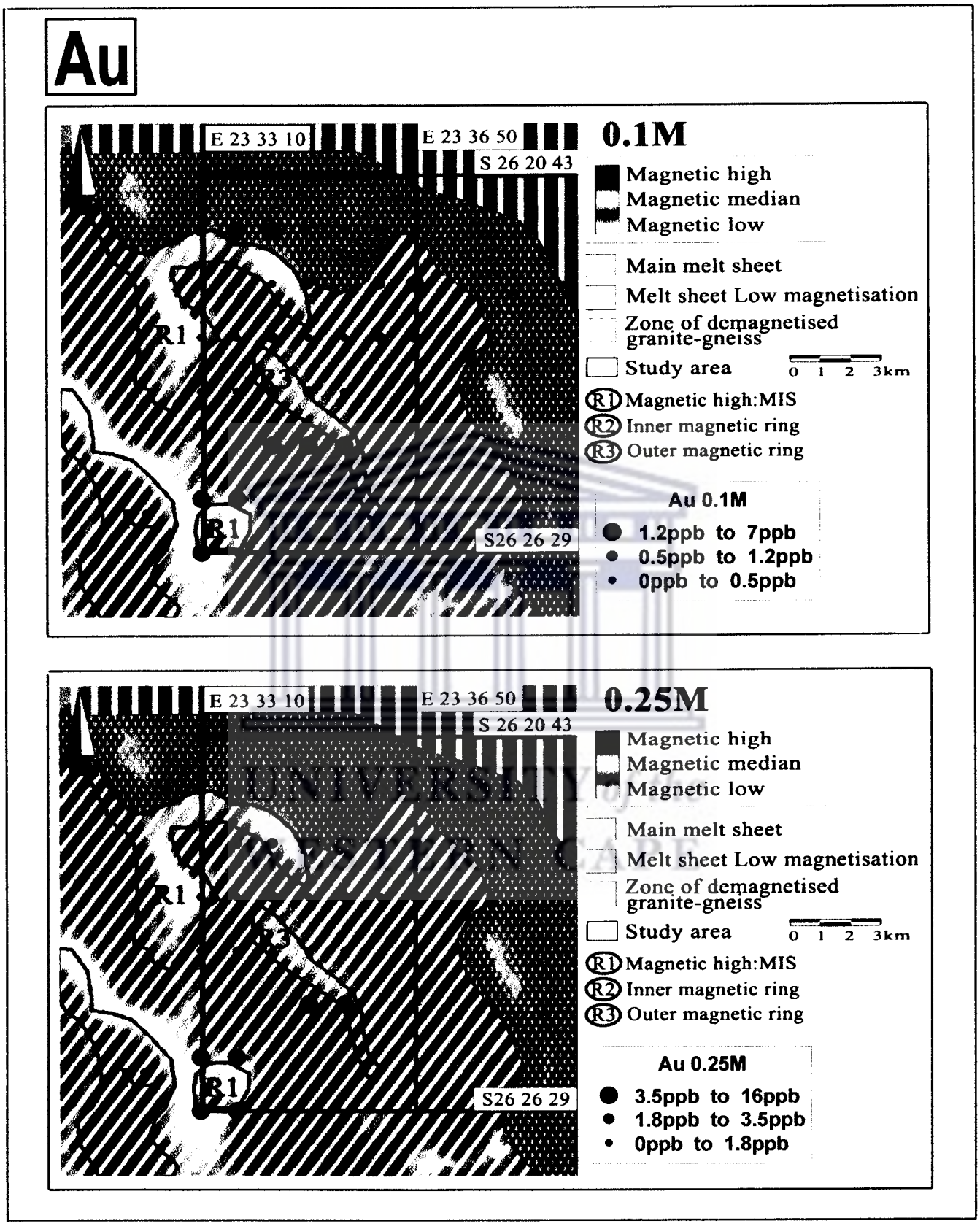

Fig. 4.3.1 Geochemical map of Au (0.1M, 0.25M hydroxylamine concentration)

Palladium

Palladium in the MIS is mobile in the secondary environment and is commonly scavenged by Fe-Mn oxyhydroxides. Pd contents of up to 0.04% have been reported in the ores associated with the impact melt rock of the MIS. Unmineralized rocks show Pd contents of about 57ppb (McDonald et al., 2000). Palladium contents by partial extraction vary from 0.1-2.5ppb and its contents in 0.1M partial extraction are lower than that of 0.25M concentration. These have average values of 0.67 and 0.81ppb for both 0.1M and 0.25M partial extraction with an estimated background anomaly values at 0.67ppb and 1ppb respectively. Distribution pattern of palladium in 0.1M and 0.25M geochemical maps are dissimilar. Elevated values above 0.67ppb (0.1M) and 1ppb (0.25M) occur in the northern part.

The box and whiskers plots show three outliers palladium values of 0.6ppb, 1ppb, 2.5ppb (0.25M) occur in the north (boundary of Zone A and Zone B) These areas are coincident with the occurrence of high magnetic anomalies or trends. Palladium distributions in 0.1M occur in the northwestern part (Zone A) and south (Zone B). Palladium distribution is similar to those of Ru, Re, Rh though some of the elevated values may not coincide with each other (Fig. 4.3.3).

Platinum

PGE mobility in the secondary environment is hampered by their low concentration in geomaterials. Pt contents of up to 0.05% have been reported in the ores associated with the impact melt rock of the MIS. Unmineralized rocks show Pt contents of about 73ppb (McDonald et al., 2001).

Platinum contents vary from 0.21-0.7ppb. Platinum in 0.1M partial extraction are lower than 0.25M and these have average values of 0.04 and 0.06ppb and an estimated background anomaly values at 0.05ppb and 0.08ppb respectively.

Distribution pattern of platinum in 0.1M and 0.25M geochemical maps are not similar. Elevated values above 0.05ppb (0.1M) and 0.08ppb (0.25M) occur in the northern parts of the project area (Fig. 4.3.4).

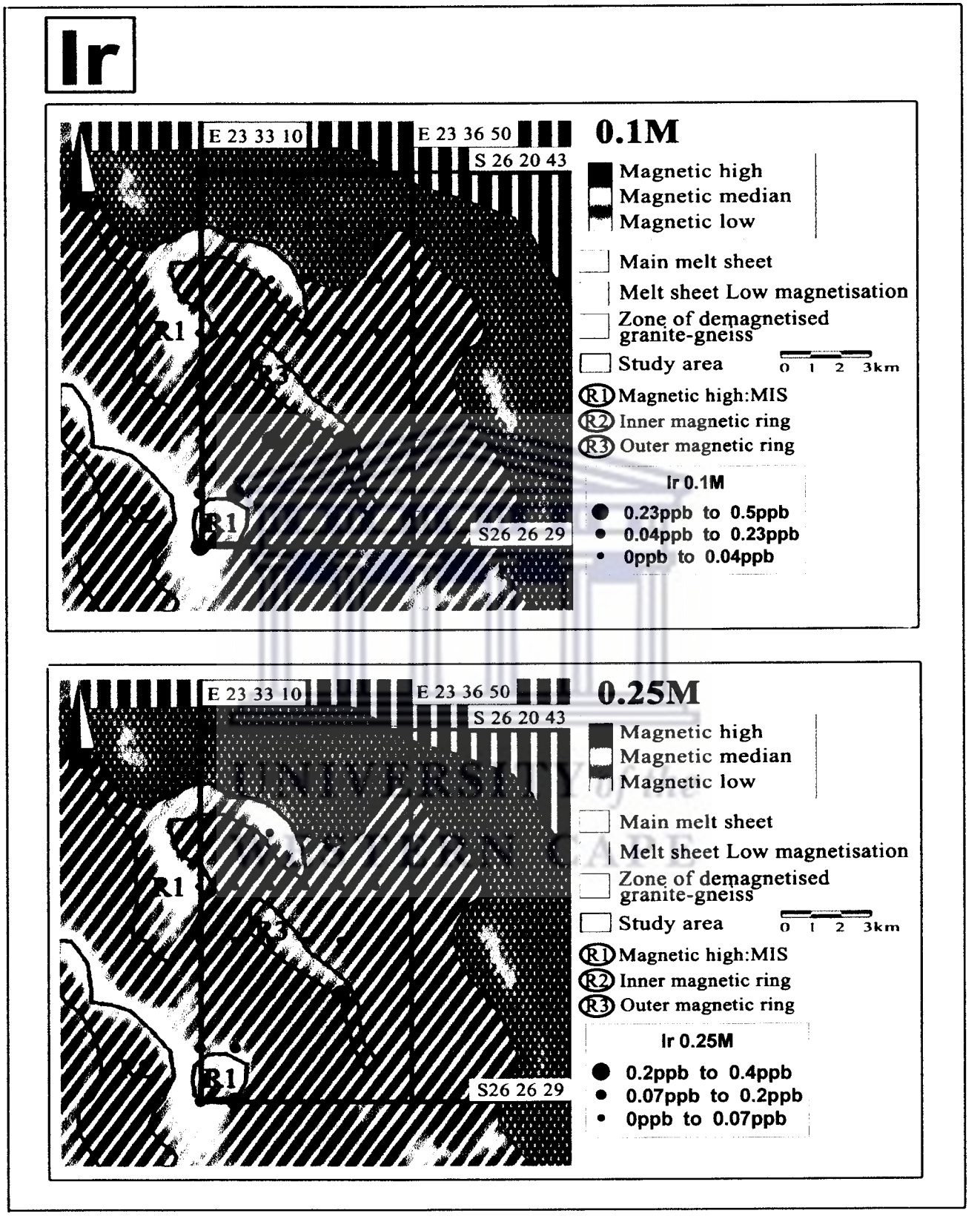

Fig. 4.3.2 Geochemical map of Ir (0.1M, 0.25M hydroxylamine concentration)

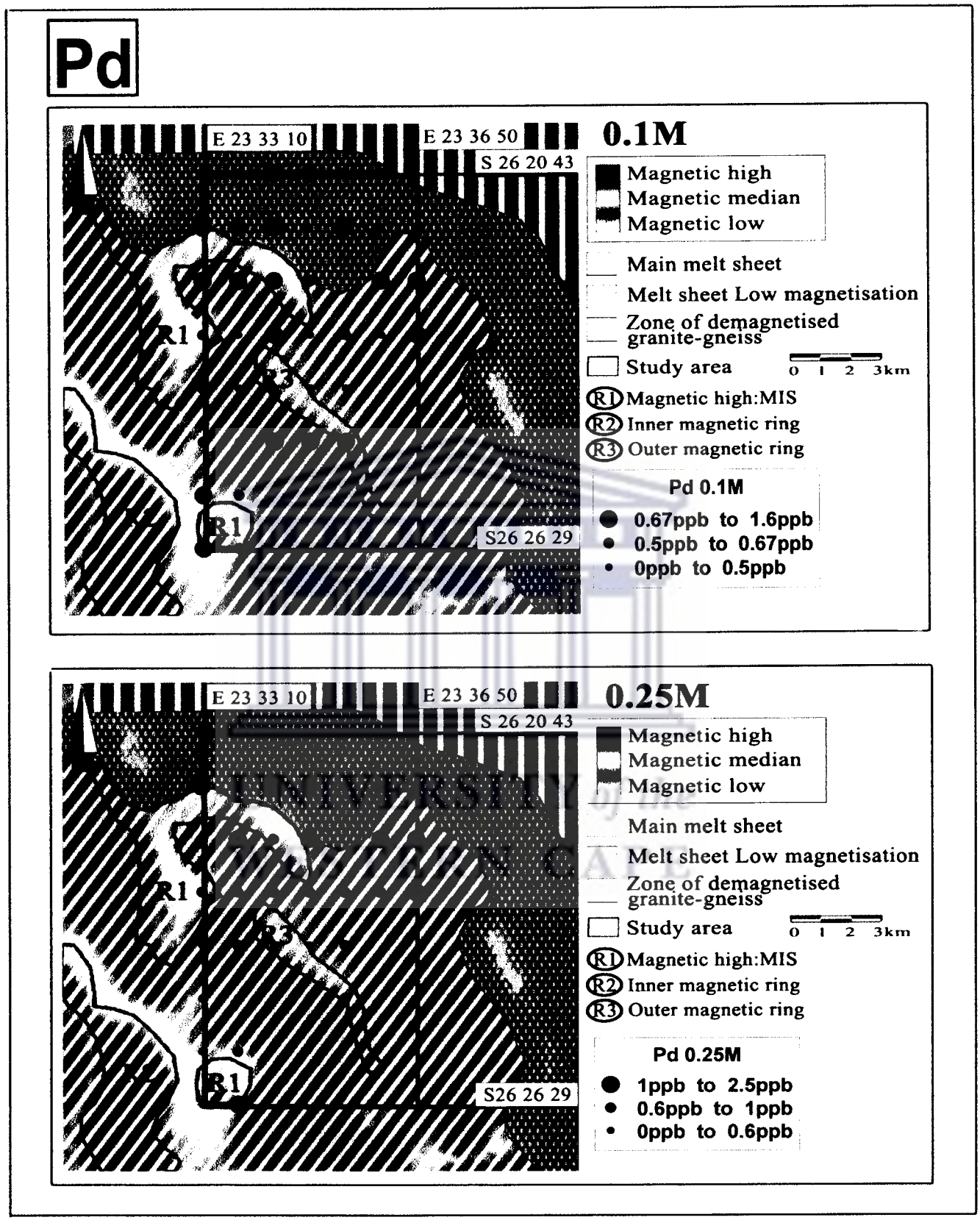

Fig. 4.3.3 Geochemical map of Pd (0.1M, 0.25M hydroxylamine concentration)

The box and whiskers plot shows three outliers platinum values of 0.03ppb, 0.08ppb, 0.7ppb (0.25M) occur mostly in the north (Zone A) and a few elevated values in the south (Zone B). Elevated values in 0.1M are generally occurring in the north part (Zone A). These areas are coincident with occurrence of high magnetic anomalies or trends (Fig. 4.3.4).

Silver

Silver contents vary from 0.03-0.94ppb. Silver in 0.1M partial extraction are higher than 0.25M and these have average values of 0.1ppb and 0.07ppbppb and an estimated background anomaly values at 0.18ppb and 0.13ppb respectively.

The Distribution pattern of silver in 0.1M and 0.25M geochemical maps are not similar. Elevated values above 0.18ppb (0.1M) occur in the northeastern part and southeastern part of project area and 0.13ppb (0.25M) occur in a band from northwestern to northeastern part of the project area.

The box and whiskers plot shows three outliers silver values of 0.14ppb, 0.18ppb, 1ppb (0.1M) which occur most in the northeastern part (Zone A and boundary Zone A with Zone B) and a few elevated values in the southeastern part (Zone B). Commonly elevated values occur in 0.25M, which is a band from northwestern to northeastern part in Zone A and Zone B (Fig. 4.3.5).

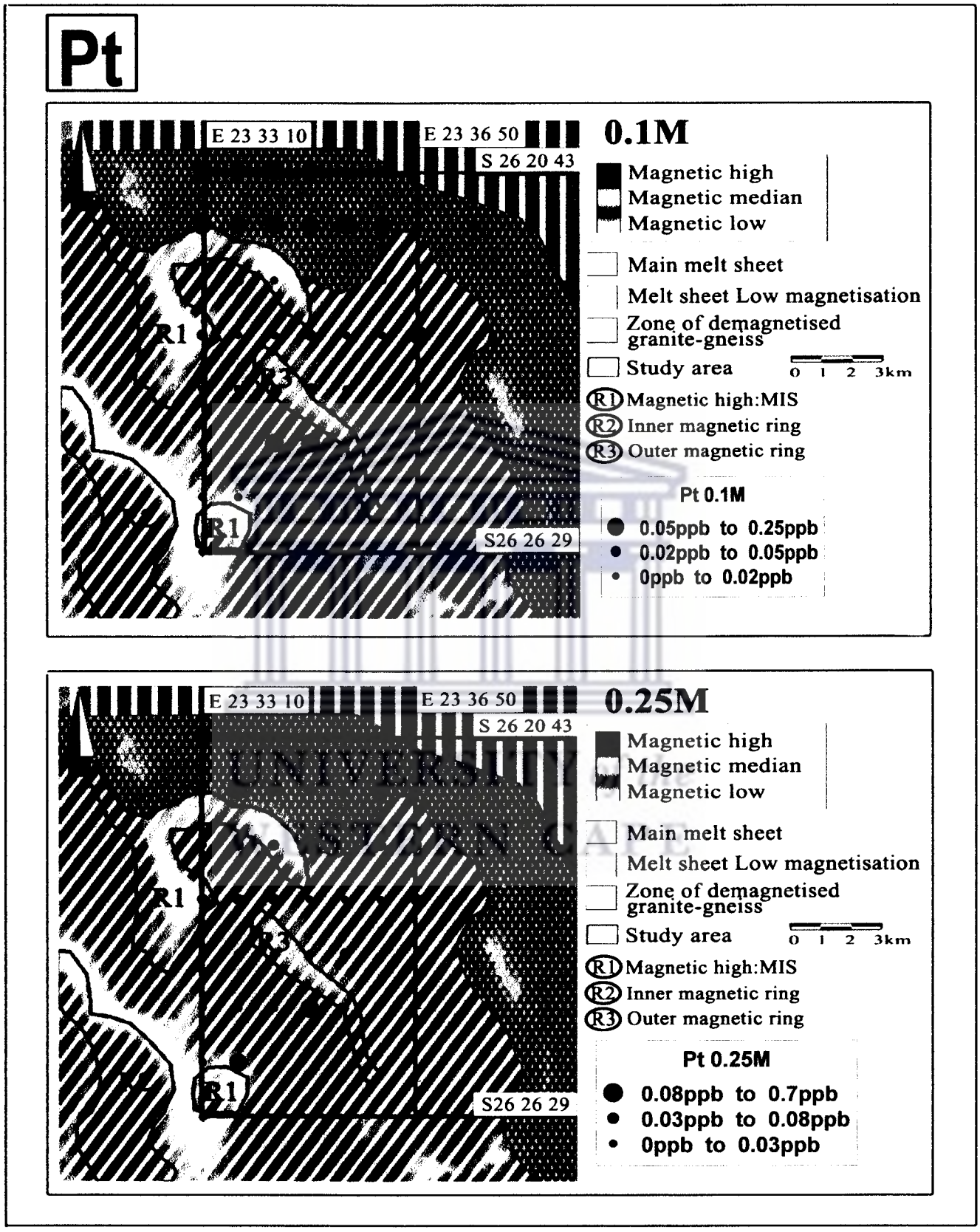

Fig. 4.3.4 Geochemical map of Pt (0.1, 0.25M hydroxylamine concentration)

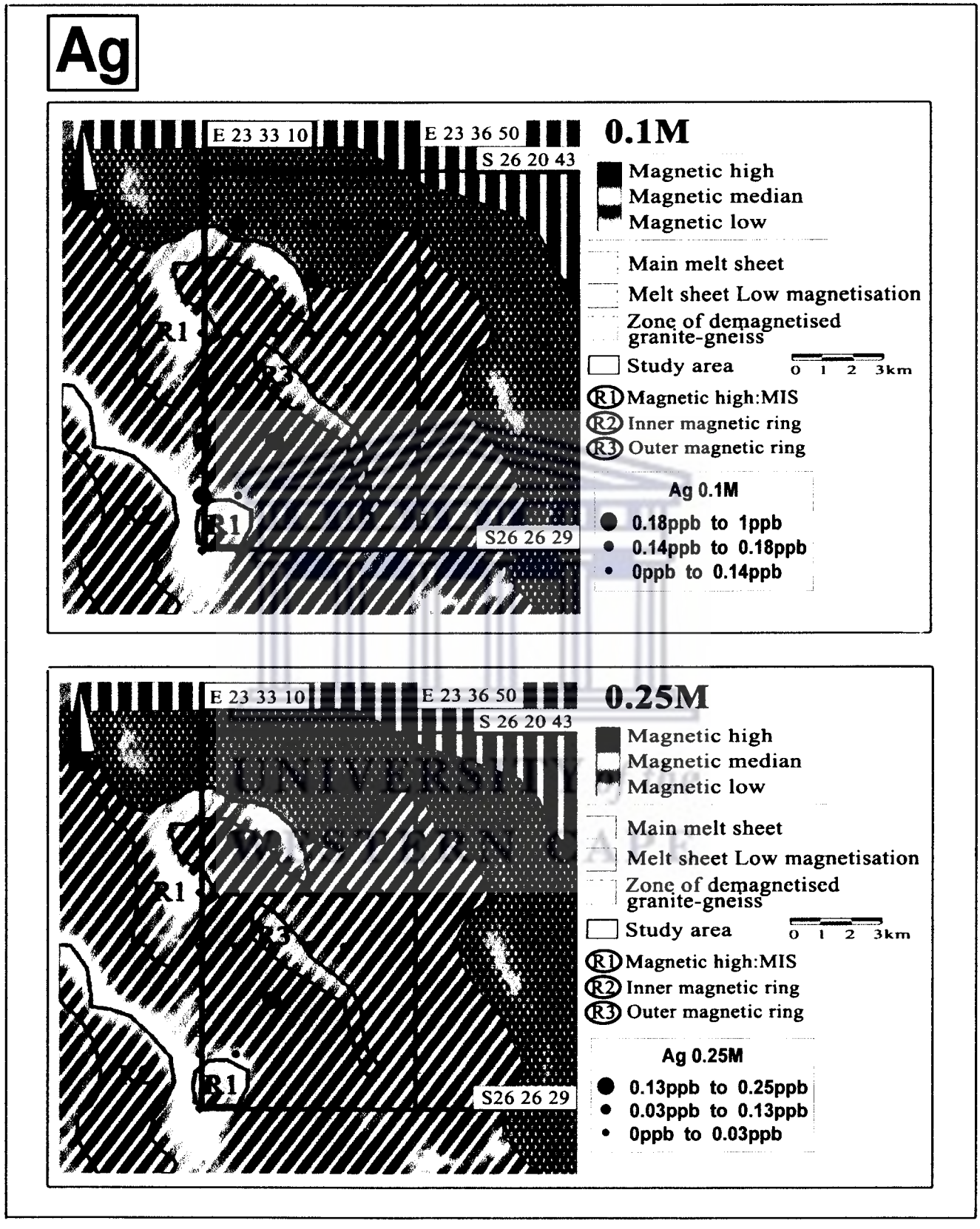

Fig. 4.3.5 Geochemical map of Ag (0.1M, 0.25M hydroxylamine concentration)

Chapter 5

Discussion

This study is part of a currently ongoing project at the Department of Earth Science, University of the Western Cape to map concealed bedrocks beneath aeolian regolith Its main objective is appraising techniques which are able to 'fingerprint' concealed bedrock by using geochemical signatures that can distinguish between the impact melt zone with its associated mineralization and the surrounding shock metamorphosed basement rocks. The chemistry of the rocks associated with the MIS e.g. the granites, quartz norite, zones of mafic nodules have been outlined by Hart et al (2002). These rocks vary widely in their chemical composition and especially the melt rocks that are highly enriched in the PGE, Ni and Cr etc.

The regolith overlying the Morokweng Impact Structure is covered entirely by wind-blown Kalahari sand and a few isolated exposures of calcretes. Aeolian sand mainly consists of quartz that is coated by Fe-Mn oxides. These appear to be the major components and phase in aeolian sand that control the distribution patterns of mobile metal ions, either bound or unbound (Okujeni et al., 2005). A hydroxylamine hydrochloride partial leach was therefore selected by this study to investigate the distribution of trace metals in aeolian sand. Davy et al., (1999), Okujeni et al., (2005) and various authors have also recommended the use of hydroxylamine hydrochloride for selectively targeting Fe-Mn oxides in regolith.

Several recent publications have focused on optimizing hydroxylamine partial leach in insitu regolith and transported overburden. The use of hydroxylamine hydrochloride in selective extraction of Fe-Mn oxide in aeolian terrain is yet to be reported. Hence, the major outcomes for this study are as follow:

1. Element extractability is more pronounced using sieved <75μm fractions of aeolian sand during partial extraction. This combined with a much reduced sample weight of 1g produced the optimum extraction levels for most elements

that were investigated. The results corroborated with findings of Hall et al., (1995), Hlavay et al., (2004), who used other transported sediments and insitu regolith samples.

2. However, high levels of element extractability may not always reflect the chemistry of underlying bedrock or mineralization (Nolan et al., 2003; Darlymple et al., 2005). This study has been tailored and linked to investigating the extractability of 24 elements by varying the hydroxylamine concentration and resultant pH at a temperature of 50℃. This reportedly provides the most suitable leach condition for the Mn-Fe related metal group (Darlymple et al., 2005). The overall results show a pattern of extractability of elements, which may be subdivided into three groups; rapid reaction metal group, Mn-Fe related and the hydroxylamine-stabilized metal group (Darlymple et al., 2005).

3. A comparison of low pH, low hydroxylamine concentration (0.1M) and high pH high hydroxyl (0.25M) partial leaches shows overall similarity in most of the elements presented, especially the PGEs. The element in geochemical maps shows a strong resemblance to MMI results from previous exploration work. The results show elevated As, V, Os, Ir, Pt, Ni and Au values located around the magnetic highs in the western and northern part of the project area. Other element such as Ba, Rb, and Sr do not reflect anomalies around these areas despite their high level of extractability.

The elevated element contents to the western and northern parts of the area are an integral part of a NE-SW trending band of anomalous Ni, Ag values. This was previously outlined in a regional geochemical survey of the MIS (Xu, 2004). These anomalies which are aligned along the NE-SW trending radial faults and dykes are same crosscut the shock metamorphosed basement rocks, possibly the impact melt rock and associated mineralized layers. A possible regolith geochemical model can be formulated in which mobile metal ions are dispersed from underlying mineralization concealed in the melt sheet via these faults into regolith; first into calcretes and then recycled into the overlying aeolian sand (Cameron and Hattori, 2003; Kelly et al., 2002). Elevated element contents may therefore be encountered along the radial faults as well as around the interface between the melt rock and the shock metamorphosed

basement (Fig. 5.1)

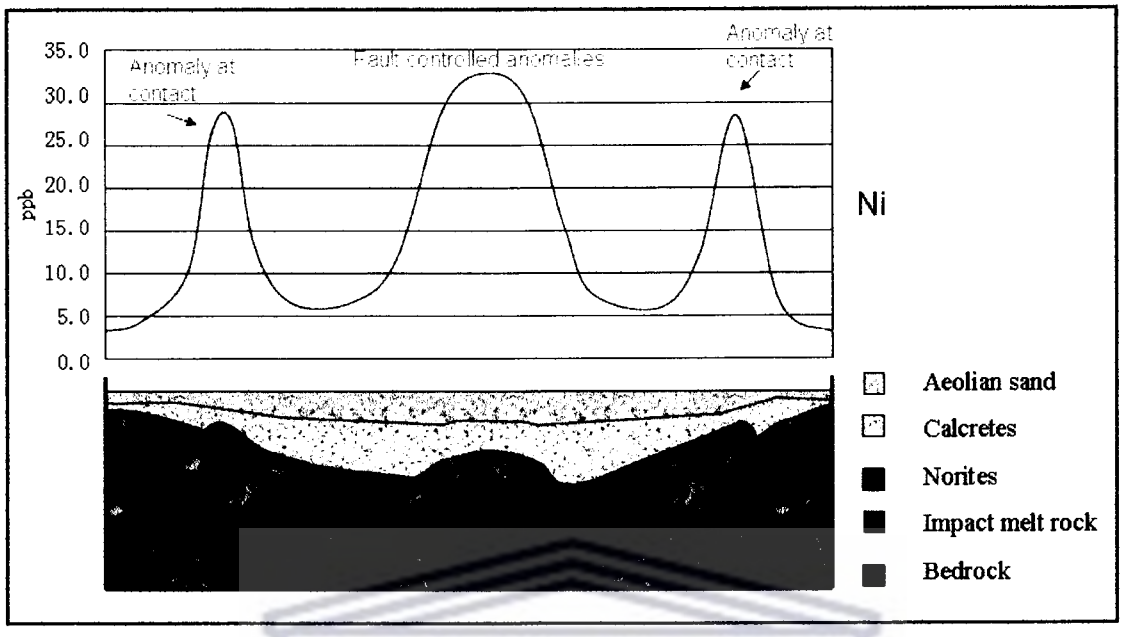

Fig. 5.1 Regolith geochemical model showing alignment of anomalies along faults intercepting Ni-PGE mineralization within the impact melt rock and at the contacts to shock metamorphosed basement.

Geochemical sampling should be extended to cover the entire melt sheet as well as a portion of the Outer Ring. This will allow interpretation of the contact between the basement rocks and the melt sheet and facilitate identification of structures with the potential to host offset type mineralization in the basement.

Chapter 6

Conclusion

1. Patterns of element extractability can be grouped into: 1.) the rapid reaction group comprising of Mn, Ba, Cu, Sr, Pb, Ni, Co, Pd and U. 2.) Those with higher extractability with an increased hydroxylamine concentration As, V, Au and Cr. 3.) Elements with variable extractability patterns Zn, Se, Ag, Pt, Ru, Cd, Ir, Re and Rh, other element such as Ba, Rb and Sr do not reflect anomalies around these areas despite their high level of extractability.
2. Elevated As, V, Ir, Pt, Ni and Au values are located around the magnetic highs in the western part and at the boundary between the impact melt rock and the surrounding basement rocks. These zones of geochemical anomalies coincide with the orientation of radial dykes / faults emanating from the impact melt structure, which is located over the impact melt rock zone.
3. A regolith geochemical dispersion model involving vertical transport of elements from concealed mineralization along faults and unconformities into overlying regolith is proposed. The nature of occurrence of anomalies in sediments can be diverse due to the complex nature of element adsorption to Fe-Mn oxides.

References

Andreoli, M.A.G., Ellis, S., Webb, S.J., Pettit, W., Haddon, J., Ashwal, L.D., Gabrielli, F., Raubenheimer, E., and Ainslie L., (1999), The 145 Ma Morokweng impact, South Africa: an unusual ~90 km crater with associated multi-ring structures and Early Cretaceous mafic dykes. Meteoritics and Planetary Science, Vol. **34**, n 4, p 9.

Andreoli, M.A.G., Ashwal, L.D., Hart, R.J. and Huizenga, J.M., (1999), A Ni- and PGE-enriched quartz norite impact melt complex in the Late Jurassic Morokweng impact structure, South Africa. Large Meteorite Impacts and Planetary Evolution II (eds. B.O. Dressler & V.L. Sharpton). Geological Society of America Special Paper **339**, pp. 91-108.

Anhaeusser C.R., and Walraven F., (1999) Episodic granitoid emplacement in the western Kaapvaal Craton: evidence from the Archaean Kraaipan granite-greenstone terrane, South Africa. Journal of African Earth Sciences, Vol. **28**, n 2, pp. 289-309.

Bootsman C.S., Reimold W.U. and Brandt D. (1999) Evolution of the Molopo drainage and its possible disruption by the Morokweng impact event at the Jurassic-Cretaceous boundary, Journal of African Earth Sciences, Vol. **29**, pp. 669-678.

Cameron E.M., Hattori, K.H., (2003) Mobility of palladium in the surface environment: data from a regional lake sediment survey in northwestern Ontario. Geochemistry: Exploration, Environment, Analysis, Vol. **3** 2003, pp 299-311.

Corner. B, W.U. Reimold, D. Brandt, C. Koeberl. (1997) Evidence for a major impact structure in the northwest province of South Africa- The Morokweng impact structure, 27th Lunar and Planetary Science Conference, Houston TX, Ext, Abstract, **1**, 1996, pp.257-258.

Darlymple, I.J., Cohen, D.R. & Gatehouse S.G. (2005). Optimization of partial extraction chemistry for buffered acetate and hydroxylamine leaches. Geochemistry:

Exploration, Environment, Analysis, Vol. **5** 2005, pp. 279-285.

Davis, J. (1986). Statistics and data analysis in Geology. Wiley, New York, 646pp.

Davy, R., Pirajino, F., Sanders, A. J. and Morris, P.A. (1999). Regolith geochemical mapping as adjunct to geological mapping and exploration: examples from three contiguous Proterozoic basins in Western Australia. Journal of Geochemical Exploration, Vol. **66**, 37-53.

Fang, G.C., Chang, C.N., Chu, C. C., Wu, Y.S., Fu, P.P.C., Yang, I.L., Chen, M.H., 2003. Characterization of particulate, metallic elements of TSP, $PM_{2.5-10}$ aerosols at a farm sampling site in Taiwan, Taichung, Sci. Total environ.308 (1-3), 157-166.

Gray, D.J., Lintern, M.J. and Wildman, J.E., (1999). Selective and partial extraction analyses of transported overburden for gold exploration in the Yilgarn Craton, Western Australia, Journal of Geochemical Exploration, Vol. **67**, 51-66.

Hall, G.E.M., Vaive, J.E., Beer, R., Hoashi. M., (1995). Selective leaches revisited, with emphasis on the amorphous Fe oxyhydroxide phase extraction. Journal of Geochemical Exploration,Vol. **56**, 59-78.

Hall, G.E.M., Maclaurin, A.I., Vaive, J.E., (1995). Readsorption of gold during the selective extraction of the "soluble organic" phase of humus, soil and sediment samples. Journal of Geochemical Exploraiton, Vol. **54**, 27-38.

Hall G.E.M., (1998), Analytical perspective on trace element species of interest in exploration. Journal of Geochemical Exploration Vol. **61**, p.1–19.

Hart R. J., Andreoli M. A. G., Tredoux M., Moser D., Ashwal L. D., Eide E. A., Webb S. J., and Brandt D. (1997) Late Jurassic age for the Morokweng impact structure, southern Africa. Earth and Planetary Science Letters, Vol.**147**, pp. 25-35.

Hart, R. J., Cloete, M., McDonald, I., Carlson, R. W., Andreoli, M.A.G., (2002), Siderophile-rich inclusions from the Morokweng impact melt sheet, South Africa: possible fragments of a chondritic meteorite. Earth and Planetary Science Letters, Vol. **198**, 49 – 62.

Hart, R.J., Martinus, C., McDonald, I., Carlson, R.W., Andreoli, M.A.G. (2002) Siderophile-rich inclusions from the Morokweng impact melt sheet, South Africa; Possible fragments of a chondritic meteorite. Earth and Planetary Science Letters **198** 49-62.

Hlavay, J., Prohaska, T., Weisz, M., Wenzel, W.W., Stingeder, G., (2004), Determination of trace elements bound to soils and sediment fractions. Pure Appl. Chem., Vol. **76**, 2, 415-442.

Kelley, D.L., Hall, G.E.M., Closs, L.G., Hamilton, I.C., McEwen, R.M., (2003), The use of partial extraction geochemistry for copper exploration in northern Chile. Geochemistry, Exploration, Environment, Analysis, Vol. **3**, pp.85-104.

Koeberl C., Armstrong R.A., and Reimold W.U. (1997) Morokweng, South Africa: A large impact structure of Jurassic-Cretaceous boundary age. Geology, Vol. **25**, pp 731–734.

Koeberl C., Armstrong R.A., and Reimold W.U. (1997) Morokweng, South Africa: A large impact structure of Jurassic-Cretaceous boundary age. Geology, Vol. **25**, pp731–734.

Koeberl C. and Reimold W.U. (2003). Geochemistry and petrography of impact breccias and target rocks from the 145 Ma Morokweng impact structure, South Africa. Geochemica et Cosmochimica Acta, Vol. **67**, No.10, pp.1837-1862.

McDonald I., Andreoli M. A. G., Hart R. J., and Tredoux M. (2001). Platinum-group elements in the Morokweng impact structure, South Africa: Evidence for the impact of a large ordinary chondrite projectile at the Jurassic-Cretaceous boundary. Geochimica et Cosmochimica Acta, Vol. **65**, (2), pp. 299-309.

Nolan, A.L., Baltpurvins, K., Hamilton, I.C. & Lawrence, G.A (2003).Chemostat-controlled selective leaches of model soil phases-the hydrous manganese and iron oxides. Part 1.Geochemistry: Exploration, Environment, Analysis, Vol. **3**,157-168.

Okujeni C.D., Ackon P., Baugaard W. and Langa N., (2005), Controls of element dispersion in aeolian sand and calcrete-dominated regolith associated with gold mineralization in the Kraaipan greenstone belt, South Africa. Geochemistry: Exploration, Environment, Analysis; Vol. **5**, No. 3; pp.223-231.

Poujol M., Anheausser C. R., and Armstrong R. A. (2000) Episodic Archaean granitoid emplacement in the Amalia-Kraaipan terrane, South Africa: New evidence from single zircon U-Pb geochronology with implications for the age of the Western Kaapvaal Craton. Univ. of the Witwatersrand, Johannesburg, Econ.Geol.Res. Inst. Inf.Circ. Vol. **346**, 21pp.

Pwa, A. Maqueen, K.G., Scott, K.M., and Van Moort, J.C. (1999). Regolith geochemical exploration using acid insoluble residue as a sample medium for gold and base metal deposits in the Cobar region, N.S.W. Australia. Journal of Geochemical Exploration, Vol. **67**, 15-31.

Reimold W.U., Koeberl C., Brandstatter F., Kruger F.J., Armstrong R.A., and Bootsman C. (2000) Morokweng impact structure, South Africa: Geologic, petrographic and isotopic results, and implications for the size of the structure. Geol.Soc.America Spec. Paper **339**, 61-90.

Reimold W.U., Armstrong R.A. and Koeberl C. (2002). A deep drillcore from the Morokweng impact structure, South Africa: petrography, geochemistry, and constraint on the crater size. Earth planet. Sct. Lett. **201**, 201, 221-232.

Reimold, W.U., and Koeberl, C., (2003), Petrography and geochemistry of a deep drill core from the edge of the Morokweng impact structure, South Africa. In: Impact Markers in the Stratigraphic Record (eds. C. Koeberl and F. Martinez-Ruiz). Impact Studies, Vol. **3**, Springer, Heidelberg, pp. 271-292.

Xu, J.J., (2004). Evaluation of geochemical survey data from the Morokweng impact structure using statistical techniques and response ratios: Earth Science Department, University of the Western Cape, B.Sc (Honours) thesis (Submitted)

Yang, J., (2006). Geochemical mapping of the North-West sector of Morokweng

Impact Structure, South Africa: Earth Science Department, University of the Western Cape, M.Sc thesis.

The Earth Impact Database, Planetary and Space Science Centre, University of New Brunswick, 2006, http://www.unb.ca/passc/impactdatabase.

APPENDIX I

Raw analytical data set for samples from orientation study

(All values are in ppm and grain sizes in μm)

	I.D	1g					2g					3g				
		Mn	Co	Ni	Fe	Cu	Mn	Co	Ni	Fe	Cu	Mn	Co	Ni	Fe	Cu
0.1M	1	9.54	2.7	0.72	10.08	1.71	0.68	1.5	0.23	1.58	1.08	5	1.14	0.45	4.35	0.84
	2	4.41	3.6	0.45	4.5	1.89	4.37	0.63	0.36	4.01	1.08	2.5	0.87	0.24	3.06	0.81
	3	2.16	2.16	0.09	2.88	1.89	1.85	0.9	0.86	2.66	1.08	1.7	1.08	0.12	2.73	0.84
	4	2.07	3.96	0.36	2.7	1.98	1.94	2.43	0.05	2.66	1.08	1.6	2.52	0.36	2.31	0.84
	5	0.99	4.14	0.45	3.33	2.07	1.31	0.95	0.05	1.93	1.13	1.2	1.47	0.18	1.41	0.84
0.15M	1	9.72	1.44	0.13	12.2	2.7	1.44	2.7	0.45	9.45	1.4	0.45	1.78	0.27	4.78	0.93
	2	0.27	2.25	0.81	6.48	2.61	0.27	2.07	0.18	3.06	1.35	0.36	2.28	0.27	0.26	0.93
	3	0.63	5.04	0.9	3.24	0.27	0.14	2.24	0.63	3.24	1.35	0.36	1.47	0.03	2.56	0.93
	4	0.27	2.79	0.72	3.24	0.27	0.14	0.99	0.54	3.06	1.4	0.27	2.31	0.18	2.61	0.93
	5	0.54	3.24	0.81	3.6	2.7	0.09	2.21	0.59	2.34	1.35	0.39	1.68	0.42	2.52	0.93
0.2M	1	0.72	7.74	1.2	13.05	2.79	0.32	2.7	0.27	8.96	1.44	0.33	2.23	0.21	4.41	0.99
	2	0.63	5.76	0.99	8.01	2.88	0.27	3.24	0.27	5.36	1.4	0.15	1.74	0.54	4.35	0.96
	3	0.36	3.87	1.2	7.2	2.79	0.36	4.01	0.72	4.32	1.49	0.27	1.92	0.42	2.85	0.99
	4	0.45	6.03	0.81	6.3	2.88	0.18	4.59	0.68	3.69	1.44	0.24	1.86	0.03	3.39	0.96
	5	0.36	6.03	0.11	6.03	2.88	0.23	3.47	0.32	3.33	1.44	0.27	3.03	0.69	2.61	0.96
0.25M	1	0.81	5.85	1.8	7.83	2.88	0.5	4.86	0.95	6.93	1.49	0.15	0.3	0.63	0.51	0.99
	2	0.9	9.27	1.4	4.5	2.97	0.36	3.24	1	4.32	1.49	0.27	2.58	0.48	2.97	1.02
	3	0.63	6.84	2	2.7	2.88	0.59	4.41	0.54	2.16	1.53	0.24	2.79	0.45	2.28	0.99
	4	0.81	9.81	1.6	3.15	2.97	0.36	3.78	1.3	2.3	1.49	0.27	2.34	0.57	1.98	1.02
	5	0.63	4.05	1.9	3.24	2.88	0.36	4.64	0.81	1.89	1.49	0.3	1.89	0.6	1.92	0.99

		0.1M					0.15M					0.2M					0.25M				
I.D	Minutes	Ni	Co	Cu	Mn	Fe	Ni	Co	Cu	Mn	Fe	Ni	Co	Cu	Mn	Fe	Ni	Co	Cu	Mn	Fe
1	10	1.98	11	3.06	5.58	5.49	1.44	9.54	2.97	1.98	5.67	1.71	8.73	3.15	1.08	6.12	1.89	8.73	2.97	1.17	6.84
2	10	1.53	7.65	2.97	3.78	4.68	1.44	9.09	2.97	1.17	5.31	1.8	5.94	2.97	1.17	7.29	1.98	8.1	2.97	1.08	7.56
3	10	1.8	4.56	2.97	3.42	4.68	1.44	7.83	2.97	0.99	5.67	1.26	9.54	2.97	1.53	6.57	1.62	11.5	2.97	0.99	6.48
4	10	1.53	10.3	2.97	2.61	3.87	2.34	7.56	2.97	0.9	5.49	1.89	9.63	2.97	0.9	5.31	2.25	6.02	2.97	0.99	7.65
5	10	0.99	8.55	2.97	2.25	5.49	2.16	6.66	2.88	0.9	4.86	1.89	7.11	2.97	0.9	5.85	2.34	8.91	2.97	0.9	7.92
1	30	1.89	8.73	2.97	9.99	10.3	2.25	9.63	2.97	1.71	9.9	1.62	10.5	2.97	1.71	11.2	1.71	10.1	2.97	1.08	2.79
2	30	2.49	10.6	2.97	5.58	9.27	2.61	11.07	2.97	1.62	9.27	2.34	10.4	2.97	1.71	10.1	2.25	11.3	2.97	1.17	4.05
3	30	2.61	8.28	3.15	3.42	7.83	2.43	10.26	3.06	1.35	9.54	1.62	11.7	2.97	1.26	10.5	2.34	9.99	3.06	1.26	2.34
4	30	2.43	7.74	3.06	3.78	8.46	2.07	9.81	2.97	1.35	9.54	2.79	9.18	3.06	0.9	9.99	2.43	8.55	3.06	1.44	2.79
5	30	1.98	9.18	2.97	2.79	8.82	2.07	10.53	2.97	1.26	8.91	2.61	6.03	2.88	1.26	11.8	2.79	10.5	3.06	1.26	2.7
1	60	3.15	9.63	2.97	5.85	5.85	2.97	10.35	2.97	1.8	5.67	3.42	11.7	3.06	1.62	4.23	2.7	9.27	2.97	1.44	5.4
2	60	2.07	9.81	2.97	3.15	4.59	3.69	11.34	2.88	1.71	3.96	3.06	9.54	2.97	1.89	4.86	3.15	11.3	2.97	1.26	4.41
3	60	2.97	9.63	2.97	4.05	4.59	2.79	10.89	2.97	1.62	4.05	2.88	10.5	2.97	1.71	5.76	3.6	11.3	2.97	1.26	4.95
4	60	2.52	9.18	2.97	4.23	3.24	2.97	8.28	2.88	1.44	3.78	3.33	11.5	2.97	1.71	4.95	2.7	11.9	3.06	1.53	6.12
5	60	2.61	6.48	2.97	2.43	4.32	2.88	11.79	2.97	1.44	3.06	2.79	8.37	2.97	1.71	3.69	2.79	9.81	2.88	1.89	6.84
1	90	2.97	12.2	2.97	10.3	7.47	2.88	10.44	3.06	1.98	7.29	3.96	11.7	2.97	1.8	8.37	3.87	11.8	2.97	1.8	7.11
2	90	2.88	10.7	3.06	6.12	8.37	3.42	11.88	2.97	2.25	6.66	2.97	12.4	2.97	1.89	6.66	3.51	10.9	2.97	1.71	8.37
3	90	3.96	8.46	2.97	3.33	6.57	2.34	11.07	2.97	1.53	8.1	3.24	11.7	2.97	1.98	7.47	3.51	11	3.06	1.98	8.1
4	90	3.15	9.99	2.97	4.23	8.01	3.78	11.52	2.97	1.89	5.31	3.06	10.6	3.06	1.98	6.66	3.78	9.36	2.97	1.89	9.18
5	90	3.15	13.3	3.06	3.06	5.85	2.97	11.88	2.97	1.8	5.85	3.15	11.1	2.97	2.7	7.83	3.87	11.5	2.97	2.07	8.37

APPENDIX II

Hydroxylamine hydrochloride sample analyzed by ICP-MS

(All values are in ppb and grain sizes in μm)

0.1M	Mn	Ni	V	Cu	Zn	As	Sr	Ba	Os	Rb	Pb	Au	Co	Pd	Se	U	Pt	Ag	Cd	Re	Ru	Ir	Rh	Cr
19	1726	23.3	32.4	14.9	136	20.8	67.2	495	*0.00*	12.1	16.1	*0.00*	21.4	0.66	10.1	0.082	*0.00*	*0.00*	0.35	*0.00*	*0.00*	*0.00*	*0.00*	*0.00*
20	848	19.3	30.0	45.0	30.7	20.9	61.3	174	158	12.5	16.5	5.40	13.3	1.23	13.7	0.14	*0.00*	*0.00*	0.27	0.054	0.086	0.35	0.032	*0.00*
39	448	11.9	40.7	31.3	0.7	28.1	22.0	159	83.8	4.93	9.38	6.11	7.24	0.64	9.12	0.075	*0.00*	*0.00*	0.66	*0.00*	0.25	0.23	0.23	19.2
40	805	15.6	33.7	211	73.0	28.7	41.5	166	30.8	10.7	16.1	5.84	13.1	0.72	*0.00*	0.17	*0.00*	0.94	0.41	*0.00*	0.35	0.19	0.077	35.2
56	1088	22.4	30.3	51.4	25.7	25.2	58.4	294	9.32	14.6	18.5	3.42	16.6	1.03	1.99	0.17	*0.00*	*0.00*	0.44	0.011	0.12	0.26	0.054	15.9
57	1331	16.9	34.5	29.0	33.0	24.4	33.2	194	1.94	13.8	22.8	3.19	23.9	1.40	14.7	0.26	0.16	*0.00*	0.20	0.21	0.35	0.13	0.12	26.4
58	1703	20.3	11.9	32.4	40.2	18.8	42.4	206	235	14.6	20.9	4.25	21.8	1.34	5.92	0.19	0.21	0.32	0.34	0.14	*0.00*	0.43	*0.00*	*0.00*
59	778	19.2	21.7	3.86	13.0	19.1	37.3	159	47.3	11.1	12.1	*0.00*	12.6	0.27	1.73	0.13	*0.00*	*0.00*	0.043	*0.00*	*0.00*	0.045	*0.00*	*0.00*
60	1363	16.7	30.1	12.4	17.9	22.7	37.4	172	13.2	12.4	19.8	*0.00*	27.7	0.51	*0.00*	0.16	*0.00*	0.25	0.070	0.030	*0.00*	*0.00*	*0.00*	*0.00*
76	873	6.33	49.3	8.03	33.6	17.1	36.5	148	1.31	13.7	11.8	0.36	15.7	0.23	17.4	0.11	*0.00*	*0.00*	0.35	*0.00*	0.043	*0.00*	*0.00*	*0.00*
77	1198	12.9	62.6	15.2	40.5	15.9	59.9	197	0.25	18.3	10.6	0.50	19.8	0.16	9.01	0.068	0.021	0.012	0.65	*0.00*	*0.00*	*0.00*	*0.00*	*0.00*
78	1796	14.9	67.3	5.36	46.4	17.7	70.2	207	*0.00*	25.8	9.79	0.53	27.2	0.13	19.5	0.099	*0.00*	*0.00*	1.15	*0.00*	0.022	*0.00*	*0.00*	*0.00*
79	771	6.64	67.0	13.0	53.4	17.0	46.2	206	*0.00*	12.0	10.9	0.48	14.8	0.21	10.0	0.075	*0.00*	*0.00*	0.19	*0.00*	*0.00*	*0.00*	*0.00*	*0.00*
80	1393	15.4	25.9	20.6	28.2	23.1	27.8	122	3.25	16.4	17.0	*0.00*	22.6	0.55	*0.00*	0.23	*0.00*	*0.00*	0.12	*0.00*	*0.00*	*0.00*	*0.00*	*0.00*
94	599	*0.00*	32.5	12.6	33.6	11.5	73.0	298	22.6	14.2	16.2	1.04	17.0	0.70	6.47	0.24	0.086	0.058	0.11	*0.00*	*0.00*	0.044	*0.00*	*0.00*
95	821	*0.00*	43.5	19.1	26.9	13.7	131	168	11.8	13.4	14.4	0.64	18.0	0.43	6.04	0.21	0.014	0.074	0.22	0.040	*0.00*	*0.00*	*0.00*	*0.00*
96	634	1.38	44.1	7.31	34.9	16.1	62.2	172	5.46	11.6	14.0	0.35	13.4	0.62	10.6	0.16	*0.00*	*0.00*	0.23	*0.00*	*0.00*	*0.00*	*0.00*	*0.00*
97	828	*0.00*	43.4	13.8	55.0	13.7	43.2	184	3.52	12.3	18.1	0.39	14.4	0.46	8.64	0.26	0.020	*0.00*	0.14	*0.00*	*0.00*	*0.00*	*0.00*	*0.00*
98	720	5.11	65.2	15.3	24.3	20.4	54.4	169	1.92	12.7	18.9	0.60	15.7	0.78	9.47	0.20	*0.00*	*0.00*	0.54	0.017	*0.00*	*0.00*	*0.00*	*0.00*
99	1053	2.98	63.2	6.85	25.9	18.6	52.3	220	0.34	10.3	18.6	0.34	20.1	0.48	17.9	0.14	0.013	*0.00*	0.45	*0.00*	*0.00*	*0.00*	*0.00*	*0.00*
100	827	6.68	61.6	13.0	39.7	20.2	50.4	185	*0.00*	12.4	20.1	0.38	11.5	0.61	17.2	0.16	0.042	0.012	0.34	0.042	0.083	*0.00*	*0.00*	*0.00*
114	716	10.7	32.8	19.0	52.1	13.9	44.0	128	30.2	12.1	21.0	1.42	23.6	0.86	20.4	0.19	*0.00*	0.15	0.39	*0.00*	*0.00*	0.033	*0.00*	*0.00*
115	720	5.93	52.2	47.1	37.4	21.8	39.6	157	15.7	11.4	17.6	0.67	10.8	0.85	13.0	0.22	*0.00*	0.092	0.44	*0.00*	*0.00*	*0.00*	*0.00*	*0.00*
117	1579	12.1	66.6	11.4	55.7	15.9	162	835	9.03	13.2	15.7	0.67	29.1	0.60	10.8	0.15	*0.00*	0.21	0.58	*0.00*	*0.00*	*0.00*	*0.00*	*0.00*
118	676	10.7	61.1	25.3	146	18.5	42.8	96.7	4.42	12.1	58.2	0.34	14.3	0.86	18.4	0.38	*0.00*	0.14	1.07	*0.00*	*0.00*	*0.00*	0.020	*0.00*
119	537	19.7	66.1	35.6	53.8	23.4	51.6	172	1.39	13.7	52.0	0.36	13.9	0.77	3.86	0.22	0.044	0.14	0.57	0.031	*0.00*	*0.00*	*0.00*	*0.00*
120	467	7.64	64.3	31.7	46.5	22.9	25.9	160	*0.00*	11.5	64.2	0.042	10.8	1.12	9.16	0.24	0.013	0.14	1.04	*0.00*	*0.00*	*0.00*	*0.00*	*0.00*
135	570	10.8	70.7	15.0	73.9	24.3	81.5	149	*0.00*	12.3	26.8	1.01	14.7	0.43	20.2	0.21	0.076	0.12	0.61	0.019	0.092	*0.00*	0.012	4.02
136	209	17.4	71.0	25.6	101	23.9	47.8	117	*0.00*	12.7	25.9	0.091	6.1	0.70	12.4	0.32	0.051	0.14	0.42	*0.00*	*0.00*	*0.00*	*0.00*	*0.00*
137	1099	19.6	79.9	15.9	36.2	27.3	64.0	301	*0.00*	8.94	44.2	0.21	16.6	0.48	14.0	0.18	0.050	0.10	0.42	*0.00*	0.021	*0.00*	*0.00*	*0.00*
138	1205	*0.00*	34.5	12.2	29.0	10.2	76.6	255	83.0	13.2	23.0	3.13	25.3	0.97	9.23	0.25	0.12	0.11	0.29	0.048	*0.00*	0.13	0.057	*0.00*
139	584	*0.00*	50.9	22.6	52.9	11.9	75.1	174	39.1	11.8	19.0	1.42	14.8	0.72	12.0	0.14	0.16	0.18	0.26	0.036	*0.00*	0.036	0.018	*0.00*
140	720	*0.00*	57.5	10.5	27.7	15.9	48.4	229	20.4	10.9	23.6	1.17	11.5	0.83	*0.00*	0.15	0.051	0.13	0.63	0.044	*0.00*	0.024	0.018	*0.00*
155	969	*0.00*	43.5	11.3	48.6	9.47	86.1	246	8.60	11.8	21.3	0.29	18.5	0.52	*0.00*	0.25	0.023	0.12	0.30	0.041	*0.00*	*0.00*	*0.00*	*0.00*
156	823	*0.00*	45.4	12.9	29.8	10.8	51.1	272	3.76	11.7	30.8	*0.00*	15.8	0.57	*0.00*	0.11	*0.00*	0.076	0.79	0.033	*0.00*	0.017	*0.00*	*0.00*
157	1579	21.7	48.5	13.3	42.7	18.8	65.4	209	5.76	15.9	29.0	1.13	24.1	0.87	6.18	0.27	0.052	0.083	0.48	0.037	*0.00*	*0.00*	*0.00*	54.0
158	2210	3.38	40.2	8.63	29.3	10.9	53.7	297	*0.00*	16.0	28.3	*0.00*	28.1	0.71	12.1	0.25	0.072	0.044	0.63	0.017	*0.00*	*0.00*	0.021	*0.00*
159	637	7.32	48.1	17.1	67.8	11.2	68.0	139	*0.00*	12.4	27.2	0.37	16.7	0.51	5.55	0.21	0.097	0.16	0.53	0.020	*0.00*	*0.00*	0.048	*0.00*
160	841	6.91	61.2	18.9	42.9	18.4	42.9	185	*0.00*	13.6	30.8	*0.00*	18.7	0.66	2.40	0.16	0.087	0.054	0.51	0.017	*0.00*	*0.00*	0.012	*0.00*

0.15M	Mn	Ni	V	Cu	Zn	As	Sr	Ba	Os	Rb	Pb	Au	Co	Pd	Se	U	Pt	Ag	Cd	Re	Ru	Ir	Rh	Cr
19	238	9.57	41.3	8.48	74.4	28.8	6.08	57.3	0.00	3.25	13.4	0.42	1.98	0.61	23.6	0.10	0.00	0.00	0.00	0.00	0.00	0.00	0.00	0.00
20	60.1	7.70	34.4	18.6	52.6	29.8	4.07	15.3	111	2.43	13.0	4.59	0.67	1.27	1.93	0.090	0.00	0.00	0.15	0.00	0.40	0.088	0.00	0.00
39	89.9	8.92	50.5	38.5	32.1	37.2	3.00	32.4	63.8	1.33	8.37	7.89	1.34	0.62	0.00	0.19	0.20	0.00	0.26	0.033	0.22	0.20	0.37	29.5
40	82.6	8.36	47.5	57.3	28.5	37.4	3.13	19.7	26.0	2.52	10.5	7.82	1.26	0.61	1.81	0.12	0.015	0.00	0.64	0.076	0.31	0.20	0.13	28.5
56	81.6	10.1	42.2	28.4	27.2	36.6	3.91	16.4	6.52	3.20	11.9	3.82	1.30	0.99	13.1	0.16	0.35	0.00	0.39	0.11	0.22	0.13	0.057	15.4
57	101	11.0	43.4	42.4	28.0	36.4	3.95	17.5	2.24	3.51	11.2	4.25	1.33	1.21	0.00	0.21	0.26	0.00	0.12	0.093	0.15	0.13	0.12	43.6
58	79.6	7.86	28.2	27.7	26.5	31.7	3.88	15.7	152	3.05	10.2	3.59	0.85	0.78	25.7	0.13	0.00	0.27	0.00	0.14	0.00	0.31	0.00	0.00
59	52.3	7.45	33.0	2.33	43.0	32.0	3.32	11.4	39.4	2.70	7.52	1.06	0.24	0.65	16.1	0.086	0.00	0.10	0.00	0.19	0.00	0.068	0.00	0.00
60	58.4	6.78	35.2	29.1	24.2	34.4	3.55	12.9	7.45	2.52	8.49	0.00	0.48	0.37	8.55	0.10	0.00	0.00	0.009	0.024	0.00	0.00	0.00	0.00
80	51.6	5.88	30.5	3.48	13.7	32.3	2.82	8.52	1.21	2.79	7.95	0.00	0.62	0.32	0.70	0.15	0.00	0.00	0.00	0.00	0.00	0.00	0.00	0.00

0.2M	Mn	Ni	V	Cu	Zn	As	Sr	Ba	Os	Rb	Pb	Au	Co	Pd	Se	U	Pt	Ag	Cd	Re	Ru	Ir	Rh	Cr
19	103	10.3	60.3	11.0	29.5	49.4	3.56	14.4	424	2.26	19.6	21.2	1.20	3.83	38.6	0.29	0.35	0.00	0.28	0.21	0.40	0.91	0.35	11.0
20	37.6	8.70	45.8	22.6	31.8	45.1	2.36	6.12	81.6	0.86	7.76	5.66	0.39	1.08	16.0	0.11	0.00	0.00	0.20	0.09	0.37	0.01	0.00	0.00
39	64.7	10.9	56.1	54.0	4.13	44.1	2.53	23.5	49.5	0.90	11.1	10.0	1.20	1.94	0.00	0.14	0.17	0	0.06	0.04	0.21	0.22	0.27	29.0
40	65.3	10.4	62.1	61.6	36.3	47.1	3.71	11.6	17.5	1.18	8.13	9.56	0.82	0.75	0.00	0.18	0.16	0.00	0.24	0.04	0.43	0.23	0.10	39.2
56	58.0	9.80	51.0	13.6	18.7	42.7	2.71	4.76	4.44	1.69	10.3	7.38	0.65	1.03	10.4	0.17	0.00	0.00	0.22	0.07	0.16	0.18	0.11	19.0
57	64.7	11.0	52.4	48.4	58.4	53.5	2.91	8.39	0.31	1.41	9.21	4.62	0.86	0.65	0.00	0.14	0.46	0.00	0.31	0.09	0.33	0.02	0.03	30.5
58	27.9	8.17	42.4	10.0	23.6	42.3	2.87	4.47	98.5	1.12	6.01	2.11	0.00	0.21	1.18	0.14	0.00	1.47	0.00	0.01	0.00	0.17	0.00	0.00
59	22.4	7.62	51.8	3.33	16.4	46.3	2.69	5.64	30.1	1.06	5.33	1.25	0.00	0.27	0.00	0.11	0.00	0.25	0.00	0.10	0.00	0.06	0.00	0.00
60	25.4	8.16	53.3	15.5	154	46.1	5.25	10.0	6.16	1.55	7.22	0.00	0.00	0.23	7.71	0.14	0.00	0.00	0.00	0.09	0.00	0.00	0.00	0.00
80	19.8	7.30	41.5	30.0	11.9	42.8	2.77	4.52	0.018	0.83	4.09	0.00	0.00	0.013	0.98	0.16	0.00	0.00	0.00	0.00	0.00	0.00	0.00	0.00

0.25M	Mn	Ni	V	Cu	Zn	As	Sr	Ba	Os	Rb	Pb	Au	Co	Pd	Se	U	Pt	Ag	Cd	Re	Ru	Ir	Rh	Cr
19	58.82	11.30	67.42	12.73	15.83	54.75	3.11	9.74	252.96	1.00	9.63	13.49	0.53	1.56	*0.00*	0.20	*0.00*	*0.00*	0.30	0.08	0.15	0.38	0.19	*0.00*
20	36.47	10.33	58.52	24.29	23.95	52.63	3.09	17.32	61.06	0.74	6.90	5.86	0.68	0.51	27.00	0.17	*0.00*	*0.00*	0.09	0.17	*0.00*	0.10	*0.00*	*0.00*
39	60.98	12.61	73.32	32.93	34.40	59.34	3.51	18.16	41.24	0.80	9.33	10.99	0.79	0.61	*0.00*	0.18	0.43	*0.00*	0.50	0.05	0.25	0.20	0.17	39.17
40	62.18	11.48	67.04	34.95	16.27	54.85	3.00	4.82	13.50	0.84	7.29	9.31	0.98	0.59	6.06	0.16	*0.00*	*0.00*	0.20	0.04	0.34	0.20	0.06	21.89
56	52.33	13.45	60.49	36.54	47.94	61.22	3.82	13.51	2.39	1.00	10.28	5.97	0.37	0.79	*0.00*	0.17	*0.00*	*0.00*	0.19	0.08	0.12	0.25	0.02	30.32
57	59.99	13.86	70.96	24.95	74.24	60.17	6.47	15.20	*0.00*	1.32	11.18	6.42	0.95	0.45	5.72	0.18	0.58	*0.00*	0.46	*0.00*	0.36	0.08	0.03	29.18
58	20.53	9.95	58.55	7.72	22.92	52.37	3.10	3.86	69.70	0.65	5.05	1.73	*0.00*	0.03	14.54	0.12	*0.00*	0.19	*0.00*	0.08	0.09	0.12	*0.00*	*0.00*
59	11.22	11.06	70.01	3.64	49.40	60.03	4.31	3.01	18.99	0.60	3.88	0.26	*0.00*	*0.00*	*0.00*	0.07	*0.00*	*0.00*	*0.00*	0.04	*0.00*	*0.00*	*0.00*	*0.00*
60	15.24	9.91	71.60	5.62	51.45	56.40	3.41	4.67	2.72	0.83	4.15	*0.00*	*0.00*	*0.00*	*0.00*	0.20	*0.00*	*0.00*	*0.00*	0.07	*0.00*	*0.00*	*0.00*	*0.00*
76	47.40	4.92	139.15	8.16	5.94	58.93	2.84	*0.00*	1.36	6.16	10.58	1.33	0.38	0.63	9.90	0.16	0.04	*0.00*	*0.00*	*0.00*	*0.00*	*0.00*	0.03	4.46
77	85.27	5.04	139.10	12.35	10.66	49.55	4.27	7.82	*0.00*	8.95	16.03	1.08	1.15	0.52	24.56	0.09	*0.00*	0.07	*0.00*	*0.00*	*0.00*	*0.00*	*0.00*	3.02
78	89.70	6.81	150.45	7.41	16.19	51.67	3.92	2.71	*0.00*	10.27	13.93	1.00	1.53	0.53	28.63	0.12	*0.00*	0.01	*0.00*	*0.00*	*0.00*	*0.00*	0.03	5.33
79	61.12	*0.00*	127.87	14.83	8.22	57.32	3.11	1.89	*0.00*	5.37	10.11	1.17	0.55	0.64	15.26	0.13	*0.00*	*0.00*	0.06	*0.00*	*0.00*	*0.00*	*0.00*	15.99
80	16.31	8.58	82.56	5.32	52.45	50.74	3.39	3.95	0.82	0.68	3.69	0.28	0.02	0.11	15.52	0.16	*0.00*	*0.00*	*0.00*	*0.00*	*0.00*	*0.00*	*0.00*	*0.00*
94	59.20	1.68	115.52	11.41	9.50	57.83	4.94	28.14	15.87	5.71	12.50	2.48	0.70	1.20	17.92	0.40	0.06	*0.00*	*0.00*	0.02	*0.00*	0.03	0.03	16.07
95	46.06	*0.00*	93.37	3.89	3.16	42.72	5.81	0.74	8.01	5.02	25.23	1.20	0.18	0.91	15.63	0.18	*0.00*	0.03	*0.00*	*0.00*	*0.00*	0.03	*0.00*	*0.00*
96	47.63	2.33	121.22	6.03	6.92	47.78	3.27	*0.00*	6.26	4.08	9.22	1.93	0.33	0.77	12.72	0.21	*0.00*	0.09	0.13	*0.00*	*0.00*	0.02	0.02	5.37
97	50.44	*0.00*	102.95	5.91	18.14	51.27	2.40	*0.00*	2.78	4.57	7.48	1.56	0.17	0.80	26.60	0.26	*0.00*	*0.00*	*0.00*	*0.00*	*0.00*	*0.00*	*0.00*	1.82
98	60.56	3.61	114.56	10.46	12.18	57.30	3.11	*0.00*	2.42	5.24	10.40	1.86	0.82	0.97	13.17	0.22	0.05	*0.00*	0.08	0.01	*0.00*	*0.00*	0.01	11.10
99	69.66	5.56	138.86	7.33	13.51	59.92	2.64	1.07	0.62	4.26	10.72	1.56	0.76	0.85	27.01	0.23	0.06	*0.00*	*0.00*	*0.00*	0.12	*0.00*	0.02	15.90
100	46.12	2.42	114.55	12.84	27.34	54.59	2.39	*0.00*	*0.00*	3.38	8.07	1.19	*0.00*	0.78	13.17	0.18	0.06	*0.00*	0.02	0.02	*0.00*	*0.00*	*0.00*	3.04
114	67.48	6.47	108.51	9.23	7.79	59.87	2.90	*0.00*	21.88	4.70	9.67	3.07	1.01	1.17	18.24	0.19	0.05	0.14	*0.00*	*0.00*	*0.00*	0.06	0.03	16.26
115	61.60	6.93	132.94	21.99	11.73	63.79	1.77	*0.00*	12.90	3.33	9.76	2.84	0.07	1.06	11.78	0.20	0.03	0.12	0.04	*0.00*	0.03	0.03	0.02	14.86
117	114.44	13.62	146.69	11.14	40.34	61.59	9.44	70.80	7.82	5.73	18.77	2.26	2.63	1.27	6.65	0.18	0.14	0.11	0.15	0.01	0.04	*0.00*	0.02	15.68
118	56.61	9.16	113.65	9.87	3.49	54.81	1.62	*0.00*	3.79	3.65	8.31	1.96	0.40	0.89	31.86	0.22	0.07	0.18	0.07	0.04	0.12	*0.00*	0.03	6.48
119	52.42	16.76	139.07	19.05	9.36	64.18	2.25	*0.00*	1.35	4.46	9.67	2.01	0.54	1.08	9.57	0.18	0.05	0.19	0.11	*0.00*	0.13	*0.00*	*0.00*	7.85
120	40.21	11.13	124.45	16.20	19.20	60.50	1.57	*0.00*	*0.00*	3.46	14.30	1.56	0.62	0.89	20.96	0.25	0.01	0.09	0.17	0.02	*0.00*	*0.00*	*0.00*	1.97
135	46.37	10.61	128.85	9.37	24.59	60.25	3.07	*0.00*	*0.00*	4.70	9.03	1.21	0.44	0.73	*0.00*	0.19	0.08	0.08	0.07	*0.00*	*0.00*	*0.00*	0.01	*0.00*
136	38.47	12.34	141.89	13.44	13.75	66.98	2.71	*0.00*	*0.00*	4.43	14.83	1.28	0.60	0.81	6.82	0.27	0.02	0.23	0.35	0.04	*0.00*	*0.00*	0.02	2.12
137	81.27	13.24	74.25	18.87	28.21	54.03	4.17	18.95	141.12	4.80	19.47	7.07	1.07	1.92	2.19	0.25	0.07	0.21	0.29	0.04	*0.00*	0.32	0.04	5.42
138	55.90	*0.00*	102.64	11.97	26.69	48.68	3.92	10.62	55.99	5.86	35.58	3.05	0.94	1.20	2.75	0.31	0.04	0.16	0.68	0.03	0.04	0.08	0.05	*0.00*
139	45.86	8.42	110.19	17.40	27.66	59.11	3.70	6.77	32.87	4.48	28.68	1.95	0.96	0.96	5.72	0.19	0.14	0.21	0.52	0.07	*0.00*	0.02	0.04	12.24
140	39.75	5.65	86.84	8.50	18.08	43.11	2.26	6.19	14.67	4.05	9.78	0.77	0.26	1.03	3.39	0.14	*0.00*	0.09	0.09	0.04	*0.00*	0.05	0.02	0.89
155	52.79	*0.00*	92.24	8.63	26.41	44.42	4.58	10.37	6.56	4.94	42.63	0.58	0.56	0.89	4.93	0.20	*0.00*	0.06	0.71	0.02	*0.00*	0.02	0.02	0.89
156	43.95	9.13	89.28	10.71	37.96	44.57	2.75	7.61	2.41	4.12	10.72	0.47	0.48	0.70	4.60	0.15	0.04	0.13	0.21	0.02	0.05	*0.00*	0.03	2.36
157	82.06	9.41	92.63	8.93	21.55	48.73	3.52	7.17	*0.00*	5.76	11.45	0.47	0.90	0.89	5.59	0.21	*0.00*	0.10	0.18	0.04	*0.00*	*0.00*	0.02	8.33
158	88.12	8.24	85.32	7.86	19.63	40.34	2.73	14.15	*0.00*	6.10	12.07	0.22	1.15	0.98	5.90	0.27	*0.00*	0.09	0.05	0.03	*0.00*	*0.00*	0.02	*0.00*